EFFECT OF HIGH TEMPERATURES ON NORMAL STRENGTH CONCRETE AND HIGH PERFORMANCE CONCRETE CONTAINING STEEL FIBERS

ALAN LAU

M. PHIL.

THE HONG KONG

POLYTECHNIC UNIVERSITY

2003

ABSTRACT

This thesis reports a study of some of the mechanical properties of steel fiber reinforced concrete (SFRC) after being subjected to different elevated heating temperatures, ranging between 105 °C and 1200 °C, in relation to non-reinforced concrete properties. The properties evaluated consist of compressive strength, flexural strength, and elastic modulus. Three grades of concrete, included two normal strength concrete (NSC) mixes and one high performance concrete (HPC) mix, have been studied for their behavior after exposure to different heating temperatures, and those same mixes reinforced with 1% steel fibers by volume of concrete incorporated have also been studied. The main variables taken into consideration were maximum temperature of exposure, and moisture content of heated specimens at the start of heating. In addition, changes of color to the heated concrete were observed and changes in microstructure were also studied using mercury intrusion porosimetry (MIP) analysis.

The results showed that the loss of concrete strength was significant and increased with the increase of maximum heating temperature and with initial moisture content. The percentage loss occurs over a wide range of maximum heating temperatures between 105 and 1200 °C. For maximum exposure temperatures below 400 °C, the loss in compressive strength was relatively small. Significant further reductions in compressive strength are then steadily observed, as maximum temperature increases, for all concrete mixes heated to temperatures exceeding 400 °C. HPC mixes, however, started to suffer from higher compressive strength loss than NSC at maximum exposure temperatures of

600 °C. It is suggested that HPC suffered both chemical decomposition and pore-structure coarsening of hcp where C-S-H is the main hydration product, which starts to decompose at this high temperature. For maximum exposure temperatures exceeding 800 °C, HPC suffers a higher strength loss than NSC. Strengths for all mixes reached minimum values at 1000 or 1100 °C.

In this research study, no evidence of spalling was encountered. Concrete that incorporates steel fibers, at 1 per cent, retains better crack resistance and better mechanical properties than concrete without steel fibers if not heated to exposure temperatures above 1000 °C. Flexural strength results also reflected that concrete with steel fibers performs better than concrete without steel fibers under temperature effects, at about 800 °C, even though the residual strength was very low at this high temperature.

From visual inspection, it is revealed that variations with color, which is mainly depending on the composition of aggregates, occurred in concrete is associated with maximum temperature of exposure and loss in mechanical properties. For steel fiber concrete, a network of hair cracks appeared after heating to maximum temperatures between 400 and 600 °C, which become deeper when heated beyond 600 °C. For ordinary concrete mixes, hair cracks first appeared in specimens heated to 300 °C.

It is concluded overall that (a) fiber reinforcing concrete has higher strength and better performance in crack resistance than non-fiber concrete after exposure to high temperature. (b) high performance concrete can withstand higher heating temperature,

below 600 °C, than normal strength concrete without spalling. (c) initial moisture content before firing affects the ultimate strength of concrete.

PREFACE

This thesis is submitted for the degree of Master of Philosophy at the Hong Kong Polytechnic University (HKPU). The research work presented in this thesis was carried out by the candidate during the years 1998 to 2000 in the Department of Civil and Structural Engineering at the HKPU, initially under the supervision of Dr. Sammy Chan and then, on his departure from the University, under the supervision of Professor M. Anson, the Chief Supervisor; and Professor Sun Wei, the Co-Supervisor.

ACKNOWLEDGMENTS

This thesis was prepared under the direction of Prof. Mike Anson, Dean of the faculty of Construction and Land Use, The Hong Kong Polytechnic University for most of the study period. The author wishes to express his sincere gratitude to Prof. Anson for his invaluable guidance and inspiration during the preparation of this thesis.

The author wishes to give thanks to Prof. Sun Wei, Professor of The South East University, Nanjing, China, who has provided inspiration and valuable suggestions. Thanks are due to Dr. Sammy Y.N. Chan, whose inspiration and contributions have greatly influenced the author.

The author would also like to acknowledge the kind assistance received from the laboratory technicians who helped with various technical difficulties throughout the entire laboratory investigation.

Thanks are also due to Dr. Lam Lik who provided information of great importance to author's research work and for the arrangements he made for the carrying out of tests in the Concrete Laboratory. The author is particularly indebted to Mr. Lam for his very great help in keeping the author on the right track and for always being ready to discuss matters related to the thesis. Special thanks are also due to Dr. Kou S.C. for valuable discussions and his important guidance throughout the laboratory testing.

Thanks are also extended to the Research Committee of the University and the provision of facilities by the Department of Civil and Structural Engineering of the Hong Kong Polytechnic University for providing financial support for the author's Master of Philosophy program, of which this thesis is a requirement.

The author is grateful for the support and encouragement received from his parents throughout the research study. The support of God to the people named above is also acknowledged.

NOTATION

All symbols are defined where they first appear in the thesis. For convenience, the notation is defined as follows.

b	width of concrete test beam
CSH	calcium silicate hydrates
d	depth of concrete test beam
d_p	mercury intruded pore diameter
E	modulus of elasticity of concrete
E_c	modulus of elasticity of cylinder
f	flexural strength
$f_c^{'}$	compressive strength of cylinder
f_{ck}	characteristic cylinder strength
L	span of concrete test beam
m	moisture content of concrete
P	maximum total load on concrete test beam
P_{In}	intrusion pressure
R	total evaporable water percentage of a fully saturated specimen
S	span of beam
v	volume fraction of cement paste in concrete
W_d	constant weight of oven-dried specimen

W_f	total evaporable water quantity within specimen at the time of test
W_t	actual weight of specimen at the time of test
W_0	weight of the fully saturated specimen
W_i	total evaporable water quantity within fully saturated specimen
W/C	water-to-cement ratio
ΔW	difference of water loss within specimen
γ	surface tension of mercury
θ	contact angle
ϕ	volumetric moisture content of concrete
ϕ_p	volumetric moisture content of cement paste
ρ	density of dry concrete at room temperature
ρ_w	density of wet concrete

TABLE OF CONTENTS

LIST OF TABLES

LIST OF FIGURES

CHAPTER ONE INTRODUCTION

1.1 BACKGROUND TO THE STUDY

The study has been carried out is because fire remains one of the most serious potential risks to buildings and structures, and, only a limited range of relevant studies has been previously carried out, especially for high performance concrete, and knowledge gaps in this area exist. As well as steel fiber effects, the study is also intended to gain a better understanding of the effects on, and the differences in, the mechanical properties of normal strength concrete (NSC) and high performance concrete (HPC) under temperature effects, and with different moisture contents.

The initial impetus for the study of the fire resistance of concrete came from problems associated with the fire resistance of buildings. To understand the influence of elevated temperature on the mechanical properties of concrete is important for fire-resistance studies. In recent years, the use of fiber reinforced concrete, which has enhanced toughness and crack resistant properties, has become increasingly common. It is technically and economically feasible to produce reinforced concrete incorporating high strength steel fibers. As the use of fiber reinforced concrete becomes more common, the probability of its exposure to high temperatures also increases.

As a matter of fact, concrete itself is incombustible and has excellent properties in this regard [1-3] compared with other materials and can be used effectively to shield other

structural materials such as steel. The British Standard Definition for fire resistance states that the term fire resisting should not be applied to a material, but only to structural elements of which it forms a part. Nowadays, fire remains one of the most serious potential risks to buildings and structures. The extensive use of concrete as a structural material has led to a demand for further exploration of the effect of fire on concrete. With the further development and the usage of HPC, however, particular doubts about the fire resistance of HPC have emerged [4]. This will be discussed in more detail below.

1.1.1 High Performance Concrete (HPC)

Urban development has given rise to taller and more extensive buildings whose contents are of increasing commercial value and has offered an increasing risk to life at the same time. High performance concrete (HPC) has gained substantial attention globally in the last 10 years. Buildings, however, must offer some resistance to delay the destructive effects of fire to give time for escape and the use of HPC in building construction requires careful study because of the risk of spalling violently in fire producing sudden local weakening. Only a limited number of studies on the subject have been carried out so far and our knowledge of the behavior under fire of HPC is very limited.

HPC is high in both durability and strength. It is commonly used in industry nowadays due to its advantages, as it is easy to place and does not segregate during placing. It gains strength quickly enabling the formwork to be reused after a shorter time interval with cost benefit implications. It also allows the sizes of columns and shear walls to be

substantially reduced, hence increasing the available living space and allowing buildings to be significantly taller. In this research study, high performance concrete in terms of strength will be taken as a compressive strength in excess of 80 MPa.

Although many research studies have been carried out relating to the fire resistance of concrete, HPC is a relatively new type of concrete. Thus, knowledge about the performance of HPC subjected to fire is inadequate, as stated above, compared with that for normal strength concrete (NSC). Until recent years, only a small number of research studies [5,6] have been carried out on HPC subjected to fire or high temperatures. These research studies found HPC to be prone to spalling under high temperature in some cases. A possible reason might be that the dense hardened cement paste (HCP) keeps the moisture vapor from escaping under high temperatures, also as stated above. Considerable pore pressure is therefore established. In addition, a thermal incompatibility between HCP and aggregate, and between the outer and inner part of a sections of concrete is produced. Naturally, the spalling problem has cast doubts on the behavior of HPC under fire conditions. Apart from spalling, whether HPC suffers from fire damage in terms of mechanical strength to a greater degree than NSC is also very important to ensure that HPC can be used safely in buildings.

1.1.2 Steel Fiber Reinforced Concrete (SFRC)

Steel fiber reinforced concrete (SFRC) has various excellent properties as a composite material; for instance, flexural strength, tensile strength, shear strength, toughness,

impact resistance, crack resistance and resistance to frost damage are improved by the use of steel fiber. It must be realized that the main contribution of a small percentage of fibers is to increase the toughness of a fiber reinforced concrete while a large percentage of fibers can improve tensile strength of FRC. Hence, steel fiber reinforced concrete has been commonly used in industry such as for tunnel lining and road paving. Although steel fiber may not offer any obvious advantage from a fire-endurance point of view, results have shown that steel fibers can delay the occurrence of cracking [18] and hence potentially improve the performance of concrete after exposure to high temperatures. Thus, steel fiber-reinforced concrete, including steel fiber reinforced HPC and NSC, has been included in this project for investigation of its behavior under high temperature conditions.

1.1.3 High Temperature Effects on Concrete

When concrete is subjected to high temperatures, there is deterioration in its properties such as compressive strength, flexural strength, modulus of elasticity, bond with reinforcement, etc. However, one of the specific characteristics of HPC is the occurrence of explosive spalling when associated with high temperatures. When HPC is subjected to fire or very high temperature conditions, the dense hardened cement paste (HCP) keeps the water from escaping, thus causing a considerable vapor pressure to be established internally, often resulting in spalling.

1.1.4 Moisture Content Effects on Concrete under High Temperatures

It is realized that the fire resistance depends on many factors, such as the materials, their properties, shape and thickness of the structural members, high temperature conditions including the rate of heating and the maximum temperature reached, moisture content, and many other factors such as the configuration and the layout of the reinforcement. All of these may simultaneously be relevant to the likelihood or not of the occurrence of explosive thermal spalling. All in all, research [16] has shown that the three main factors that determine the fire resistance of concrete are the moisture content, the heat conductivity and the heat capacity. Among these factors, moisture content is the primary cause for explosive spalling when HPC is subjected to very high temperatures. It can be stated more generally that the moisture content is the most important factor for determining the structural behavior of concrete at higher temperatures. The higher the rate of rise in temperature and the lower the permeability of the concrete, the greater the risk to HPC of explosive spalling [16]. It is also shown later in this dissertation that the strength loss of concrete after exposure to higher temperatures is greater for initially saturated wet concrete than for initially dry concrete. This difference is due to the influence of moisture content at the time of fire testing [16].

1.1.5 Temperature Effects on Cracking

When concrete cube specimens are heated in the furnace, there is a rise in the temperature of the concrete. If this rise occurred uniformly throughout a given concrete element without any external restraint, then the element would expand uniformly throughout until the maximum temperature has been reached. Thereafter, uniform contraction would occur as the concrete cools due to the loss of heat to the ambient atmosphere. Thus, there would be no thermal stresses within the element [16].

In fact, however, the surface of concrete loses heat to the atmosphere first, and there develops a temperature difference between the cool exterior and the hot core of the concrete element, the heat not being dissipated to the outside fast enough due to the low thermal diffusivity of the concrete. As a result, the thermal contraction is unequal in the various parts of the concrete element. Restraint to the free movement results in stresses, compressive in one part of the element and tensile in the other. If the tensile stress at the surface of the element due to the restraint to contraction induced by the hotter core exceeds the tensile strength of concrete, or if the tensile strain capacity is exceeded, surface cracking will develop [16].

1.2 THE OBJECTIVES OF THIS RESEARCH WORK

The main objectives of this study are:

(1) To investigate the effects on steel fiber reinforced concrete (SFRC) of exposure to high temperatures, up to 1200 °C.

(2) To add to our knowledge of the behavior of HPC, also in relation to that of NSC, under high temperatures.

(3) To establish a relationship between its fire exposure and the mechanical properties by studying the behavior of SFRC exposed to the high temperatures that occur during a fire.

(4) To determine the effects of initial moisture content on concrete under fire (both SFRC and non-SFRC) since high temperature induces stress variations and its behavior may be affected by moisture.

The significance of this study is to provide useful input into the issue of the fire resistance rating to use for SFRC and so that a fire resistance for SFRC can be added to the rating list.

1.3 SCOPE

This study was limited to two steel fiber reinforced normal strength concretes and one steel fiber reinforced high performance concrete obtained from conventional materials and mixing methods. For the concrete mixes, ASTM type F superplasticizer was used and no silica fume or fly ash was added.

The normal strength concretes, without fibers had 28-day cube strengths of 39 and 53 MPa respectively. The high performance concrete, without fibers had a 28-day cube strength of about 99 MPa. For mixes containing steel fibers, the percentage was 1.0% in all cases.

All of the specimens were exposed to maximum high temperatures ranging from 105 °C to 1200 °C and their mechanical properties compared to those obtained are specimens of the same mix proportions maintained constantly at room temperature (25 °C). During the increase in temperature, the moisture in the unsealed specimens was allowed to escape freely. Simulations of firing tests have been carried out for three different initial moisture contents for each concrete mix. The moisture contents studied were 20, 60 and 100% respectively.

CHAPTER TWO LITERATURE REVIEW OF RESEARCH INTO THE FIRE RESISTANCE OF CONCRETE

2.1 INTRODUCTION

Limited information exists on the performance of high performance concrete (HPC), especially on steel fiber reinforced high performance concrete. In the past, a considerable number of research studies [4-7, 9, 10-12, 15, 23-25, 27, 28, 36, 45, 46] have been conducted on the fire resistance of concrete. These studies were mainly based on normal strength concrete (NSC) and high strength concrete (HSC). HPC is a relatively new type of high strength concrete, and knowledge about the performance of HPC subjected to fire is limited in comparison with that of the NSC and HSC, thus, it is important to improve our knowledge of its properties under fire.

Since the work of the research pioneers, F.C. Lea and R. Stradling [5,6], who in the 1920s investigated the factors influencing the concrete strength at high temperatures, a number of research studies which are related to the fire resistance of concrete have been carried out. Due to the various high temperature conditions and various constituent materials of concrete used, a range of explanations for the behavior of concrete subjected to high temperatures have been proposed. Initially, research paid attention to the chemical and physical changes within the concrete, such as the decomposition of calcium hydroxide ($Ca(OH)_2$), the incompatibility at the aggregate-HCP boundary and the crystal transformation of quartz (SiO_2). After 1970, the influences of different environmental

and material factors on the fire resistance of concrete were gradually investigated. Some measurements were made following the employment of thermally stable aggregates to enhance the strength of concrete subjected to high temperatures.

The actual behavior of concrete exposed to high temperatures is dependent on many simultaneously interacting factors, which include the environment to which the concrete is exposed and the constituent materials. The environmental factors include: the rate of heating; the maximum temperature attained; the duration of exposure at the maximum temperature; the method of cooling after the maximum temperature is reached; the post-cooling treatment and the level of applied load [7]. The material factors include the types of aggregates, the types of mineral admixtures and the moisture content of the concrete.

2.2 ENVIRONMENTAL FACTORS

Among the environmental factors, heating rate and maximum temperatures reached are the two main factors that have a significant influence on the concrete properties. Under certain heating conditions, the dehydration of an amorphous C-S-H phase (CaO, SiO_2 and H_2O), the thermal incompatibility between the aggregates and cement paste and the pore pressure within the cement paste are the main detrimental factors [2,8,9].

As stated earlier, fire resistance applies to the behavior of structural elements rather than to individual materials forming the elements. However, one of the major factors

determining the fire resistance of a concrete structure is the capacity of the concrete materials to insulate the embedded reinforcement, to withstand heating itself and the subsequent action of water, and to withstand cooling, without losing strength unduly and the explosive spalling characteristics.

Researchers [14] noticed that the bending modulus, when the sample is tested in the hot state, is higher than when tested in the cooled state. Dehydration and transformation reactions, changes in porosity and pore pressures, and differential deformation of hardened cement paste and aggregates that occur at high temperatures may have important effects on the strength of concrete. The results published by different investigators on the strength of concrete exposed to high temperatures have often indicated wide differences. These differences are due not only to factors such as the mix proportions and the nature of the materials used in the concrete but also to the different conditions under which the tests were carried out. Factors such as the duration of exposure at a particular temperature level and the rates of heating and cooling cause significant changes in the residual strength of heated concrete.

A recent research study [11] showed the strength loss of concrete when conventional aggregates were used. At the heating temperature of 400 °C, the strength loss of concrete was between 1% and 10% for HSC and 15% for NSC. A more severe compressive strength loss occurred mainly after heating to between 400 and 800 °C. After heating to a temperature between 400 °C to 600 °C, HSC nevertheless confirmed to show a better performance than NSC as the residual strength of HSC was higher. It was also observed

that after heating above 800°C, only about 9 to 20% of the original compressive strength were left. However, after heating to a temperature of 1200 °C, the compressive strength of concrete then slightly increased.

Other experimental results [15] indicated that for a wide variety of ordinary concrete mixes made with conventional aggregates, there was a reduction in strength after heating to 500 °C from a minimum of 15% to a maximum of 60%. Results [15] also indicated that there is an approximately linear reduction in the strength ratios as the temperature increases from 200 to 500 °C. The result [15], at higher temperatures, indicated that at 600 °C, the residual compressive strength ratios vary between about 80 and 25%. At 700 °C, the ratios vary between 70 and 20%. At 800 ^{0}C, the ratios vary between 50 and 20% of the initial unheated compressive strength.

Other investigations [30] were carried out in Norway where different types of concretes were exposed to hydrocarbon fire where the temperature reached almost 1100 °C (2000 °F) in 30 minutes. The strength of the elements ranged between 40 and 80 MPa (5,800 and 11,600 psi). Test results showed that spalling and damage occurred earlier than expected and that increasing the moisture content of the hardened concrete increased the severity of the effects.

2.3 MATERIAL FACTORS

The type of aggregate influences the response of concrete to high temperature. Abrams [17] confirmed that siliceous aggregate concrete loses a greater proportion of its strength at temperatures above about 430 °C (810 °F) when compared with concretes made with limestone or lightweight aggregates. Once the temperature has reached some 800 °C (1470 °F), the difference disappears. For practical purposes, about 600 °C (1100 °F) can be considered as the limiting temperature for structural integrity of concrete made with Portland cement; at higher temperatures, refractory concrete has to be used [16].

With all aggregates, the percentage loss of strength was found to be independent of the original level of strength but the sequence of heating and loading influences the residual strength. Specifically, concrete heated under load retains the highest proportion of its strength, whereas heating unloaded specimens leads to the lowest strength of the subsequently cooled concrete. Application of load while the concrete is still hot leads to intermediate values [16].

Concretes made with siliceous or limestone aggregate show a change in color with temperature. The color change is dependent on the presence of certain compounds of iron; however, there is some difference in the response of different concrete [16].

2.4 EFFECTS OF STEEL FIBERS IN CONCRETE

Swamy [41] confirmed that fibers have little effect on increasing compressive strength in concrete. However, including fibers in concrete can increase ductility in a compressive failure. The major benefits of steel fiber reinforced concrete have often been used on the resistance of the concrete to cracking and there is no doubt that steel fibers can delay the occurrence of cracking due to its strong bond strength [18].

In refractory applications, many researchers [31-34] agreed that refractory concretes reinforced with stainless steel fibers have good performance at temperatures up to 1500 °C. The properties required are resistance to large crack formation, spalling and abrasion, resistance to impulsive loads, and increased flexural strength. Materials properties have been measured by Nishioka *et al.* [34] on refractory castables after exposure to temperatures up to 1200 °C. Improvements in flexural strength and energy absorption were observed at steel fiber concentrations between 5 per cent and 10 per cent by weight whereas compressive strength was not affected [18].

Thus it seems that fiber reinforced concrete has better resistance to high temperatures than plain concrete because fibers delay the occurrence of cracking. In considering the behavior and strength of steel fiber reinforced concrete exposed to fire, the major variables taken into consideration are the type of steel fiber used, the fiber content, the temperature of exposure and the duration.

A research report presented by M.M. Kamal, H.H. Bahnasawy and F.E. Ei-Refai [22] concluded that exposure to fire has a destructive effect on concrete and consequently a reduction in the mechanical properties which increase with the increase of the temperature of exposure and the fire duration. It was reported that the inclusion of steel fibers in the concrete mix led to an increase in mechanical properties; the higher the fiber content in a concrete mix, the higher the resistance to the fire destructive effect. However, for a fiber content higher than 1.5% by volume of concrete, the improvement in mechanical properties may be insignificant or reduced. It was found that the reduction in mechanical properties of plain concrete due to exposure to high temperature is higher than concrete specimens incorporated with fibers. A distinct loss in mechanical properties was reported after heating to 600 °C. The reduction in mechanical properties was further increased with the increase of the exposure duration. The report showed that steel fiber reinforced concrete (SFRC) beams exhibited higher flexural rigidity, initial cracking loads and ultimate loads than those without steel fibers. The appearance of hair cracks with discoloring of concrete surfaces after exposure to fire before loading was reported. It was found that the color of concrete darkened after exposure to a temperature of 400 °C for 4 and 6 hours duration time. Non-SFRC exhibited a larger number of cracks with greater widths than SFRC. These phenomena increased with the increase of the exposure duration to fire. A network of hair cracks was also reported at 600 °C.

Another similar experiment conducted by the same group of researchers on fiber reinforced concrete beams also showed that there was a loss in the mechanical properties [22]. The range of loss depends on the time of exposure to high temperature and the

cooling condition of concrete specimens. The results showed that in the temperature range of 25 to 400 °C, the loss in strength decreased slightly. At temperatures between 400 and 600 °C, the strengths of concrete dropped sharply and reached their lower limits. These investigators further concluded that fiber reinforced concrete has better performance in resisting high temperature than plain concrete.

Similar conclusions were drawn from an experiment carried out by M. R. Resheidat and M. S. Ghanma [35]. According to the experimental results, it was concluded that the compressive strength of concrete is highly influenced when it is subjected to elevated temperatures. Loss in concrete strength is proportional with the increase of temperature values. The loss of concrete strength increases with the increase of duration of heat.

2.5 FIBER LENGTH AND L/D RATIO

The selection of steel fiber is important since the fiber type influences the flexural strength of SFRC [22]. The length / diameter ratio has a crucial influence on the volume of fibers. Long thin fibers of *l/d* greater than 100 have a tendency to interlock in some fashion to form a mat, or a type of bird's nest from which it is very difficult to dislodge them by vibration alone. Short stubby fibers of *l/d* less than 50 are not able to interlock and can easily be dispersed by vibration. Research done by Johnston, Swamy, Lankard and Edgington [18] on flexural strength of fiber reinforced concrete showed that steel fiber improves the flexural strength of reinforced concrete. This investigation also

showed that the flexural strength can be further increased if the volume fraction and the *l/d* ratio of fibers are both increased. The use of steel fiber on improving the compressive strength of concrete is relatively small although steel fiber can provide a better ductility in a compression failure.

2.6 MOISTURE CONTENT

Experimental results reported on moisture condition of concrete influence on strength are very limited. Investigations reported by several researchers [40] on effects of moisture changes on flexural and fatigue strength of concrete stated that a beam specimen tested in a dry condition exhibited a lower modulus of rupture than a similar specimen tested in a wet condition. This effect is due to the tensile stresses induced by restrained shrinkage prior to the application of the load and induces tension in the extreme fiber. The magnitude of the apparent loss of strength depends on the rate at which moisture evaporates from the surface of the specimen.

S. Popovics [37] reported that for compression test, a cube specimen tested in a dry condition leads to a higher strength. A quantitative result which reported by W. S. Butcher [38] on 34 MPa (5000 psi) concrete cube specimens exhibited an increase in compressive strength up to 10 per cent on thorough drying. The behavior of loss in strength for concrete specimens when tested in a wet condition, it is suggested by R. H.

Mills [39] is due to the dilation of cement gel by absorbed water and hence decreasing the forces of cohesion between the solid particles.

T. Z. Harmathy [23] reported an investigation showing that the maximum amount of moisture that can be held by a porous material, say at 100 per cent relative humidity, is determined by the volume fraction of interconnected pores in the material, in other words, by porosity. The estimation of moisture content of concrete was given by:

$$\phi \approx v\phi_p$$

where ϕ is the volumetric moisture content of concrete, ft^3/ft^3; v is the volume fraction of cement paste in concrete, ft^3/ft^3; ϕ_p is the volumetric moisture content of cement paste. The fire endurance of concrete directly depends on ϕ. ϕ can be calculated from moisture content, conventionally expressed as weight fraction, m, as

$$\phi = m\frac{\rho}{\rho_w}$$

where m is usually determined by measuring the weight loss of concrete on sufficiently long heating at 105 °C (221 °F). T. Z. Harmathy also concluded that the thermal fire endurance of concrete is determined by the thermal properties of the material and the moisture content.

2.7 STATIC MODULUS OF ELASTICITY

The deflection of structures is directly affected by the modulus of elasticity of concrete, and this modulus is strongly affected by temperature. However, when water is expelled from concrete, there is a progressive decrease in the modulus of elasticity after heating concrete to between 50 and 800 °C (120 and 1470 °F) [16]. The extent of the decrease in the modulus depends on the aggregate used, but a generalization on this subject is difficult. However, the variation of strength and of modulus with temperature is of the same form. In fact, the modulus of elasticity of concrete is highly dependent on the properties and the proportions of coarse aggregate.

Edgington *et al.* (1974) investigated the modulus of elasticity of concrete and confirmed that it is largely controlled by the volume and modulus of the aggregate. Small additions of steel fiber would not be expected to greatly alter the modulus of the composite. Experimental results [18] indicated that the compressive stress-strain measurements on plain and fiber reinforced 10 mm concrete showed similar increases in modulus, the values in tension and compression being essentially equal.

The behavior of structures is often dependent on the modulus of elasticity of the concrete, and this modulus is strongly affected by temperature. Research studies [24, 25] of the influence of temperature on modulus of elasticity of concrete indicated that the loss in static modulus of elasticity of concrete increases with the increase of heating temperature.

K. W. Nasser and A. M. Neville [26] presented experimental results on mass-cured concrete, there is no difference in modulus in the range of 21 to 96 °C (70 to 205 °F). K. W. Nasser and M. Chakraborty [27] also reported that the modulus of elasticity is reduced after heating to temperatures in excess of 121 °C (250 °F).

U. -M. Jumppanen and J. C. Maréchal [25, 28] reported that when water can be expelled from concrete, there is a progressive decrease in the modulus of elasticity between about 50 and 800 °C (120 and 1470 °F). The extent of the decrease in the modulus depends on the aggregate used, but a generalization on this subject is difficult. In fact, the variation of strength and of modulus with temperature are similar to each other.

2.8 POISSON'S RATIO

Experimental data on the values of Poisson's ratio for high strength concrete are very limited. A report [16] stated that based on available information, Poisson's ratio of concrete lies generally in the range of 0.15 to 0.22 when determined from strain measurements under a compressive load.

2.9 DETERMINATION OF CONCRETE MIX PROPORTIONS

The design of high performance concrete mixtures is more complicated than that of the normal strength concrete mixtures. The complication is mainly due to the consideration of more parameters, such as the content of mineral admixtures and the dosage of chemical admixtures. Many researchers [55-59] have proposed different methods to optimize the proportions of the materials that need to produce high performance concrete.

In the past two decades, researchers and engineers [55-59] consolidated their experience in using high strength concrete where they developed their own mix design method for proportioning high strength concrete. By modifying the mix design method for normal strength concrete, a new design method for high strength concrete up to Grade 60 was developed in 1974 [55]. A researcher [56] proposed to fix the total binder content and the fine to coarse aggregate ratio. It was assumed that the concrete strength was controlled by the quality of the binder. De Larrard, F. [57] suggested to use low binder paste content but with high content of superplasticizer to produce high strength concrete. A statistical method was also proposed to minimize the number of trials and to optimize the mix proportion of high strength concrete [58]. Two other researchers, Gutierrez and Canovas [59] proposed empirical mathematical models and derivations based on large series of studies to determine the proportion of high strength concrete mixture.

In American method of selection of mix proportions, the ACI Standard Practice ACI 211.1-91 [47] describes a method of selection of mix proportions of concrete containing Portland cement, cementitious materials and admixtures.

The British method of mix design [48] that is similar to the ACI approach. The British method is based on the experience of British materials so that the results may not be applicable in other parts of the world.

A generalized systematic approach to the selection of mix proportions of high performance concrete has not yet been developed, however, some useful guidance for the mix selection of high performance concrete can be obtained from ACI 211.4R-93 [49]. As a result, the mix design method and selection for high performance concrete can only be achieved by experimental trials.

CHAPTER THREE EXPERIMENTAL DETAILS

3.1 THE SCOPE OF THE TESTING PROGRAM

In this research study, all of the concrete specimens were tested at The Hong Kong Polytechnic University. A total number of eight hundred and fifty two concrete specimens were cast. The concrete specimens were cured for 28 days and then heated at that age of 28 days.

A total number of 666 specimens, including 486 cubes, 72 cylinders and 108 beams, were tested in the furnaces of the Concrete Laboratory, The Hong Kong Polytechnic University. The maximum exposure temperatures for the different specimens were 105, 200, 300, 400, 600, 800, 1000, 1100 and 1200 °C and the duration of exposure at the maximum value was maintained for one hour. All specimens were stored in a laboratory at a temperature of 25±3 °C. Two hundred and twenty two groups (162 groups of cubes, 36 groups of beams and 24 groups of cylinders), of three specimens per group, with different moisture contents of 20, 60 and 100 per cent were exposed to each maximum temperature level and cooled to room temperature before testing. Each batch also included 3 cube specimens that were normally cured to form a reference to the ultimate compressive strength of unheated concrete. All concrete cube specimens were subjected to a compressive test, beam specimens to a flexural test and cylinder specimens to an elastic modulus test. These mechanical properties, for the heated specimens, were

compared with the unheated reference concrete that had been stored and tested at room temperature, in order to establish the effect of heating on strength and elasticity loss. The program showing scope of the tests is shown in Table 3-1 and Table 3-2 below.

Table 3-1. Testing Program for the Determination of Mechanical Properties of Concrete Specimens at Three Initial Moisture Contents and Subjected to a Wide Range of Maximum Heating Temperatures.

Maximum Heating Temperatures	Six Concrete Mixes that were Tested for Mechanical Properties																	
	Non-SFRC									SFRC								
	NSC M-1			NSC M-2			HPC M-3			NSC M-1F			NSC M-2F			HPC M-3F		
(Degree Celsius)	C	E	F	C	E	F	C	E	F	C	E	F	C	E	F	C	E	F
25°C	x	x	x	x	--	x	x	x	x	x	x	x	x	--	x	x	x	x
105°C	xyz	x	x	xyz	--	x	xyz	x	x	xyz	x	x	xyz	--	x	xyz	x	x
200°C	xyz	--	x	xyz	--	x	xyz	--	x	xyz	--	x	xyz	--	x	xyz	--	x
300°C	xyz	x	x	xyz	--	x	xyz	x	x	xyz	x	x	xyz	--	x	xyz	x	x
400°C	xyz	--	--	xyz	--	x	xyz	--	--	xyz	--	--	xyz	--	--	xyz	--	--
600°C	xyz	x	x	xyz	--	x	xyz	x	x	xyz	x	x	xyz	--	x	xyz	x	x
800°C	xyz	x	x	xyz	--	x	xyz	x	x	xyz	x	x	xyz	--	x	xyz	x	x
1000°C	xyz	--	x	xyz	--	x	xyz	--	x	xyz	--	x	xyz	--	x	xyz	--	x
1100°C	xyz	x	x	xyz	--	x	xyz	x	x	xyz	x	x	xyz	--	x	xyz	x	x
1200°C	xyz	x	--	xyz	--	--	xyz	x	--	xyz	x	--	xyz	--	--	xyz	x	--

Note: All Concrete Specimens are subjected to 28 days of Water Curing prior to Testing.

Symbols: C = Compression; E = Modulus of Elasticity; F = Flexure

Moisture Contents: x = 100%; y = 60%; z = 20%

Table 3-2. Scope of Testing Program

Program A: Control Specimens (Not Heated)

Types of Concrete Specimens	Total number of mixes	Mixes	7 days strength	14 days strength	28 days Strength	Total number of samples required
			Number of Samples Required for each case			
Cubes	6	M-1, M-2, M-3, M-1F, M-2F, M-3F	3	3	3	***54***
Beams	4	M-1, M-3, M-1F, M-3F	3	3	3	***36***
Cylinders	4	M-1, M-3, M-1F, M-3F	--	--	3	***12***
						102

Program B: Heated Specimens

Types of Concrete Specimens	Total number of mixes	Mixes	Number of initial moisture for each mix	Number of max. heating temperatures for each mix and moisture	Number of Samples required for each case	Total number of Samples required	Number of not heated control specimens needed	Number of molds available	Number of batches required
Cubes	6	M-1, M-2, M-3 M-1F, M-2F, M-3F	3	9	3	***486***	***36***	48	12
Beams	4	M-1, M-3, M-1F, M-3F	1	9	3	***108***	***24***	15	8
Cylinders	4	M-1, M-3, M-1F, M-3F	1	6	3	***72***	***24***	12	8
						666	***84***		

Total number of samples prepared = **852**

3.2 MATERIALS USED

All the materials used in this research study are conventionally available in Hong Kong.

3.2.1 Cement

In this research study, the Ordinary Portland cement (OPC) used was 'Green Island' cement that is equivalent to ASTM Type I. The use of OPC was in compliance with the limits of the British Standard BS 12:1996 and with a strength class of 52.5N. Its physical properties and chemical composition are given in Table 3-3:

Table 3-3. Properties of Cement

Chemical Composition (% by weight)	
CaO	66.9
SiO_2	22
Al_2O_3	5.7
Fe_2O_3	3.3
MgO	1
SO_3	2.5
Na_2O (Sodium oxide)	0.47
Bogue Compound Composition (%)	
C_3S	54.9
C_2S	21.7
C_3A	9.5
C_4AF	10
Physical Properties	
Fineness (m^2/kg)	335
Specific Gravity	3.17
Standard Consistency (%)	31
Setting (minutes)	
Initial	80
Final	125
Soundness (mm)	0.1
Compressive Strength (N/mm^2)	
2 days	22.7
7 days	40.7
28 days	58.9

3.2.2 Aggregates

The coarse and fine aggregates used were of crushed granite and river sand of zone F grading complying with BS 882:1992. The two coarse aggregates were of nominal sizes 20 mm and 10 mm. Their gradings and properties are shown in Table 3-4 and Table 3-5. Their sieve analysis plots are shown in Fig.3-1, 3-2 and 3-3 in Appendix VIII.

Table 3-4. Gradings of Aggregates

	Percentage Passing		
BS Sieve Size (mm)	20mm single sized crush granite	10mm single sized crush granite	River Sand (Zone F)
37.5	100		
20	95.1	100	
10	21.01	93.53	100
5	4.54	21.67	100
2.36		4.88	96.76
1.18			87.76
0.6			70.66
0.3			26.2
0.15			1.18
Pan	0.03	0.04	0

Table 3-5. Specific gravity, water absorption, and fineness modulus of aggregates

	20mm single sized crush granite	10mm single sized crush granite	River Sand (Zone F)
Specific gravity (Saturated Surface Dried)	2.64	2.63	2.63
24hr. Water absorption (% by weight)	0.6	0.7	1.1
Fineness Modulus	--	--	2.4

3.2.3 Superplasticizer

The superplasticizer used in this research study is a high range water reducer formulated to provide improved slump retention characteristics. It is an aqueous solution of naphthalene sulfonate and other components, which in combination react to greatly enhance performance in workability. It is also an essential constituent in the production of high strength concrete.

In this study, the amount of superplasticizer which has been added to concrete in order to achieve the specified workability was determined by slump tests complying with BS 1881: Part 102: 1983. Slump values between 57 and 150 mm were recorded for concrete mixes and slumps have been successfully maintained at their normal conditions. The Daracem 100 superplasticizer was selected, which is commercially available and is in the form of an aqueous solution dark brown in appearance. This superplasticizer is Naphthalene based, it contains no added chlorides and is formulated to comply with specifications for Chemical Admixtures for Concrete, BS 5075 Part 3: 1985 and ASTM Designation: C494 as a Type F or a Type G Admixture. Its specific gravity is approximately 1.20 and the solid content is 40%. Details of its properties are listed below in Table 3-6.

Table 3-6. Technical Data for Superplasticizer (sulphonated naphthalene formaldehyde condensates)

Standard (type)	British Cement Association Classification	Appearance	Specific Gravity	Solid Content (%)
ASTM C494 (A, F)	B	Dark brown solution	1.2	40

3.2.3.1 Effects of Superplasticizer

Superplasticizer is an essential constituent in the production of high strength concrete. It helps to improve the initial low workability caused by the low free water content. However, in the existing British Method [48], there is no guideline for the use of superplasticizer.

In normal strength concrete, no matter which types of superplasticizer are used to acquire adequate workability, there is an optimum dosage level, beyond which, the effectiveness of superplasticizer in reducing the water content is diminished [50]. This phenomenon appeared also in the case of high performance concrete mixtures. It is necessary to make tests on a trial concrete mix because only such tests give reliable data on slump loss and strength gain.

3.2.4 Steel Fiber

In this research study, Dramix cold drawn stainless steel fiber of 25-mm length and 0.40 mm diameter with aspect ratio (l/d) 62.5 was used for the concrete reinforcement. This

type of steel fiber has hooked ends; bright coating; a standard tensile strength (≤1700 N/mm^2); a melting temperature of 1538 °C; a density of 7.87g/cm^3 and is loose in form at delivery.

3.3 PREPARATION OF CONCRETE AND TEST SPECIMENS

3.3.1 Concrete Mix Proportioning

The study has been performed on 6 mixtures: 3 non-steel fiber reinforced concrete M-1, M-2 and M-3; 3 steel fiber reinforced concrete M-1F, M-2F and M-3F. M-3 is a high performance concrete whereas M-1 and M-2 are normal strength concretes. These three mixes were chosen because it was intended to compare NSC with HPC under high temperature effects. The proportion of steel fiber added to each of the concrete mixes was 1.0% of concrete volume (see mix proportion). The mix proportion, the relative 28-day compressive strength results of concrete and their scatters are summarized in Table 3-7.

Table 3-7. Concrete Mix Proportions by Weight and their Relative Compressive Strengths

Cement	Aggregate		Sand	Water	W/C ratio	Without Steel Fiber		With Steel Fiber (1% of concrete volume)	
	20mm	10mm					Compressive Strength at Age of 28 Days		Compressive strength at Age of 28 Days
(kg/m3)	(kg/m3)	(kg/m3)	(kg/m3)	(kg/m3)	(kg/m3)		(MPa)		(MPa)
311	780	390	665	205	0.66	M-1	39	M-1F	45
366	771	385	623	205	0.56	M-2	53	M-2F	60
458	938	469	408	147	0.32	M-3	99	M-3F	110

Note: Values reported are average of 10 tests (See Table A-A in Appendix)

3.3.2 Determination of Concrete Mix Proportions

3.3.2.1 Introduction

The general principle of designing a concrete mixture is to proportion cement, aggregate, water, and admixtures appropriately to produce a concrete with sufficient workability in the fresh state, and with the required mechanical and durability properties in the hardened state.

Grade 40 concrete was normally the highest strength commercially produced in Hong Kong until the end of the 1980s. This was changed in the early 90s when Grade 60 concrete was first used for the construction of the 378m high Central Plaza. However, with the increasing demand for taller buildings, longer span bridges/beams and higher space/structure efficiency, high strength concrete, defined as Grade 60 or above, became an important construction material. In the late 90s, Grade 100 concrete was used in several major projects such as Tai Koo Sing Phase I Redevelopment and Hong Kong Electric Headquarters Redevelopment. Concrete with a 28-day compressive strength of 160 MPa and with a slump retention of over 1.5 hours has also been developed, using conventional local materials, casting and curing methods. Today, in research laboratories, concrete strengths of 800 MPa are being produced. One major remarkable quality is the virtual elimination of voids in the concrete matrix which are mainly the cause of the ills that generate deterioration.

3.3.2.2 Mix Proportioning Method

A systematic mix design method for proportioning a high strength concrete mixture was developed by several researchers [51]. This method is a modification of the existing mix proportioning method for normal strength concrete. The "Design of Normal Concrete Mixes" is abbreviated in the D.O.E manual [48]. This Method is described in the Appendix IV with a mix design example for normal concrete of 30 MPa as shown in Appendix V.

The plot of the compressive strength against w/c ratio is given in Figure 3-4 in Appendix VIII and it is superimposed on the relationship between the compressive strength and w/c ratio from the existing D.O.E manual.

3.3.3 Concrete Mix and Preparation

The preparation of concrete specimens followed the recommendations stipulated in BS 12:1991, BS 1881:Part 108: 1985, and BS 1881: Part 110: 1983, respectively. With aggregates whose maximum size is up to 20-mm, the use of 100-mm cubes and 100 by 200-mm cylinders are recommended [16].

Concrete mixes were prepared using a horizontal pan mixer with a nominal capacity of $0.05m^3$. Aggregates were firstly mixed with one third of mixing water for 2 minutes

followed by the addition of the remaining mixing water. Superplasticizer was added 2 minutes later to attain an initial slump of greater than 120 mm and the mixing process then continued for a further 2 minutes.

The freshly mixed concrete was tested for slump and was re-mixed in the mixer to maintain the homogeneity before casting the specimens for the determination of hardened concrete properties. In casting the steel fiber reinforced concrete (SFRC) specimens, the fresh SFRC mixtures were allowed to mix for a further 10 minutes, to ensure steel fibers were mixed thoroughly in the concrete, after carrying out the slump test prior to casting specimens.

The 100 mm cube molds were clamped firmly to an electrically driven steel-vibrating table. The molds were cleaned and oiled by spraying mold oil on the interior surfaces of the mold and wiped evenly with a cloth. Fresh concrete was then transferred from the concrete mixer with a scoop. The fresh concrete was then placed in the mold in layers of approximately 50 mm in depth and each layer was compacted on the vibrating table. After the top layer had been compacted, it was leveled to the top of the mold with a steel float. The molds were transferred to a horizontal surface, which was free of vibration and covered with a polythene sheet in order to prevent the fresh concrete incurring an excessive loss of moisture content. The hardened fresh concrete cubes were taken out from the mold and labeled after a further 24 hours. Concrete cube specimens were then immediately placed in a water curing tank with the water temperature maintained at

27±3°C for the water curing procedure which was carried out in accordance with Section 10 of CS 1:1990.

3.3.3.1 Mixing Sequence for Concrete

According to British Standard, BS 5075: Part 3: 1985, it is stipulated that superplasticizer is dispersed in the second addition of mixing water. However, the delay in addition of superplasticizer reduced the requirement for superplasticizer for a given workability [52, 53]. Two minutes mixing starting from the time when cement first came in contact with the water is adequate for allowing the hydration of C_3A to ettringite so that the adsorption of superplasticizer on the aluminate phase was significantly reduced [54]. The mixing sequence was in accordance with British Standard, BS 1881: Part 125:1986, and BS 5075: Part 3: 1985 with minor modification. The procedure of concrete mixing is described in Section 3.3.3 and need not be repeated.

3.3.4 Compressive Strength Development in the 28 Days Curing Period

The compressive strength development for the concrete mixes during the progress of water curing was recorded at 1 day, 3 days, 7 days, 14 days and 28 days. The compressive strength results are shown in Figure 3-5 in Appendix VIII.

After 28 days of water curing, specimens were taken from the water-curing tank and sent to the compression test machine for their 28-day compressive strength determination. The compression test was carried out in accordance with BS 1881: Part 116: 1996. The specimens were tested with a calibrated 3000 kN capacity hydraulic testing machine at a loading rate of 200 kN/min. until failure occurred.

3.3.5 Moisture Condition of Concrete

The cube specimens were taken from the water-curing tank at 28 days. They were then transferred to a furnace with a temperature of 105 °C (221 °F) and weighed intermittently until their weights were compatible with their designed moisture contents. Once the desired weights were reached, the specimens were sealed immediately with polyethylene film. Trials, not reported here, proved that the specimens which were sealed with polyethylene film succeeded in keeping their moisture contents for a couple of days until the fire test was carried out.

3.4 TESTING AND INSTRUMENTATION

3.4.1 Slump Test

The slump test equipment was standard and included a slump cone, a steel rod, a measuring meter and a steel platform.

3.4.2 High Temperature Test

A series of simulated fire tests were carried out using a Nabertherm electric furnace as shown in Fig. 3-6 in Appendix I. The electric furnace was built with sand bricks and covered on the inside with thermal bricks. It has a vent in the roof. The heating temperature is controlled by an electronic panel. For this electric furnace, the maximum

operating temperature is 1600 °C. Polyethylene film has been used throughout this research study for sealing the 100 mm concrete cube specimens and film are removed from concrete specimens just before the fire test.

3.4.3 Compressive Strength Test

The compressive strength of the concrete cube specimens were measured with a Samuel Denison compression material test machine with a load capacity of 3,000 kN, as shown in Figure 3-7 in Appendix I. The loading rate ranges from 0.2 to 0.4 N/mm^2 sec. in this machine but a constant rate of 0.3 N/mm^2 sec. was used for all tests in this research study.

3.4.4 Flexural Strength Test

The flexural strengths of the concrete beam specimens were also determined with the Denison compression machine with a load capacity of 3,000 kN, as shown in Figure 3-11 in Appendix VII. A constant loading rate of 0.3 MPa per second was used for the flexural strength test in this research study.

3.4.5 Static Modulus of Elasticity Test

The static modulus of elasticity test was conducted using the Samuel Denison compression machine and according to BS 1881:Part 121:1983. In this test, concrete cylinders were loaded via a load cell with a maximum load capacity of 1,000 kN. The load cell is connected to a data logger and hence the loading force could be accurately determined. The specimens were also instrumented with strain gauges to allow strains to be also measured as the load was applied. The load cycling and the equipment arrangement of the test are shown in figure 3-8 in Appendix and figure 3-9 below respectively.

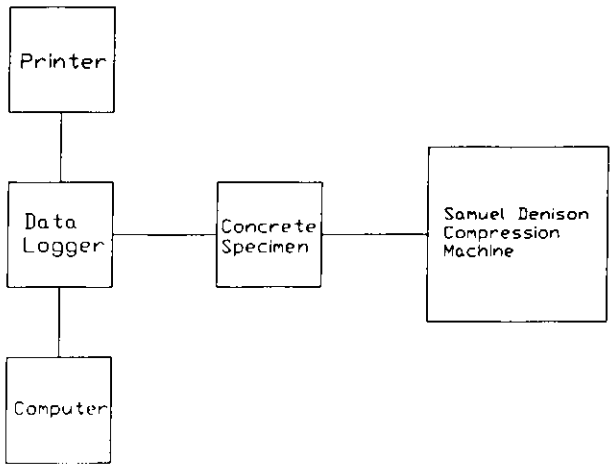

Fig. 3-9 Arrangement for Static Modulus of Elasticity Test.

3.4.6 Mercury Intrusion Porosimetry (MIP)

The MIP test was carried out using a Pore Sizer 9320 mercury intrusion porosimeter with a maximum mercury intrusion pressure of 210 MPa which enables penetration into pores with diameters ranging from approximately 360 μm to 6 nm.

3.5 TESTING METHODS AND PROCEDURES

3.5.1 Workability Retention

Concrete slump values were measured in accordance with BS 1881: part 102: 1983. During the workability retention study, the slump of the fresh concrete was measured periodically. The fresh concrete was moved back into the pan mixer after each slump test and re-agitated in the mixer for a further 15 seconds to ensure homogeneity before each measurement.

3.5.2 Moisture Content Test

The moisture content of hardened concrete is an important parameter that affects the measured compressive strength of concrete at elevated temperatures. Tests have been carried out for three different moisture contents for each concrete mix. The effect on strength was studied for three moisture contents of 20, 60 and 100 per cent.

Three representative concrete cube specimens from each mix batch were chosen after their 28 days of water curing. Their weights and densities were measured and recorded under a saturated surface-dry condition (SSD). Concrete cubes were then placed in a furnace and dried at a temperature of 105 °C (221 °F) until they reached constant weights, and hence the value of total loss of internal evaporable water content was obtained for each one. The constant dried weights of the concrete specimen representatives were used for the determination of the moisture content of other concrete specimens as to be described in section 3.5.3.

3.5.3 Determination of Moisture Content

3.5.3.1 Introduction

The moisture contents at the time of application of loading influences the compressive strength of concrete. Testing concrete in a dry condition, for example, leads to a higher strength [20]. For this reason, the moisture effect on the measured strength of concrete should be taken into account. For concrete beam specimens, it was also found there is an increase in strength if the test specimen is small and drying takes place very slowly, so that the internal stresses can be redistributed and alleviated by creep. However, wetting a completely dry specimen prior to testing causes a reduction in strength [21].

The behavior of concrete specimens described above accords with the suggestion [43] that the strength loss in wetting of a compression test specimen is due to the dilation of

cement gel by absorbed water and the forces of cohesion of the solid particles are then decreased. A quantitative report [44] on 34 MPa concrete, which has been dried thoroughly, showed an increase in compressive strength up to 10 per cent. However, the increase in strength is less than 5 per cent if the drying period is less than 6 hours.

3.5.3.2 Moisture Content Determination Method and Procedures

A moisture content determination method [45] is shown in Appendix VI. The moisture content determination followed the procedures described in section 3.3.5. When the concrete specimen has been dried to a constant weight (i.e. no more moisture can be driven off) using Equation (6), the total evaporable water percentage of a fully saturated specimen, R, is determined. Once the total evaporable water percentage of concrete, R, is obtained, W_t can be determined from Equation (9). When the W_t value is obtained, a number of concrete cube specimens at 28 days were transferred from a water-curing tank to a furnace at a temperature of 105 °C (221 °F) for drying. Once the desired weights, W_t, of the concrete specimens were reached, the specimens were sealed immediately with polyethylene film. In this research study, the moisture content of all concrete cube specimens was controlled within ±5% of the target.

3.5.4 Elevated Temperature Test

The simulated fire test has been carried out using the 100-mm cube specimens with the specified moisture contents values heated in an electrical furnace. After the polyethylene

film sealing was removed (see section 3.3.5), specimens with their designated moisture content values were immediately put into the electric furnace to be heated. The concrete cube test specimens were placed evenly and heated in the electric furnace. The maximum temperature reached was maintained for one hour. The time-temperature curve of the furnace complied with the standard curve recommended in BS476:Part20:1987 as shown in Figure 3-10.

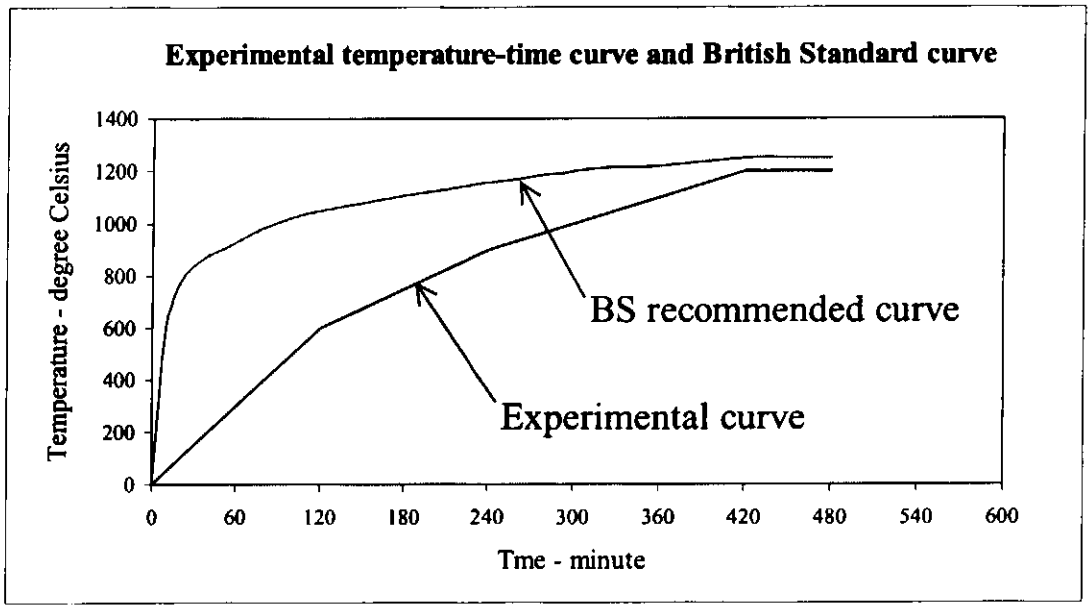

Fig. 3-10 Experimental and BS recommended temperature-time curves.

In this research study, this elevated temperature test was repeated for nine different designated maximum temperatures: 105, 200, 300, 400, 600, 800, 1000, 1100 and 1200 °C. It must be realized that, for the heating rate, the experimental curve is slower than the BS recommended one due to the limitation of the equipment provided. It is not likely that the relative temperature effects would bear exactly the same absolute ratios if the BS curve had been used, but in qualitative terms, it is not thought that the different

rate of heating would affect the trends. In both cases, the concrete would have been held for one hour at the constant maximum temperature anyway.

3.5.5 Compressive Strength Test

The compressive strength test was carried out using the 'unstressed residual' method [15], in which the unloaded specimen is heated to the required peak temperature and maintained for one hour, and then allowed to cool slowly to room temperature. The ultimate compressive strengths were determined by loading to failure in compression when the concrete specimens were cool enough to handle. In this study, the compression load was applied at the rate of 200 kN/min.

3.5.6 Flexural Strength Test

The flexural strength test is also known as the modulus of rupture test. In this test, a concrete beam is subjected to flexure using symmetrical four-point loading until failure occurs as illustrated in Fig. 3-11 in Appendix VII.

Flexural strength tests have been carried out according to the British Standard BS 1881:Part 118:1983. Beams with dimension 100 by 100 mm (4 by 4 in.) supported over a span of 300 mm (12 in.) were used. The load was applied as two equal point loads so as to ensure a constant bending moment over the central 100 mm of the beam at the rate of 6kN/min until the beams failed in tension at their undersides.

3.5.7 Static Modulus of Elasticity

The static modulus of elasticity test was carried out according to the British Standard BS 1881:Part 121:1983. The preparation of the test specimens is very time consuming and extra caution is needed. Concrete cylinders with dimensions 100 mm in diameter by 200 mm in length were used in this test. When tested in compression, the top surface of the test cylinder is brought into contact with the platen of the testing machine and, because this surface is not obtained by casting against a machined plate but finished by means of a float, stress concentrations are introduced and the apparent strength of the concrete is thus reduced. Convex end surfaces cause a greater reduction than concave ones as they generally lead to higher stress concentrations. The reduction in the measured loss in strength is particularly high in high strength concrete [29]. For this reason, concrete test cylinders were initially ground smooth both on the top and bottom contact surfaces using a grinding machine [16, 63]. The level of the ground surfaces were then examined by a leveling meter. The surfaces where strain gages were attached were sandpapered and cleaned with alcohol. Thereafter, the pores were filled with epoxy and allowed to dry. Strain gauges were then glued on the marked vertical and horizontal axis of the cylindrical specimens with the P-2 adhesive. The glued strain gauges were set aside to allow the adhesive to dry before being connected to the electrical wires. The strain gauges used were models PL-60-11 and PFL-30-11 manufactured by Tokyo Sokki Kenkyujo Co., Ltd. The specifications for the strain gauges used are shown in Appendix II.

At this stage, the test specimens are ready to connect to a Kyowa UCAN-10B data logger, which is connected to the compression-testing machine. Both the top and bottom of the ground surfaces of the concrete cylinders were loaded via a load cell and set in the centerline of the compression machine. Once the compression has started, the strain gauges will transmit data to the data logger. Data is then taken by the data logger and the modulus of elasticity is determined from a straight-line plot.

According to the British Standard BS 1881:Part 121:1983, it is suggested that the compressive strength of the concrete on three companion specimens should be tested in a moist condition. The specimens should be obtained from the same batch as those to be used for the determination of the static modulus of elasticity. The specimens are required to be made and cured under conditions, similar to that of compression test specimens carried out in accordance with BS 1881: Part 116. The mean value of the compressive strength, f_c, is used to determine the maximum stress to be applied in the determination of static modulus of elasticity.

The test specimen was placed centrally in the compression machine, a basic stress (σ_b) of 0.5 N/mm^2 was applied and the strain gauge readings was taken at each load stage. A load was applied in uniform increments, each time at a constant rate of 0.6 ± 0.4 N/(mm^2•s) until the stress was equal to one-third of the compressive strength of the concrete ($\sigma_a = f_c/3$). Loading was stopped for 60 seconds at each load increment to allow strain and load readings to be taken.

Figure 3-8 in Appendix III illustrated a load cycling of the test. Two pre-loading cycles were carried out by applying load to, and then unloading, the concrete cylinder specimens before the ultimate stress and strain was determined. The stress (σ_a and σ_b) was maintained for 60 seconds and the strain readings were recorded during the succeeding 30 seconds at each load stage. After the completion of the last pre-loading cycle, a wait for a period of 60 seconds under the basic stress (σ_b) of 0.5 N/mm^2 took place, and the mean strain (ε_b) was recorded. The specimen was then reloaded to the next loading stress (σ_a), and the mean strain (ε_a) was recorded.

In case of misalignment of test specimens producing uneven horizontal and vertical strain values, tests were terminated when it was not possible to reduce the differences to a range of within ±10%. Test specimens were unloaded and re-centered in the compression machine until the individual strains were within a range of ±10% of their mean value at σ_a. Once the test specimen was accurately centered, the applied load was reduced accurately to the basic stress of 0.5 N/mm^2 at the same rate as during loading.

3.5.8 Mercury Intrusion Porosimetry (MIP)

Porosity is a measure of the proportion of the total volume of concrete occupied by pores, and is usually expressed in percent. Porosity can be measured by mercury intrusion, this technique was used to determine the pore size distribution and the porosity of the concrete paste samples using a Pore Sizer 9320 mercury intrusion porosimeter with a maximum mercury intrusion pressure of 210 MPa.

The MIP test method is based on the fact that a liquid (mercury in this case) that does not wet a porous solid will enter its pores only under pressure. If the pores are assumed to be cylindrical, the intrusion pressure, P_{In} , needed to force the liquid into them is given by the Washburn equation:

$$P_{In} = -4\gamma \cos \theta / d_p$$

where γ is the surface energy of the liquid, θ is the contact angle, and d_p is the mercury intruded pore diameter. For mercury (Hg), γ =0.483 Mm^{-1}, the surface tension of mercury [19]. In this study, cylindrical pore geometry and a contact angle θ of 140 °C were assumed.

The paste samples for the MIP measurement were obtained from the crushed concrete cubes after the compression test. The fragments of mortars were soaked in acetone to stop hydration, and were dried in a furnace at 60 °C for 24 hours before the measurement

was carried out. The Pore Sizer 9320-mercury intrusion porosimeter will enable penetration of pore diameter sizes ranging from approximately 360 μm to 6 nm.

The specimens used in this test were fragments of mortar of about 5 grams in weight taken from the 100 mm concrete cubes. Fragments of mortar samples were weighed and placed in a tube-shaped penetrometer. After the specimen environment was evacuated to a pressure below 50 μm of Hg in the penetrometer, the penetrometer was filled with mercury which was pressure intruded into the specimen by compressed air at 0.021 MPa. Thereafter, the penetrometer was transferred to a hydraulic chamber where a maximum hydraulic pressure of 210 MPa was applied. Using a series of increments in pressure, pores of smaller and smaller size were mercury intruded. By incrementing the pressure and measuring the amount of mercury entering the sample at each pressure step, the intruded volumes of mercury at different levels were recorded, and the corresponding pore size distribution was obtained.

CHAPTER FOUR RESULTS AND DISCUSSION

4.1 MECHANICAL PROPERTIES

4.1.1 Compressive Strength Results

The compressive strength results for specimens after having been heated to a series of maximum temperatures up to 1200 °C and the percentage strength difference from the unheated specimen control values are summarized in Table 4-1 and Table 4-2 respectively. The related plots are shown in Figures 4-1 to 4-13 in Appendix VIII. Each figure in Table 4-1 represents an average of the ultimate compressive strength of three specimens and Table 4-2 compares the Table 4-1 results with the compressive strength of saturated cubes at room temperature (25 °C). Table 4-1 gives results for specimens that have been heated and are respectively saturated to the 20, 60 and 100 per cent levels at the start of the heating process. Results illustrated in Table 4-3 compares the compressive strength results of fiber and non-fiber concrete given in Table 4-1.

Table 4-1. Compressive Strengths for Concrete after Heating and Tested at Room Temperature, (MPa)

	Moisture	Maximum Temperature, (°C)									
	Content	25	105	200	300	400	600	800	1000	1100	1200
M-1	20%	-	40	38	36	32	24	14	6	5	11
	60%	-	37	35	34	30	21	12	6	5	10
	100%	39	35	32	30	28	18	10	4	4	6
M-2	20%	-	50	46	39	36	34	17	8	8	15
	60%	-	47	39	38	33	29	16	8	7	15
	100%	53	45	36	34	32	22	13	6	6	10
M-3	20%	-	101	99	96	94	56	33	12	11	19
	60%	-	98	97	93	87	56	30	12	11	18
	100%	99	96	95	90	85	50	26	8	19	15
M-1F	20%	-	46	42	38	35	32	16	8	7	14
	60%	-	42	38	36	32	24	14	7	6	13
	100%	45	41	34	32	30	20	12	5	5	8
M-2F	20%	-	60	58	54	50	37	19	8	9	18
	60%	-	53	50	47	44	36	18	8	8	17
	100%	60	50	48	45	40	33	17	6	8	14
M-3F	20%	-	112	106	102	100	69	37	14	12	19
	60%	-	107	104	96	94	69	33	14	11	19
	100%	110	100	97	94	90	65	28	12	10	17

Note: Control specimens at laboratory temperature about 25 °C
Values reported are average of 3 tests (See Table A-B in Appendix for scattered results)

Table 4-2. Compressive Strengths for concrete after Heating, as a Percentage Change from that for Fully Saturated Unheated Concrete Tested at Room Temperature, (per cent)

	Moisture	Maximum Temperature, (°C)								
	Content	105	200	300	400	600	800	1000	1100	1200
M-1	20%	3	-3	-8	-18	-38	-64	-85	-87	-72
	60%	-5	-10	-13	-23	-46	-69	-85	-87	-74
	100%	-10	-18	-23	-28	-54	-74	-90	-90	-85
M-2	20%	-6	-13	-26	-32	-36	-68	-85	-85	-72
	60%	-11	-26	-28	-38	-45	-70	-85	-87	-72
	100%	-15	-32	-36	-40	-58	-75	-89	-89	-81
M-3	20%	2	0	-3	-5	-43	-67	-88	-89	-81
	60%	-1	-2	-6	-12	-43	-70	-88	-89	-82
	100%	-3	-4	-9	-14	-49	-74	-92	-91	-85
M-1F	20%	2	-7	-16	-22	-29	-64	-82	-84	-69
	60%	-7	-16	-20	-29	-47	-69	-84	-87	-71
	100%	-9	-24	-29	-33	-56	-73	-89	-89	-82
M-2F	20%	0	-3	-10	-17	-38	-68	-86	-86	-70
	60%	-12	-17	-22	-27	-40	-70	-87	-87	-72
	100%	-17	-20	-25	-33	-45	-72	-90	-87	-77
M-3F	20%	2	-4	-7	-9	-37	-66	-87	-89	-83
	60%	-3	-5	-13	-15	-37	-70	-87	-90	-83
	100%	-9	-12	-15	-18	-41	-75	-89	-91	-85

Note: Values reported are average of 3 tests

Table 4-3. Compressive Strength for Concrete which incorporates Steel Fiber, as a Percentage Change from that for Non-fiber Concrete Tested at Room Temperature, (per cent)

	Moisture	Maximum Temperature, (°C)									
	Content	25	105	200	300	400	600	800	1000	1100	1200
M-1F	20%	--	15	11	6	9	33	14	33	40	27
	60%	--	14	9	6	7	14	17	17	20	30
	100%	15	17	6	7	7	11	20	25	25	33
M-2F	20%	--	20	26	38	39	9	12	6	6	20
	60%	--	13	28	24	33	24	13	0	13	13
	100%	13	11	33	32	25	50	31	0	33	40
M-3F	20%	--	11	7	6	6	23	12	17	9	0
	60%	--	9	7	3	8	23	10	17	4	6
	100%	11	4	2	4	6	30	8	50	11	13

Note: Control specimens at laboratory temperature about 25 °C
Values reported are average of 3 tests

The measurements of compressive strength for the control specimens (at a room temperature of 25 °C) are given in Fig. 4-1. It can be observed from Fig. 4-1 that the compressive strengths of SFRC (M-1F, M-2F and M-3F) are higher than for the same mixes without steel fibers incorporated (M-1, M-2 and M-3).

The measurements of compressive strength, as a function of the maximum exposure temperature, are given in Figures 4-2 to 4-4, each figure for a different test specimen saturation condition. It can be seen that as the temperature increases, there is a decrease in compressive strength. The decrease occurs over a wide range of temperatures. Significant reductions in strength are observed for the HPC mixes, M3 and M3F, for temperatures exceeding 400 °C and strengths for all mixes reached minimum values at 1000 or 1100 °C. For maximum temperatures up to 400 °C, the loss in strength was small. Above 1000 or 1100 °C, there is a slight increase in strength.

Figures 4-5 to 4-13 showed the relationship of compressive strength to moisture content after heating to the nine peak heating temperatures of 105, 200, 300, 400, 600, 800, 1000, 1100 and 1200 °C respectively. It can be seen that there is nearly always a slight reduction in compressive strength as moisture content increases for different maximum heating temperatures. Thus, moisture content of concrete specimens at the time of the firing test affects the compressive strength. Concrete specimens with higher moisture content leads to a slightly lower strength and this is quantified below. The loss in strength may be due to the dilation or softness of the cement gel by adsorbed water and the forces of cohesion of the solid particles are then attenuated [16, 39].

4.1.2 Percentage Difference in Compressive Strength

The compressive strength of concrete after exposure to high temperature is highly variable. The percentage strength differences between the original unheated values for both the non-SFRC (M-1, M-2 and M-3) and the SFRC (M-1F, M-2F, M-3F) specimens are shown in Table 4-2.

For a maximum temperature of 105 °C with initial moisture content of 20%, there were about 2 to 3% increases in strength for the non-SFRC (M-1 and M-3), however, M-2 suffered from a 6% loss in strength and there was about 2% strength gain for the SFRC (M-1F and M-3F). For initial moisture content of 60%, the strength loss for the non-SFRC was between 1 and 11% and about 3 to 12% for the SFRC. For initial moisture

content of 100%, the strength loss varies from 3 to 15% for the non-SFRC and 9 to 17% for the SFRC.

When heated to a maximum temperature of 200 °C with initial moisture content of 20%, the non-SFRC, M-1 and M-2 suffered from 3 to 13% loss in strength. Meanwhile, M-3 sustained their original strength. The strength loss for the SFRC was 3 to 7%. For initial moisture content of 60%, the strength loss was between 2 and 26% for non-SFRC and 5 to 17% for SFRC. For initial moisture content of 100%, the reduction in strength was 4 to 32% for non-SFRC and about 12 to 24% for SFRC.

For a heating temperature of 300 °C and initial moisture content of 20%, the strength loss ratios vary between 3 and 26% for non-SFRC and between 7 and 16% for SFRC. For initial moisture content of 60%, the strength loss was 6 to 28% for non-SFRC, and 13 to 22% for SFRC. For initial moisture content of 100%, the strength loss starts with 9% and ends with 36% for non-SFRC, and 15 to 29% for SFRC.

When a maximum temperature reached 400 °C, it can be seen that the loss in strength for an initial concrete content of 20%, the reduction in strength was between 5 and 32% for non-SFRC and between 9 and 22% for SFRC. For moisture content of 60%, the strength loss was 12 to 38% for non-SFRC and 15 to 29% for SFRC. For moisture content of 100%, the reduction in strength varies from about 14 to 40% and 18 to 33% for SFRC.

For a maximum temperature of 600 °C and moisture content of 20%, the strength loss was 36 to 43% for non-SFRC, and 29 to 38% for SFRC. For 60%, the loss in strength was between 43 and 46% for non-SFRC, and 37 to 47% for SFRC. For 100%, the strength loss was between 49 and 58% for non-SFRC and between 41 and 56% for SFRC.

At 800 °C and an initial moisture content of 20%, there was about 64 to 68% of the compressive strength loss for both non-SFRC and SFRC mixes. For 60%, the loss in strength was about 69 to 70% for both non-SFRC and SFRC. For 100%, the loss was 74 to 75% for non-SFRC and 72 to 75% for SFRC.

At maximum heating temperature of 1000 °C, the strength loss percentages reached their greatest values. For moisture content of 20%, the original strength losses vary from between 85 and 88% for non-SFRC and between 82 and 87% for SFRC. For the moisture content of 60%, the original strength losses were 85 to 88% for non-SFRC and 84 to 87% for SFRC. For moisture content of 100%, the losses vary between 89 and 92% for non-SFRC and 89 to 90% for SFRC.

After heating to a temperature of 1100 °C, it can be seen that there was a further reduction in the overall compressive strength for all mixes. When the maximum heating temperature of 1200 °C is reached, it can be seen that the losses in the original strengths were less when compared to those after heating to 1000 °C.

Table 4-3 summarizes the relative compressive strength results as a percentage change for concrete, which incorporates steel fibers from that for non-fiber concrete and tested at room temperature. It can be seen from the results that concrete, which incorporates steel fibers has an overall compressive strength gain up to 50 per cent after exposure to high temperatures up to 1200 °C.

4.1.3 Discussion on Compressive Strength

The amount of strength loss for both NSC and HPC after exposure to temperatures below 200 °C for one hour is small. The overall loss in strength is up to about 32 per cent. For an exposure temperature reaches between 200 and 400 °C, the strength loss of concrete is slightly increased up to 40 per cent. Following exposure to temperatures greater than 400 °C, there is a rapid decrease in strength. As can be seen from Fig. 4-3 to 4-4, the strength of concrete for all mixes reaches its lowest value after exposure to about 1000 °C and started to converge to one very low value for concrete exposed to 1100 °C. It is suggested that the structure of concrete is destroyed at a temperature of 1000 °C. After exposure to temperatures exceeding 1000 °C, there is a slight increase in strength, which is suggested is due to the hardening, resulting from the sintering of the materials in the concrete after changes have taken place in the sorel binding.

A higher exposure temperature leads to a lower indicated strength. It is suggested that the factors affecting the losses in strength could be caused by damage to the aggregate, weakening of the bond between the aggregate and cement paste, and reduction in the

strength of hardened cement paste due to an increase in porosity, partial breakdown of calcium silicate hydrates, chemical transformation due to hydrothermal reactions and the development of cracking.

It can be stated more generally that concrete which incorporates steel fibers retains better crack resistance and better mechanical properties, in compressive strength in this case, up to about 1100 °C for NSC, however, HPC containing fiber suffered from a greater strength loss at this high temperature.

4.1.4 Flexural Strength Results

The flexural strength of concrete beams after heating to different maximum temperatures up to 1100 °C is summarized in Table 4-4 and the related plot is given in Fig. 4-14. Each figure in Table 4-4 represents an average of the ultimate flexural strength of three specimens compared with the flexural strength at room temperature (25 °C). The percentage difference of flexural strength of the original value is summarized in Table 4-5. The reduction in flexural strength of heated concrete beams appears to follow the trend of concrete cubes, except that the sudden change in the rate of loss of compressive strength that is particularly noticeable in HPC after heating to 400 °C, does not occur in the case of tensile strength. Results showed in Table 4-6 are for specimens that compares the Table 4-4 results with the flexural strength of fiber and non-fiber concrete.

Table 4-4. Flexural Strength for Concrete after Heating and Tested at Room Temperature, (MPa)

Temp. (°C)	M-1F	M-2F	M-3F	M-1	M-2	M-3
25	6.00	8.00	10.65	4.74	7.00	9.00
105	5.20	7.50	8.78	4.51	6.50	8.50
200	5.02	7.00	8.50	4.35	5.50	8.00
300	3.77	5.30	7.00	3.50	5.00	6.00
400	3.00	4.00	6.00	2.00	3.70	5.00
600	1.25	2.50	4.00	1.00	2.00	3.00
800	0.14	0.84	1.78	0.13	0.66	0.92
1000	0.17	0.24	0.42	0.10	0.20	0.28
1100	0.47	0.35	0.99	0.02	0.12	0.30

Note: Control specimens at laboratory temperature about 25 °C

Values reported are average of 3 tests (See Table A-C in Appendix for scattered results)

Table 4-5. Percentage Flexural Strength Difference from that for Fully Saturated Unheated Concrete and Tested at Room Temperature, (per cent)

Temp. (°C)	M-1F	M-2F	M-3F	M-1	M-2	M-3
105	-13.4	-6.3	-17.6	-5.0	-7.1	-5.6
200	-16.3	-12.5	-20.2	-8.2	-21.4	-11.1
300	-37.3	-33.8	-34.3	-26.1	-28.6	-33.3
400	-50.0	-50.0	-43.7	-36.7	-47.1	-44.4
600	-79.2	-68.8	-62.4	-78.9	-92.9	-66.7
800	-97.7	-89.5	-83.3	-97.3	-90.6	-89.7
1000	-97.2	-97.0	-96.1	-97.9	-97.1	-96.9
1100	-92.1	-95.7	-90.7	-99.6	-98.3	-96.7

Note: Values reported are average of 3 tests

Table 4-6. Flexural Strength for Steel Fiber Concrete, as a Percentage Change from that of Non-fiber Concrete Tested at Room Temperature, (per cent)

Temperature (°C)	M-1F	M-2F	M-3F
25	27	14	18
105	15	15	3
200	15	27	6
300	8	6	17
400	50	8	20
600	25	25	33
800	8	27	93
1000	70	20	50
1100	Immeasurable	Immeasurable	Immeasurable

Note: Control specimens at laboratory temperature about 25°C

Values reported are average of 3 tests

4.1.5 Percentage Difference in Flexural Strength

It can be seen from Table 4-5 that the reduction in flexural strength starts to occur progressively for concrete mixes at an exposure temperature of 105 °C. For the maximum heating temperature of 105 °C, percentage reduction in flexural strength was about 6 to 18% of the concrete at 25 °C for SFRC and about 5 to 7% for non-SFRC. The percentage of reduction in flexural strength becomes significant at 200 °C; the percentage loss was about 13 to 20% for SFRC and about 8 to 21% for non-SFRC. For 300 °C, the percentage reduction in flexural strength was about 34 to 37% for SFRC and between about 26 and 33% for non-SFRC. For 400 °C, the percentage loss was about 44 to 50% for SFRC and about 37 to 47% for non-SFRC. After exposure to temperature of 600 °C, the ratios of the flexural strength difference to the original flexural strength vary between about 62 and 79% for the SFRC and about 67 to 93% for non-SFRC. At 800 °C, the percentage loss ratios in flexural strength were about 83 to 98% for SFRC and about 90 to 97% for non-SFRC. With further increase in temperature to 1000 °C, there was only about 3 to 4% of the original flexural strength left for SFRC and about 2 to 3% for the non-SFRC specimens. However, for 1100 °C, the flexural strength was slightly recovered compared with 1000 °C; the residual flexural strength percentage was about 4 to 9% for SFRC and about 0 to 3% for non-SFRC.

Table 4-6 summarizes the relative flexural strength results as a percentage change for concrete incorporates steel fiber from that for non-fiber concrete and tested at room temperature. Results illustrate that concrete incorporating steel fibers has an overall

better flexural strength than concrete without steel fibers. The strength gain ranges from a low of 3% to as much as 93% depending on the mix. HPC containing fibers achieves the greatest strength gain, of 93% over HPC without fiber at a maximum exposure temperature of 800 °C.

4.1.6 Discussion on Flexural Strength

In Fig. 4-14, it is also can be seen that the reduction in flexural strength for the SFRC mixes (M-1F, M-2F and M-3F) is not as sharp as for the non-fiber mixes (M-1, M-2 and M-3). Thus, the SFRC beam specimens had an overall better performance in flexural strength compared with the ones without steel fiber incorporated, not only at normal temperatures but also after being subjected to temperatures between 200 and 1000 °C. However, the results showed that there is no significant difference in flexural strength for both the SFRC and the non-fiber mixes after exposure to a temperature of 1000 °C.

From Fig. 4-14, it is obvious that a decrease in the flexural strength of most tested concrete beams started after exposure to about 200 °C and progressed sharply until 800 °C. The strength reaches minimum values and is of virtually negligible after exposure to 1000 °C and seems to converge to one point. After exposure to any temperatures up to 200 °C, the loss in strength was small, there was only about 5 to 21 percent of the reference concrete values. There is evidence of the residual strength, of about 0 to 8 per cent, after exposure to a temperature of 1100 °C, being greater than that for concretes exposed to 1000 °C.

It is observed that concrete incorporates steel fibers retains better mechanical properties, in flexural strength in this case, after exposure to high temperatures of up to 1200 °C. There is evidence that steel fibers benefited HPC for the greatest strength gain after exposure to a very high temperature of 1000 °C.

4.2 DEFORMATION CHARACTERISTICS

4.2.1 Static Modulus of Elasticity

The results of the static modulus of elasticity based on concrete cylinder tests after heating to various maximum temperatures up to 1200 °C are summarized in Table 4-7 and the related plot is shown in Fig. 4-15. Results represent an average of the modulus of elasticity of three specimens compared to the average maximum modulus of elasticity at room temperature (25 °C).

Table 4-7. Static Modulus of Elasticity under Temperature Effect, (GPa).

Temperature, (°C)	M-1	M-1F	M-3	M-3F
25	30	35	70	82
105	28	30	53	55
300	26	28	51	53
600	15	17	34	40
800	8	10	20	23
1100	2	2	5	7
1200	Immeasurable	Immeasurable	Immeasurable	Immeasurable

Note: Values reported are average of 3 tests (See Table A-D in Appendix for scattered results)

The effect of temperature on the modulus of elasticity of concrete cylinder specimens is similar to that on the other mechanical properties discussed above. It can be seen from the results that the modulus of elasticity of concrete exposed to 600 °C was much less than for concrete exposed only to 300 °C. However, after exposure to between 800 and 1000 °C, the reduction in elastic modulus from already small values were necessarily small. At the maximum heating temperature of 1000 °C, the modulus of elasticity starts to converge to one very low value. With further increase in maximum exposure temperatures to 1100 and 1200 °C, the modulus of elasticity reaches minimum values.

4.2.2 Poisson's Ratio

The Poisson's ratio for concrete cylinders heated at different temperatures up to 1100 °C is determined and summarized in Table 4-8. A plot of Poisson's ratio, as a function of heating temperatures is given in Fig. 4-16.

Table 4-8. Poison's Ratio under Temperature Effect

Temperature, (°C)	M-1	M-1F	M-3	M-3F
25	0.15	0.16	0.21	0.22
105	0.13	0.14	0.19	0.21
300	0.11	0.13	0.16	0.19
600	0.06	0.07	0.09	0.10
800	0.04	0.05	0.07	0.08
1100	0.01	0.01	0.02	0.02

Note: Values reported are average of 3 tests (See Table A-E in Appendix for scattered results)

Table 4-8 shows that for HPC incorporates steel fibers, M-3F mix, Poisson's ratio starts at 0.22 and diminishes until 0.02. For HPC without steel fibers, M-3 mix, Poisson's ratio starts at 0.21 and attenuates until 0.02. For NSC incorporates steel fibers, M-1F mixes Poisson's ratio starts at 0.16 and ends at 0.01. For NSC without steel fibers, M-1 mix, Poisson's ratio starts at 0.15 and disappears at 0.01. It can be seen from the results that the modulus of elasticity increases with the increase in compressive strength of concrete.

4.2.3 Cracking

The results of observation on cracking are summarized in Table 5-1 in section 5.1. A network of hair cracks were observed on non-steel fiber reinforced concrete specimens heated to a maximum temperature of 300 °C. With further increases in maximum temperatures exceeding 400 °C, a considerable number of hair cracks were found and become deeper when heated to a maximum temperature of 600 °C. For maximum temperatures beyond 600 °C, severe cracking occurs on concrete specimen surfaces. It is probable that cracking is due to the neat Portland cement expanding initially upon heating subject to the normal thermal expansion, hence caused local breakdowns in bond

between the cement and the aggregate. As the maximum exposure temperature rises, drying shrinkage eventually becomes much greater than the normal thermal expansion as water is driven off. These two opposing actions progressively weaken and crack the concrete [42]. For steel fiber reinforced concrete, it is observed that hair cracks first appeared at about 600 °C and severe cracking occurs at temperatures exceeding 800 °C. Thus, it is believed that the presence of steel fibers can delay the occurrence of cracking and hence improve the performance of concrete subjected to high temperatures.

It was also observed by inspection that the SFRC specimens after being subjected to very high temperatures beyond 1100 °C, suffered severe deformation in shape. However, non-fiber concrete exposed to very high temperature of 1200 °C suffered only minor deformation in shape but severe cracking, concrete specimens in this case are generally very friable and porous.

4.2.4 Change of Colors in Concrete with Temperature Effects

The color change of concrete after exposure to high temperatures is highly depends on the type of aggregate used. The color change is summarized in Table 4-9.

Table 4-9. Change of Color in Concrete subjected to Different Temperatures

Maximum Temperature, (°C)	Color Observed
25 to 300	Grey (original gray cement color)
400 to 600	Yellowish Grey
Up to 800	Pinkish Brown
1000 to 1100	Reddish Brown
Up to 1200	Orange Brown / Golden Brown

The observed colors shown in Table 4-9 are for concrete subjected to different temperatures. Once concrete has been subjected to a high temperature, the color change is permanent. The color sequence is approximately as follows: Gray at 300 °C or below; yellowish gray between 400 °C and 600 °C; then Pink up to about 800 °C; reddish brown between 1000 and 1100 °C; and buff on surfaces with golden brown or orange brown up to 1200 °C. Thus, it looks to be possible to develop the use of color to determine what maximum temperature a specific element of concrete has been exposed to after a real fire and to estimate the residual mechanical properties of the element. Generally, concrete past the gray stage is friable and porous.

4.3 MICROSTRUCTURE ANALYSIS

It is realized that the cement paste is almost completely dehydrated at around 950 °C and steel changes its microstructure (lattice) at 900 °C, however, it is our intention to conduct tests above 1000 °C so as to investigate the change in pore structure in concrete. In fact, it still holds a mechanical meaning in reality.

4.3.1 Measurement of Porosity and Pore Size Distribution

The measurements of porosity as the percentage of the total concrete volume and average pore diameter for the concrete cube specimens after exposure to different maximum temperatures up to 1000 °C are given in Figures 4-17 to 4-28 and 4-55 to 4-58, and

summarized in Table 4-10 and 4-11. All reported results are the average of three measurements.

Table 4-10. Increase in Porosity Percentage of Concrete after Heating to Various Temperatures, per cent

	Moisture	Maximum Heating Temperature (°C)				
	Content	25	105	300	800	1000
M-1	20%	-	10	19	22	18
	60%	-	17	20	23	20
	100%	13	22	25	30	20
M-3	20%	-	7	10	12	8
	60%	-	10	11	13	10
	100%	7	12	19	20	11
M-1F	20%	-	8	14	16	14
	60%	-	13	18	19	15
	100%	12	15	20	24	17
M-3F	20%	-	5	8	9	4
	60%	-	8	9	11	5
	100%	6	9	12	14	8

Note: Control specimens at the laboratory temperature about 25 °C

Values reported are average of 3 tests (See Table A-F in Appendix for Scattered Results)

Table 4-11. Increase in Average Pore Diameter in Concrete after Heating to Various Temperatures, ($x10^{-6}$ m)

	Moisture	Maximum Heating Temperature (°C)				
	Content	25	105	300	800	1000
M-1	20%	-	0.04	0.07	0.11	0.30
	60%	-	0.06	0.08	0.18	0.35
	100%	0.05	0.07	0.09	0.24	0.55
M-3	20%	-	0.02	0.06	0.10	0.15
	60%	-	0.05	0.06	0.11	0.17
	100%	0.04	0.06	0.07	0.13	0.44
M-1F	20%	-	0.03	0.06	0.13	0.22
	60%	-	0.05	0.08	0.15	0.30
	100%	0.05	0.07	0.08	0.16	0.49
M-3F	20%	-	0.03	0.04	0.07	0.09
	60%	-	0.05	0.06	0.10	0.11
	100%	0.03	0.06	0.06	0.12	0.23

Note: Control specimens at the laboratory temperature about 25 °C

Values reported are average of 3 tests (See Table A-G in Appendix for Scattered Results)

Table 4-10 shows the porosity percentage of concrete for different maximum temperature exposures. Results show that the porosity increases as the maximum heating temperature increases. For the maximum heating temperatures above 800 °C, results are suspect due to their high variations. However, SFRC seemed to have a lower porosity percentage than the non-SFRC. Evidence is also revealed that the porosity percentage increases with the moisture content of concrete at the time of the firing test.

From Table 4-11, it is found that the average pore diameter increases as maximum heating temperature increases for all mixes. A higher moisture content leads to a larger pore diameter after exposure to high temperature. In general, for different moisture contents of concrete specimens at the time of firing test, the effect of fire on pore sizes is somewhat highly variable. The cause of the variations is not known.

As can be seen from Figures 4-17 and 4-18, for the control samples (25 °C), the results showed that for SFRC, both the porosity percentage and the average pore diameter were lower in values compared with those for non-SFRC.

4.3.2 Measurement of Porosity of Concrete after Exposure to High Temperatures

The measurements of porosity, as a function of maximum temperature of exposure are shown in Figures 4-19 to 4-21. Each point in the figures represents an average of the porosity of three specimens compared with the porosity at room temperature (25 °C).

It can be seen that the results are highly variable with temperature exposure. However, as stated earlier, the results revealed that the porosity percentage generally increases as the maximum temperature of exposure increases. The porosity percentage reaches its maximum values after exposure to temperature at about 800 °C. After exposure to maximum heating temperatures above 800 °C, the porosity showed decrease in values. It is suspected that substances in the concrete specimens were liquefied at very high temperatures and diffused into the pores and hence reduced porosity.

The measurements of porosity, as a function of initial moisture contents are given in Figures 4-22 to 4-25. After inspected the plots from Figures 4-22 to 4-25, the results showed that for SFRC and non-SFRC at different maximum heating temperatures, porosity percentage increases as initial moisture content percentage increases. SFRC has better resistance against porosity compared with non-SFRC. Non-fiber concrete mixes showed significant increases in porosity percentage for higher moisture contents whereas SFRC showed better resistance against porosity. Concrete with lower grade showed higher porosity percentage than concrete with higher grade regardless of steel fiber effect. On further increase to maximum temperature of 1000 °C, changes in porosity percentage between low (20%) and high (100%) initial moisture contents were not significant for any of the concrete mixes.

4.3.3 Temperature Effects on Pore Size Distribution of Concrete at Different Initial Moisture Contents

Table 4-11 illustrates the effect of moisture contents on average pore diameters for the concrete cube specimens exposed to different maximum temperatures up to 1000 °C and the related plots are shown in Figures 4-26 to 4-28.

The results reflect that the average pore diameter increases with the increase in maximum temperature of exposure at all levels of moisture content. The measurements of the average pore diameter, as a function of maximum temperature are given in Figures 4-26 to 4-28. It can be seen from the results that the maximum pore diameter varies from 0.02×10^{-6} to 0.55×10^{-6} m. Concrete specimens reached a maximum pore diameter of about 0.55×10^{-6} m after exposure to a maximum temperature of 1000 °C.

For concrete mixes reinforced with steel fiber, average pore diameter is lower than those non-fiber mixes. Exceeding maximum heating temperature of 800 °C, all concrete mixes showed significant increase in average pore diameter.

The measurements of pore diameter of concrete were determined using the mercury intrusion porosimetry method as explained above. The measurements of cumulative intrusion volume, as a function of pore diameter are given in Figures 4-29 to 4-40.

Figures 4-29 to 4-34 illustrate the cumulative intrusion volume, as a function of pore diameter at different initial moisture contents for the non-fiber mixes of M-1 and M-3. It can be seen from the results that concrete specimens exhibited a higher cumulative intrusion volume after heating to maximum temperatures exceeding about 1000 °C when compared to values after heating to lower maximum temperatures. However, in some cases, intrusion volume at higher temperatures showed a lower value than the ones at lower temperatures. These results are suspect and the cause of variations is not known. In general, concrete heated to a higher maximum temperature had a greater cumulative intrusion volume and pore size. A similar trend can also be seen for the fiber reinforced concrete mixes M-1F and M-3F.

Figures 4-35 to 4-40 demonstrate the cumulative intrusion volume, as a function of pore diameter at different initial moisture contents for the SFRC mixes of M-1F and M-3F. As can be seen from the results, the trend is similar to that for the M-1 and M-3 mixes as discussed above. Concrete specimens if subjected to higher maximum temperatures have higher intrusion volumes, larger pore sizes and are porous.

Figures 4-41 to 4-43 summarize the pore volume of concrete mixes M-1, M-1F, M-3 and M-3F with a pore size greater than 0.1μm at different moisture contents. The results confirmed the coarsening effect of high temperatures on pore structure [11, 46, 60-62]. The coarsening effect increased the porosity of hardened cement paste, the increased cumulative volume of pores larger than 0.1μm had influenced the strength of hardened cement paste, it is believed this was one of the factors that is responsible for the strength

loss of concrete. The cumulative volume of pores of hardened cement paste in concrete subjected to an elevated temperature increased with decreasing concrete strength.

The cumulative pore volume in range greater than 1.3μm in pore diameter, which should be responsible for the permeability of hardened cement paste [11, 16], was also increased after exposure to elevated temperatures as shown in Fig. 4-44 to Fig. 4-46. Thus, high temperatures have reduced the permeability and the durability of high strength concrete and normal strength concrete as well as the mechanical properties. The deterioration was more severe for normal strength concrete.

4.3.4 Moisture Effects on Pore Size Distribution of Concrete at Different Temperatures

Figures 4-47 to 4-54 summarize the cumulative pore volume for different concrete mixes with pore sizes greater than 0.1μm and 1.3 μm respectively after exposure to elevated temperatures at three different levels of initial moisture contents. The results are somewhat suspect due to their high variations. It can be seen from the figures that concrete mixes with initial moisture content of 60 per cent seems to have better performance against coarsening effect and this advantage is lost in fiber reinforced concrete mixes. More investigation to be needed to confirm this phenomenon.

The measurements of average pore diameter, as a function of initial moisture content are shown in Figures 4-55 to 4-58. The results showed that as initial moisture content

increases, there is an increase in average pore diameter after exposure to higher temperatures. A maximum average pore diameter of 0.55×10^{-6} m was recorded at 100% initial moisture content after heated to above 1000 °C.

The measurements of cumulative intrusion volume, as a function of pore diameter following exposure to different maximum temperatures are given in Figures 4-59 to 4-64.

From Fig. 4-59, it can be seen from the results that the pore size distribution for concrete specimens, without heating, incorporated with steel fiber shifted to the smaller pore size range demonstrating the pore refining effect of steel fibers. Thus, SFRC resulted in lower porosity compared to the non-fiber concrete mixes. As can be seen from Figures 4-60 to 4-64, it can be stated more generally that different concrete mixes, after heating to different degree of temperatures, with higher initial moisture contents have higher cumulative intrusion volume. However, results with suspect were found in some cases due to variations and the cause is not known.

CHAPTER FIVE CONCLUSIONS AND RECOMMENDATIONS

5.1 CONCLUDING SUMMARY

The experimental results of this research study are summarized below in Table 5-1.

Table 5-1. Conclusing Summaries

		Concrete	Initial	Maximum Heating Temperature (Degree Celsius)									
		Mix	Moisture	25°C	105°C	200°C	300°C	400°C	600°C	800°C	1000°C	1100°C	1200°C
Residual	Non-SFRC	M-1	20%	–	40	38	36	32	24	14	6	5	18
Compressive			60%	–	37	35	34	30	21	12	6	5	17
Strength			100%	39	35	32	30	28	18	10	4	5	14
(MPa)		M-2	20%	–	50	46	39	36	34	17	8	7	13
			60%	–	47	39	38	33	29	16	8	5	14
			100%	53	45	36	34	32	22	13	5	6	8
		M-3	20%	–	101	99	96	94	56	33	12	12	18
			60%	–	98	97	93	87	56	30	12	11	17
			100%	99	96	95	90	85	50	26	8	10	14
	SFRC	M-1F	20%	–	46	42	38	35	32	16	8	8	19
			60%	–	42	38	36	32	24	14	8	7	18
			100%	45	41	34	32	30	20	12	5	6	15
		M-2F	20%	–	60	58	54	50	37	19	8	9	15
			60%	–	53	50	47	44	36	18	8	8	15
			100%	60	50	48	45	40	33	17	6	8	10
		M-3F	20%	–	112	106	102	100	69	37	14	12	19
			60%	–	107	104	96	94	69	33	14	11	19
			100%	110	100	97	94	90	65	28	12	10	17
Residual	Non-SFRC	M-1	100%	4.74	4.51	4.35	3.50	2.00	1.00	0.13	0.10	0.02	NA
Flexural		M-2	100%	7.00	6.50	5.50	5.00	3.70	2.00	0.66	0.20	0.12	NA
Strength		M-3	100%	9.00	8.50	8.00	6.00	5.00	3.00	0.92	0.28	0.30	NA
(MPa)	SFRC	M-1F	100%	6	5.2	5.02	3.77	3	1.25	0.14	0.17	0.47	NA
		M-2F	100%	8.00	7.50	7.00	5.30	4.00	2.50	0.84	0.24	0.35	NA
		M-3F	100%	10.65	8.78	8.50	7.00	6.00	4.00	1.78	0.42	0.99	NA
Young's	Non-SFRC	M-1	100%	30	28	–	26	–	15	8	–	3	NA
Modulus		M-3	100%	70	53	–	51	–	34	24	–	5	NA
(GPa)	SFRC	M-1F	100%	35	30	–	28	–	17	10	–	4	NA
		M-3F	100%	82	55	–	53	–	40	25	–	7	NA
Porosity	Non-SFRC	M-1	20%	–	10%	–	19%	–	–	22%	24%	–	10%
(per cent)			60%	–	17%	–	20%	–	–	25%	23%	–	–
			100%	13%	22%	–	25%	–	–	33%	30%	–	–
		M-3	20%	–	7%	–	10%	–	–	12%	12	–	20%
			60%	–	11%	–	10%	–	–	13%	17%	–	13%
			100%	6%	12%	–	20%	–	–	20%	21%	21%	NA
	SFRC	M-1F	20%	–	8%	–	14%	–	–	16%	17%	NA	NA
			60%	–	13%	–	18%	–	–	19%	20%	23%	NA
			100%	12%	15%	–	19%	–	–	24%	27%	27%	NA
		M-3F	20%	–	5%	–	8%	–	–	9%	10%	NA	NA
			60%	–	8%	–	11%	–	–	11%	14%	21%	NA
			100%	7%	9%	–	12%	–	–	14%	17%	4%	NA
Color	Non SFRC	All	All	Gray	Gray	Gray	Gray	Y.G.	Y.G.	P.B.	R.B.	R.B.	G.B.
	SFRC	All	All	Gray	Gray	Gray	Gray	Y.G.	Y.G.	P.B.	R.B.	R.B.	O.B.
Cracking	Non-SFRC	M-1	20%	N.O.	N.O.	N.O.	N.O.	N.O.	H & m	M	S	S	S
			60%	N.O.	N.O.	N.O.	N.O.	N.O.	H & m	M	S	S	S
			100%	N.O.	N.O.	N.O.	H	H	m	M	S	S	S
	SFRC	M-1F	20%	N.O.	N.O.	N.O.	N.O.	N.O.	N.O.	m	S	S	S
			60%	N.O.	N.O.	N.O.	N.O.	N.O.	N.O.	m	S	S	S
			100%	N.O.	N.O.	N.O.	N.O.	N.O.	H	M	S	S	S
	Non-SFRC	M-3	20%	N.O.	N.O.	N.O.	N.O.	N.O.	H	m	S	S	S
			60%	N.O.	N.O.	N.O.	N.O.	N.O.	H	m	S	S	S
			100%	N.O.	N.O.	N.O.	N.O.	H	H & m	M	S	S	S
	SFRC	M-3F	20%	N.O.	N.O.	N.O.	N.O.	N.O.	N.O.	H & m	S	S	S
			60%	N.O.	N.O.	N.O.	N.O.	N.O.	N.O.	H & m	S	S	S
			100%	N.O.	N.O.	N.O.	N.O.	N.O.	N.O.	m	S	S	S

Note: Results Reported are Average of at least Three Specimens.

Symbols for Cracking: N.O. No obvious cracks observed.
S Severe cracks observed.
m Micro cracks observed.
M Macro cracks observed.
H Hair cracks observed.

Symbols for Color: Y.G. Yellowish Gray
P.B. Pinkish Brown
R.B. Redish Brown
G.B. Golden Brown
O.B. Orange Brown

5.1.1 Strength Loss due to Temperature Effects

1) Exposure to higher temperatures leads to a lower residual strength, in the cases of both compression and flexure specimens.
2) For maximum heating temperatures up to 400 °C, the further loss in compressive strength was relatively small; there was only about 1 to 40 per cent of the reference concrete values.
3) The further reduction in compressive strength becomes significant, of about 29 to 92% of the original, for concrete heated to temperatures exceeding 400 °C, and is greater the higher the maximum temperature.
4) For exposure temperatures below 1000 °C, concretes reinforced with steel fibers (at 1 per cent) showed better performance in mechanical properties, of about 2 to 50 per cent for compressive strength, than concrete without steel fibers.
5) For concrete heated to maximum exposure temperature reaching 1000 °C, the difference in mechanical properties between steel fiber and non-steel fiber concrete was up to about 50 per cent for compressive strength.
6) HPC mixes started to suffer a higher compressive strength percentage loss than NSC at maximum exposure temperature of 600 °C and above.
7) HPC mixes suffers an even higher compressive strength loss when the temperature exceeds 800 °C.
8) The reduction in compressive strength is affected significantly beyond exposures up to 400 °C and reaches the minimum strengths after exposures to 1000 or 1100 °C. At

these very high exposure temperatures, the residual strength is only about 8 to 18 per cent of the reference concrete values.

9) For maximum heating temperatures of 1200 °C, there is a slight increase in compressive strength from the very low base, a base that occurs at a maximum temperature of 1000 and 1100 °C.

10) Under temperature effect, steel fiber reinforced concrete shows a better overall performance in flexural strength over a wide range, with a low at 3 per cent and a high at 93 per cent, compared with concretes without steel fibers under the high exposure temperature of 800 °C.

11) The reduction in flexural strength starts to occur progressively for concrete after exposure to temperature of 200 °C.

12) Flexural strengths of concrete reach their minimum values after exposure to about 1000 or 1100 °C.

13) For concrete exposed to a maximum heating temperature of 1100 °C, the residual flexural strength is a little greater than that for concretes exposed to 1000 °C, of about 1 to 5 per cent from this already low base.

14) For a maximum exposure temperature of 1000 °C, the difference in flexural strength for both SFRC and non-SFRC ranges from 20 to 70 per cent although the flexural strength for both SFRC and non-SFRC was very low at this high exposure temperature.

It must be stressed that after concrete has been heated to different high temperatures, concrete is cracked under these very high temperatures and our measurements of static modulus of elasticity and Poisson's ratio do not reflect the real values for the heated materials. However, the measurements have a mechanical and a physical meaning in reality, and give values of the apparent static modulus of elasticity and Poisson's ratio of the overall body of crashed heated material.

5.1.2 Static Modulus of Elasticity

1) The behavior of concrete structures is often dependent on the modulus of elasticity of the concrete, and current experimental results showed this modulus is strongly affected by exposure temperature.
2) The reduction in static modulus of elasticity progressed sharply between maximum exposures of 300 and 800 °C.
3) The decreasing values of static modulus of elasticity reach the minimum at maximum temperature of 1100 °C.

5.1.3 Poisson's Ratio

1) Results showed that for concrete, Poisson's ratio decreases with increasing exposure temperature.
2) For concretes exposed to a maximum heating temperature of 1100 °C, Poisson's ratio reduced to about 0.01 and 0.02 was reported.

5.1.4 Moisture Content Effects

1) Generally, HPC with a higher initial moisture content leads to a greater decline in strength and a larger pore size after exposure to high temperatures.
2) After heating beyond a temperature of 800 °C, destruction of concrete specimens under fire effect becomes larger and the mechanical strength eventually reaches the minimum after exposure to 1000 °C.
3) Above the heating temperature of 1000 °C, mechanical strength showed a slight increase. As pointed out earlier, moisture content within concrete at the time of firing test affects the compressive strength. Higher moisture content leads to a lower compressive strength.

5.1.5 Color Change

1) For concrete subjected to various high temperatures, the color change induced is permanent.
2) The residual mechanical properties of concrete elements that have been exposed to a real fire can be estimated or determined by color identification.
3) The color change of concrete after exposing a high temperature is highly depends on the type of aggregate used. Concrete composed of granite as aggregate after exposure to different high temperatures, its color sequence is approximately as follows:

Gray at 300 °C or below, yellowish gray between 400 and 600 °C, pink up to 800 °C, reddish brown between 1000 and 1100 °C, buff on surface with golden brown or orange brown at 1200 °C.

4) Concrete whose colors are beyond the gray stage is friable and porous.

5.1.6 Cracking in Concrete

1) For concretes with no steel fibers incorporated, a network of hair crack appear noticeably at a maximum heating temperature of 300 °C and severe cracking occurs at a maximum heating temperature of 600 °C.
2) For steel fiber reinforced concrete, hair cracks first appeared at about 600 °C and severe cracking occurs at about 800 °C. The presence of steel fibers can delay the occurrence of cracking and hence improve the performance of concrete under fire effects.

5.1.7 Microstructure Analysis

1) There is no doubt that concrete mixes with steel fiber incorporated showed a lower porosity percentage and average pore diameter than non-fiber concrete due to the strong bond strength of steel fiber.
2) It is confirmed that increases in exposure temperatures and in moisture content at the time of heating result in higher porosity percentages in concrete.

3) Concrete specimens if subjected to higher maximum temperatures have higher intrusion volumes, larger pore sizes and are rather porous.
4) It is suspected that for concrete, higher initial moisture content leads to a smaller pore size.
5) For a maximum heating temperature of 105 °C, the change in porosity of the concrete was insignificant.
6) For concrete exposure to between 105 and 300 °C, non-steel fiber concrete starts to suffer from higher porosity than steel fiber reinforced concrete.
7) Results showed that for concrete exposures up to a maximum heating temperature of 1000 °C, a maximum pore diameter of 0.55×10^{-6} m was reported.

5.1.8 Spalling of Concrete

Silica fume is commonly used in producing HPC, because of its high fineness, it is beneficial to reduce bleeding and to improve cohesion of mix. Silica fume can also enhance concrete properties of high early strength or low permeability. HPC that contains silica fume, however, is prone to spalling under high temperatures (in excess of about 300 °C) [10]. Explosive spalling is higher, the lower the permeability of the concrete and the higher the rate of rise in temperature [16]. Moisture content and strong dense hardened cement paste preventing moisture escape under high temperatures are the two main factors that are responsible for the spalling of concrete [45, 46]. In this research study, there was no evidence of spalling for concrete specimens during the simulated fire tests. This may be due to the fact that no silica fume was incorporated in

the concrete mix [28]. Steel fibers would also be likely to protect concrete against spalling providing added security.

5.2 CONCLUSIONS

In relation to the objectives in section 1.2, and taking into account the results of the past work by others as stated earlier, the following broad conclusions can be drawn:

1. It is concluded that incorporating steel fiber is beneficial to concrete exposed to high temperatures up to 1200 °C confirming that 1 per cent steel fiber is of no disadvantage if concrete is subjected to a fire. After concrete exposure to high temperatures, steel fiber reinforced concrete shows a higher overall residual strength and better crack resistance than non-fiber concrete. HPC mixes started to suffer a higher compressive strength loss than the NSC at maximum exposure temperatures of 600 °C. In this research study, for maximum exposure temperatures below 600 °C, HPC generally suffers a lower strength loss than NSC. No spalling was encountered, even though spalling has been identified as a problem with HPC by others [10, 16, 45].
2. For the cases of SFRC and non-SFRC, HPC and NSC, it is confirmed that the higher the exposure temperature the lower the residual strength. Moisture content within concrete at the time of high temperature test also affects the ultimate strength. A higher moisture content leads to a lower residual strength [16, 37].

3. In addition, the research has identified a correlation between the final color of the heated concrete and the temperature reached.

5.3 RECOMMENDATIONS FOR FUTURE WORK

Special care is required in translating observations on laboratory-made concrete specimens into useful information on full size structures. For instance, the behavior of elements of concrete in a real fire is extremely complicated and the inner section of a heavy member differently affected from the outer areas. Small specimen tests can provide quantitative results but they may not represent what happens at full scale. It is suggested that full-scale fire tests be carried out to allow further investigation on the fire resistance of steel fiber reinforced and high performance concrete when subjected to very high temperatures.

To further understand the microstructure of concrete after exposure to high temperature, it is suggested to study also the decomposition changes in concrete due to heating before and after the sintering process. To investigate the cracking situation, X-ray diffraction (XRD) tests or scanning electron microscopy (SEM) tests are required.

The change in color of concrete after exposure to different temperatures was substantial, and thus it is recommended to further investigate the color changes which occur in concrete elements after exposure to fire in order to understand the relationship between

color change and residual mechanical properties of concrete. An established relationship between color change and maximum temperature/time exposure will also be valuable in gauging 'temperature contours' attained after a real fire has burnt out and so assist other researchers in the field of fire spread modeling.

REFERENCES:

[1] Lea, F.M. The Chemistry of Cement and Concrete. Edward Arnold (Publishers) Ltd., London, UK, 656 pp. (1983).

[2] Metha, P.K. *Concrete: structure, properties, and materials*. Prentice-Hall, Inc., USA, pp. 129-132 (1986).

[3] Curwell, S. et al. *Building and Health*. RIBA Publishers Ltd, London, UK, 156 pp. (1990).

[4] Jahren, P.A. Fire Resistance of High Strength / Dense Concrete with Particular Reference to the Use of Condensed Silica Fume - A Review. Fly ash, Silica Fume, Slag, and Natural Pozzolans in Concrete. *Proceeding of the Third International Conference*, ACI SP-114, Detroit, USA, pp. 1013-1049 (1989).

[5] Lea, F.C. *The effect of temperature on some of the properties of materials*. Engineering, pp. 110, 293-298 (1920).

[6] Lea, F.C. and Stradling, R. *The resistance to fire of concrete and reinforced concrete*. Engineering, pp. 114(2959), 341-344, 380-382 (1922).

[7] Petzold, A. and Röhrs, M. *Concrete for high temperatures*, Maclaren and Sons Ltd., London, 190 pp. (1970).

[8] Mindess, S. and Young, J.F. *Concrete*, Prentice-Hall, Inc., Englewood Cliffs, New Jersey, USA, 530 pp. (1981).

[9] Crook, D.N. and Murray, M.J. Regain of strength after firing of concrete, *Magazine of Concrete Research*. vol. 22, no. 72, pp. 149-154 (1970).

[10] Hertz, K. D. Danish investigations on silica fume concrete at elevated temperatures, *ACI Materials Journal*. vol. 89, no. 4, pp. 345-7 (1992).

[11] Chan, Y.N., Pang, G.F., and Chan, K.W. Comparison between high strength concrete and normal strength concrete subjected to high temperature. *Materials and Structures/Matériaux et Constructions*. vol. 29, pp. 616-619, (December 1996).

[12] Castillo, C. and Durrani, J.J. Effect of transient high temperature on high-strength concrete, *ACI Materials Journal*. pp. 47-53 (January-February 1990).

[14] Sheets, H. D., J.J. Bulloff and W.H. Duckworth: *Brick and Clay Record 133* No. 1, 55 pp. (1958).

[15] Bažant, Zdeněk P. and Kaplan, Maurice F. *Concrete at High Temperatures: Material Properties and Mathematical Models*. Longman Group Ltd., (London, 1996, 97).

[16] Neville, A.M. *Properties of Concrete*. Longman, 4th and final Edn., (London, 1997).

[17] Abrams, M.S. Compressive Strength of Concrete at Temperatures to 1600F, *Temperature and Concrete*. ACI SP-25, pp. 33-58 (Detroit, Michigan, 1971).

[18] Hannant, D.J. *Fiber Cements and Fiber Concretes*. John Wiley & Sons, (1978)

[19] Taylor, H.F.W. *Cement Chemistry*. Academic Press Limited, (London, 1990).

[20] Popovics, S. Effect of Curing Method and Final Moisture Condition on Compressive Strength of Concrete. *ACI Journal*. vol. 83, no. 4, pp. 650-7 (1986).

[21] Walker, S. and Bloem, D.L. Effects of Curing and Moisture Distribution on Measured Strength of Concrete. *Proc. Highw. Res. Bd*, vol. 36, pp. 334-46 (1957).

[22] Swamy, R.N. Fiber Reinforced Cement and Concrete. *Proceedings of the Fourth RILEM Internal* Symposium, E & FN Spon, (1992).

[23] Harmathy, T.Z. *Behavior of Concrete Under Temperature Extremes*, ACI SP-39, pp. 179-203 (Detroit, Michigan, 1973).

[24] Castillo, C. and Duranni, A.J. Effect of Transient High Temperature on High-Strength Concrete. *ACI Materials Journal*. vol. 87, no. 1, pp. 47-53 (1990).

[25] Maréchal, J.C. Variations in the Modulus of Elasticity and Poisson's Ratio with Temperature, *Int. Seminar on Concrete for Nuclear Reactors*. ACI SP-34, vol. 1, pp. 495-503 (Detroit, Michigan, 1972).

[26] Nasser, K.W. and Neville, A.M. Creep of Concrete at Elevated Temperatures. *J. Amer. Concr. Inst.* vol. 62, pp. 1567-79 (Dec. 1965).

[27] Nasser, K.W. and Chakraborty, M. Effects on Strength and Elasticity of Concrete, *Temperature Effects on Concrete*, ASTM Sp. *Tech. Publ. No. 858*, pp. 118-33 (Philadelphia, Pa, 1983).

[28] Jumppanen, U.–M. Effect of Strength on fire behavior of concrete, *Nordic Concrete Research*. Publication No. 8, pp. 116-27 (Oslo, Dec. 1989).

[29] Gonnerman, H.F. Effect of end condition of cylinder on compressive strength of concrete. *Proc. ASTM.* vol. 24, Part II, pp. 1036 (1924).

[30] Gjorv, O.E. High Strength Concrete. *Proceedings International CANMET Conference on Advances in Concrete Technology*. Athens ed. V. M. Malhotra, CANMET-Natural Resources Canada, Ottawa, pp. 19-82 (1992).

[31] American Concrete Institute Committee 544. State of the art report on fiber-reinforced concrete. *A.C.I. Journal*. Title No. 70-65, 729-744 (November 1973).

[32] Beckett, R. E. Patent positions and license agreements in Europe. *Conference on Properties and Applications of Fiber-reinforced Concrete*. Delft University, pp. 187-190 (1974).

[33] Lankard, D. R., and Sheets, H. D. Use of steel wires in refractory castables. *Ceramic Bulletin*. vol. 50, no. 5, pp. 497-500 (1971).

[34] Nishioka, K., Kakimi, N., and Yamakawa, S. and Shirakawa, K. Effective applications of steel fiber reinforced concrete. *Fiber-reinforced Cement and Concrete*. RILEM Symposium, pp. 425-433 (1975).

[35] Dhir, Ravindra K. and McCarthy, Michael J. Concrete Durability and Repair Technology. *Proceedings of the International Conference*. Thomas Telford, pp. 701, (Dundee, Scotland, Sep. 1999).

[36] Phan, Long T., Carino, Nicholas J., Duthinh, Dat, and Garboczi, Edward. International Workshop on Fire Performance of High-Strength Concrete. *Proc., NIST Sp.* Publ. No. 919 (Gaithersburg, MD, USA, Feb. 1997).

[37] Popovics, S. Effect of curing method and final moisture condition on compressive strength of concrete. *ACI Journal*. vol. 83, no. 4, pp. 650-7 (1986).

[38] Butcher, W. S. The effect of air-drying before test: 28-day strength of concrete. *Constructional Review*. pp. 31-2 (Sydney, Dec. 1958).

[39] Mills, R. H. Strength-maturity relationship for concrete which is allowed to dry. *RILEM Int. Symp. on Concrete and Reinforced Concrete in Hot Countries*. (Haifa, 1960).

[40] Galloway, J. W., Harding, H. M. and Raithby, K. D. *Effects of Moisture Changes on Flexural and Fatigue Strength of Concrete*. Transport and Road Research Laboratory, No. 864, pp. 18 (Crowthorne, U.K., 1979).

[41] Swamy, R. N. The technology of steel-fiber-reinforced concrete for practical applications. *Proceedings Institution of Civil Engineers*, Paper No. 7694, 1974, pp. 143-159.

[42] Lea, F. M. Cement research: retrospect and prospect. *Proc. 4th Int. Symp. On the Chemistry of Cement*, pp. 5-8 (Washington DC, 1960)

[43] Mills, R. H. Strength-maturity relationship for concrete which is allowed to dry, *RILEM Int. Symp. On Concrete and Reinforced Concrete in Hot Countries* (Haifa, 1960)

[44] Butcher, W. S. The effect of air-drying before test: 28-day strength of concrete, *Constructional Review*. pp. 31-2 (Sydney, Dec. 1958).

[45] Chan, Y.N., Peng, G.F. and Anson, M. Fire behavior of high-performance concrete made with silica fume at various moisture contents. *ACI Material Journal*. vol. 96, pp.405-409 (1999)

[46] Chan, Y.N., Peng, G.F. and Anson, M. Residual strength and pore structure of high-strength concrete and normal strength concrete after exposure to high temperatures. *Cement & Concrete Composites*. vol. 21, pp.23-27 (1999)

[47] ACI 211.1-91. Standard practice for selecting proportions for normal, heavyweight, and mass concrete, *ACI Manual of Concrete Practice, Part 1: Materials and General Properties of Concrete*, 38 pp. (Detroit, Michigan, 1994).

[48] Department of the Environment, *Design of Normal Concrete Mixes*, 42 pp. (Building Research Establishment, Watford, U.K., 1988).

[49] ACI 221.4R-93. Guide for selecting proportions for high-strength concrete with Portland cement and fly ash, *ACI Manual of Concrete Practice, Part 1: Materials and General Properties of Concrete*, 13 pp. (Detroit, Michigan, 1994).

[50] P.-C. Aïtcin, C. Jolicoeur and J. G. MacGregor. A look at certain characteristics of superplasticizers and their use in the industry, *Concrete International*, 16, No. 15, pp. 45-52 (1994).

[51] Chan, Y.N., Tsang, K.C., Chan, K.W. A systematic mix design method for high strength concrete, *Transactions of the Hong Kong Institution of Engineers*, vol.3, No.2, Sept., pp.1-6 (1996).

[52] Feng, N.Q. *Flowing Concrete*, Chinese Railway Publisher, China, (1988).

[53] Ramachandran, V.S. *Concrete Admixtures Handbook: Properties, Science, and Technology*, 2nd edition, Noyes Publications, New Jersy, (1995).

[54] Yilmaz, V.T., and Glasser, F.P. Early hydration of tricalcium aluminate-gypsum mixtures in the presence of sulphonated melamine formaldehyde superplasticizer, *Cement and Concrete Research*, vol. 21, pp.765-776 (1991).

[55] Blick, R.L., Peterson, C.F., and Winter, M.E. Proportioning and controlling high-strength concrete. *Proportioning Concrete Mixes*, SP-46. American Concrete Institute, Detroit, pp. 141-156 (1974).

[56] Metha, P.K., and Aitcin, P.C. Microstructural basis of selection of materials and mix proportions for high strength concrete, *H.S.C. Second International Symposium on Utilization of High-Strength Concrete*, Berkeley, California, SP-121. Edited by W.T. Hester, American Concrete Institute, Detroit, pp. 265-286 (1990).

[57] de Larrard, F. A method for proportioning high strength concrete mixtures, *Cement, concrete and aggregates*, CCAGDP, vol. 12, No. 2, Summer 1990, pp. 47-52 (1990).

[58] Luciano, J.J., Nmai, C.K. and DelGado, J.R. A novel approach to developing high strength concrete, *Concrete International*, May 1991, pp.25-29 (1991).

[59] Gutierrez, P.A., and Canovas, M.F. High performance concrete: requirements for constituent materials and mix proportioning, *ACI Materials Journal*, vol. 93 (3) pp.233-241 (1996).

[60] Rostasy, R.S., Weiss, R., and Wiedemann, G. Changes of pore structure of cement mortars due to temperatures. *Cement and Concrete Research 1980*; 10:157-164.

[61] Woods, H. Durability of Concrete Construction. *ACI and The Iowa State University Press*, USA, 1968.

[62] Crook, D.N. and Murray, M.J. Regain of strength after firing of concrete. *Magazine of Concrete Research 1970*; 22(72):149-154.

[63] Novokshchenov, V. Factors controlling the compressive strength of silica fume concrete in the range 100-150 MPa, *Magazine of Concrete Research*, 44, No.158, pp.53-61 (1992).

APPENDICES

APPENDIX I

PHOTOGRAPHS OF EQUIPMENT

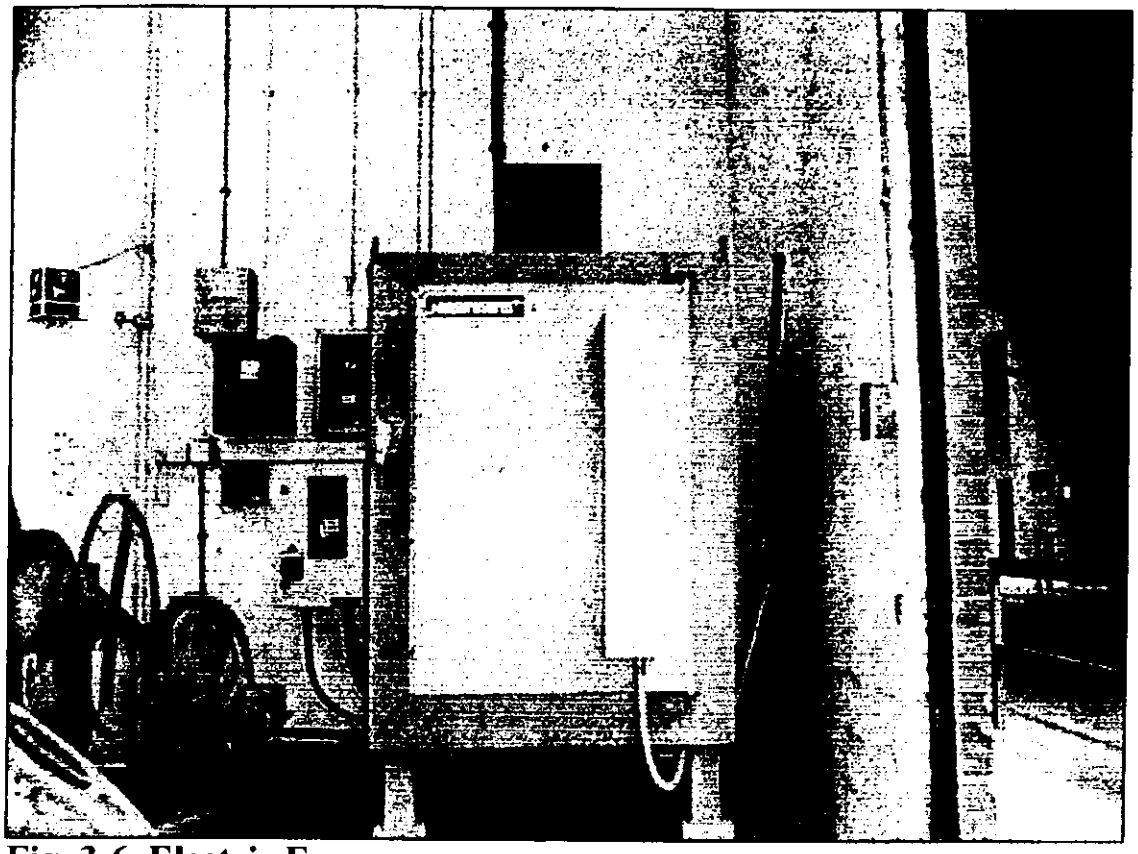

Fig. 3-6 Electric Furnace

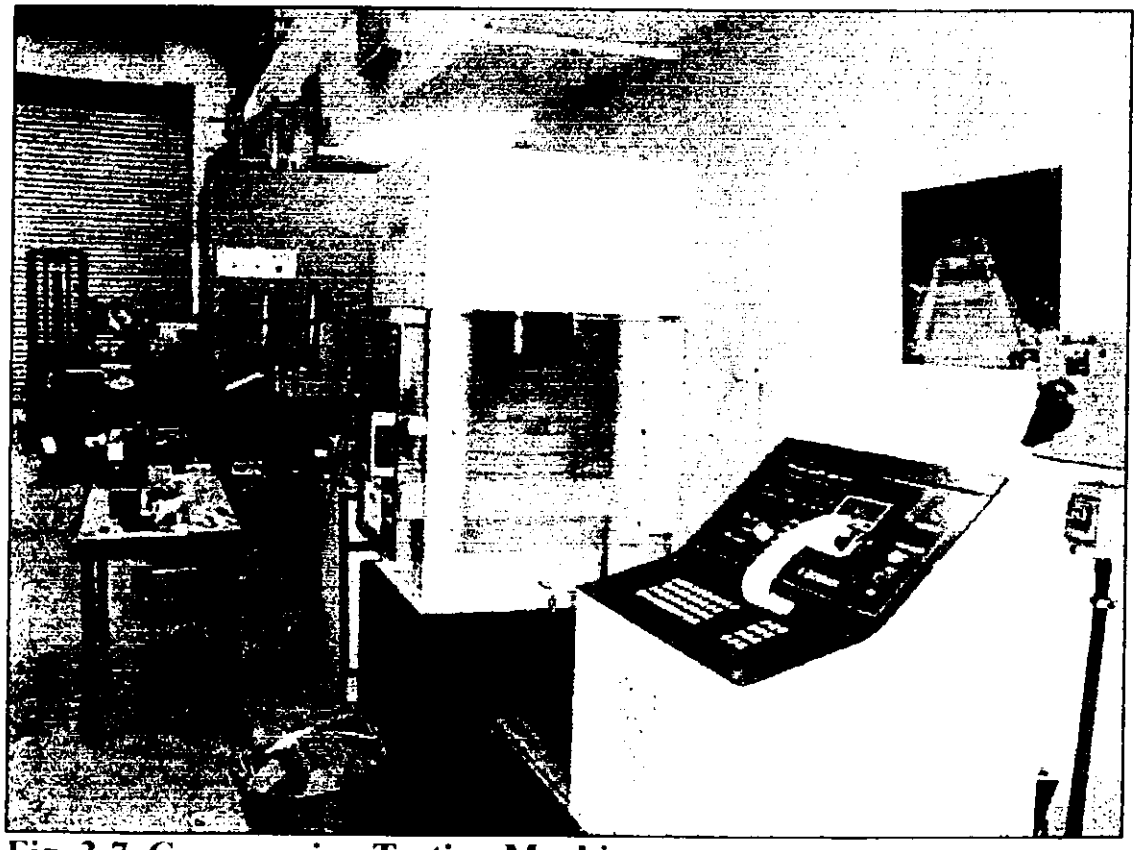

Fig. 3-7 Compression Testing Machine

APPENDIX II

SPECIFICATIONS FOR STRAIN GAUGE

The specification of PL-60-11 strain gauge is as follows:

Gauge factor = 2.09±1%,

Coefficient of thermal expansion = 11.8×10^{-6} / °C,

Temperature coefficient of gauge factor = +0.1 ± 0.05%/10 °C,

Apparent strain = $-3.12\times10^{-1}+3.01\times T^{1}-8.50\times10^{-2}\times T^{2}+6.56\times10^{-4}\times T^{3}-2.15\times10^{-6}\times T^{4}$

(μm/m) with a tolerance of ± 0.85 [(μm/m)/ °C]; where T is temperature (°C).

The specification of PFL-3-11 strain gauge is as follows:

Gauge factor = 2.13±1%,

Coefficient of thermal expansion = 11.8×10^{-6} / °C,

Temperature coefficient of gauge factor = +0.15 ± 0.05%/10 °C,

Apparent strain = $-1.62\times10^{-1}+1.63\times T^{1}-4.55\times10^{-2}\times T^{2}+2.27\times10^{-4}\times T^{3}+3.52\times10^{-8}\times T^{4}$

(μm/m) with a tolerance of ± 0.85 [(μm/m)/ °C]; where T is temperature (°C).

APPENDIX III

STATIC MODULUS OF ELASTICITY

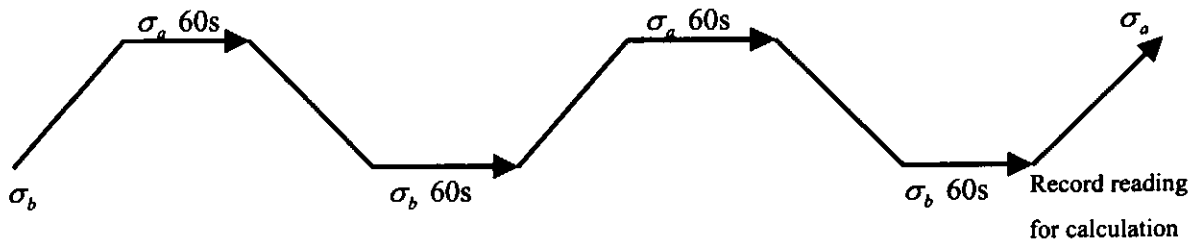

Fig. 3-8 Load cycling of Elasticity Modulus Test.

The static modulus of elasticity in compression E_c (in N/mm^2) is given by the formula:

$$\frac{\Delta_\sigma}{\Delta\varepsilon} = \frac{\sigma_a - \sigma_b}{\varepsilon_a - \varepsilon_b}$$

where

σ_a is the upper loading stress (in N/mm^2);

σ_b is the basic stress (i.e. 0.5 N/mm^2);

ε_a is the mean strain under the upper loading stress;

ε_b is the mean strain under the basic stress.

APPENDIX IV

MIX PROPORTIONING PROCEDURES

Step 1: Determination of Free Water to Cement Ratio.

First of all, find out the target mean strength by summing up the characteristic strength and the margin according to calculations Eq.1 and Eq.2,

$$M = k \times s \qquad (Eq.1)$$

Where s is the standard deviation which is stipulated in D.O.E. mix design manual and is based on the experience and the result of the laboratory test, M is the margin, and K is a value which is appropriate to the 'percentage defectives' permitted below the characteristic strength:

K for 10% defectives = 1.28

K for 5% defectives = 1.64

K for 2.5% defectives = 1.96

K for 1% defectives = 2.33

In this research study, the percentage defective value K, which was assumed for all concrete mix proportion.

The target mean strength is expressed as follows:

$$f_m = f_c + M \qquad (Eq.2)$$

where f_m is the target mean strength, f_c is the specified characteristic strength, and M is the margin.

Next, the compressive strength value is obtained from Table A-1 for a concrete mix made with specific types of aggregates and a free water / cement ratio of 0.5 at an age of 28 days.

Table A-1 Approximate Compressive Strengths of Concretes made with a Free Water/Cement Ratio of 0.5 According to the 1988 British Method.

Type of Cement	Type of coarse aggregate	Compressive Strength (N/mm^2) at an age of (days):			
		3	7	28	91
Ordinary Portland Cement (OPC)	Uncrushed	22	30	42	49
	Crushed	27	36	49	56

This strength value is then plotted on the chart of relationship between compressive strength and free water/cement ratio in 1988 British mix selection method [48]. The corresponding value for the free water / cement ratio can then be read from the abscissa. In this proportioning method, the lowest w/c ratio is limited to 0.22

Step 2: Determination of Free-Water Content.

According to the maximum size of aggregate and the types of aggregate used, the free water content can be determined in the British mix selection method [48] under the condition of 0 to 10 mm slump for HPC and 60 to 180 mm slump for NSC. The target workability is attained by incorporating an appropriate amount of superplasticizer during the trial mixing process.

In the case of coarse and fine aggregates of different types are used, the total free water content is estimated by the following equation:

$$\frac{2}{3} W_f + \frac{1}{3} W_c \qquad \textit{(Eq.3)}$$

where W_f is the free water requirement for fine aggregate and W_c is the free water requirement for coarse aggregate.

Step 3: Determination of Cement Content.

To determine the cement content, it is simply the water content divided by the water/cement ratio. This cement content must not conflict with any minimum value specified for reasons of durability or a maximum value specified for reasons of heat development. In accordance with BS 8110: Part 1, 1985, the maximum cement content is limited to 550 kg/m^3 for the consideration of crack due to thermal stresses and drying shrinkage.

Stage 4: Determination of Total Aggregate Content.

To determine the total aggregate content, this requires an estimate of the fresh density of fully compacted concrete, which can be read off from the estimated wet density chart for fully compacted concrete in the D.O.E. mix selection manual [48]. The wet density depends on the free water content and the relative density (or specific gravity) of the combined aggregate in the saturated surface-dry condition (SSD). The total aggregate content is expressed as:

Total aggregate content (SSD) = D – C – W *(Eq.4)*

Where D = the wet density of concrete (kg/m^3); C = the cement content (kg/m^3); and W = the free water content (kg/m^3).

Step 5: Determination of Fine Aggregate Content.

This procedure determines the proportion of fine aggregate in the total aggregate, using the recommended values in 1988 British mix selection method [48] according to the percentage passing the 600 μm sieve depending on the maximum size of aggregate, the level of workability, and the water/cement ratio. Once the proportion of fine aggregate has been obtained, multiplying it by the total aggregate content gives the content of fine aggregate. The content of coarse aggregate is then the difference between the total aggregate content and the content of fine aggregate. The coarse aggregate, in turn, should be divided into size fractions depending on the aggregate shape. According to the 1988 British Method [48], the proportion of coarse aggregate fractions which is approximately one-third of the total coarse aggregate content for the 10 mm coarse

aggregate and two-third of the total coarse aggregate content for the 20 mm coarse aggregate.

APPENDIX V

MIX DESIGN EXAMPLE

Step 1: The 28 days characteristic strength of 30 MPa is specified, 5% defectives is assumed, and hence $k = 1.64$. From Equations (1) and (2), M = 13.12 MPa, thus, $f_m = 30 + 13.2 = 43.12$ MPa. From the 1988 British mix selection method [48], for ordinary Portland cement and crushed aggregate, it is found that the 28-day strength to be 49 MPa. With this value corresponding to a water/cement ratio of 0.5 in D.O.E. mix design manual, we obtain a specified strength of 43.12 MPa. Finally, it gives the water/cement ratio of 0.56. Check whether the water/cement ratio is greater than the lowest w/c ratio value 0.22.

Step 2: For maximum aggregate size of 20 mm and slump ranged from 60 to 180 mm, it is found that the water requirement for the uncrushed and crushed type of aggregate to be 195 and 225 kg/m^3 respectively. From Equation (3), the free water requirement is $\frac{2}{3}(195) + \frac{1}{3}(225) = 205$ kg/m^3.

Step 3: The cement content is 205/0.56 = 336 kg/m^3. Check whether the cement content value is less than 550 kg/m^3.

Step 4: For water content of 205 kg/m^3 and aggregate with a specific gravity of 2.60, the required fresh density of concrete is found to be 2350 kg/m^3. The total aggregate content is given by Equation (4) which is 2350 – 366 – 205 = 1779 kg/m^3.

Step 5: For the maximum size of aggregate of 20 mm and a slump between 60 and 80 mm, on the line representing fine aggregate with 70 per cent passing the 600 μm sieve, at a water/cement ratio of 0.56, the particular diagram gives the proportion of fine aggregate is 35 per cent by mass of total aggregate. Hence, the fine aggregate content is 1779 × 35% = 623 kg/m^3. The total coarse aggregate content is 1779 – 623 = 1156 kg/m^3. Thus, the 10 mm aggregate content is $\frac{1}{3}(1156)$ = 385 kg/m^3, and the 20 mm aggregate content is $\frac{2}{3}$ (1156) = 771 kg/m^3.

APPENDIX VI

MOISTURE CONTENT DETERMINIATION METHOD

Moisture content is defined as the ratio of the quantity of evaporable water within a specimen at the time of the test to its original evaporable water quantity when just taken out from the water-curing tank. The moisture content percentage can be expressed in terms of W_f and W_i as:

$$m = \frac{W_f}{W_i} \times 100\% \qquad (Eq.5)$$

where m is the moisture content of specimen as a percentage; W_i is the total evaporable water quantity within the specimen when just removed from the curing water, i.e. the evaporable water in a fully saturated specimen, in kg; and W_f is the evaporable water quantity within the specimen at the time of the test, in kg.

If the total evaporable water percentage of a fully saturated specimen is R, then R can be defined as:

$$R = \frac{W_0 - W_d}{W_0} \qquad (Eq.6)$$

Where W_0 = the weight of the saturated specimen just taken from the curing water, in kg;

W_d = the weight of the oven-dried specimen reaches its constant, in kg.

If the evaporable water quantity of the saturated specimen is R multiplied by the weight of the saturated specimen, and R has been determined by using a number of representative specimens from the same concrete batch, then m can be expressed as:

$$m = (1 - \frac{\Delta W}{W_0 \bullet R}) \times 100\% \qquad (Eq.7)$$

where $\Delta W = W_0 - W_t$, in kg;

W_0 = the weight of the saturated specimen just taken from the curing water, in kg;

W_t = the actual weight of the specimen at the time of the test, in kg.

Substituting $\Delta W = W_0 - W_t$ in Equation (7) gives:

$$m = (1 - \frac{W_0 - W_t}{W_0 \bullet R}) \times 100\% \qquad (Eq.8)$$

Rearrange Equation (8), the actual weight of the specimen at the time of the test can be expressed as:

$$W_t = W_0 - (W_0 \bullet R)(1 - m) \qquad (Eq.9)$$

APPENDIX VII

DETERMINATION OF FLEXURAL STRENGTH

The flexural strength has been determined on the basis of ordinary elastic theory:

$$\text{Flexural strength: } f = \frac{P \bullet L}{b \bullet d^2} \qquad \textit{(Eq.10)}$$

where P is the maximum total load on the beam, L is the span, b is the width of the beam, and d is the depth of the beam.

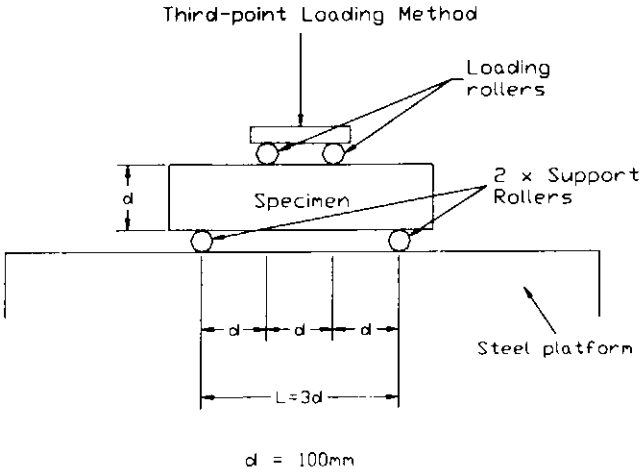

Fig. 3-11 Flexural Strength Test.

APPENDIX VIII

RAW DATA

Table A-A. Scattered Results of 28-Day Compressive Strength for All Concrete Mixes subjected to No Heating.

Mixes	**Compressive Strength (MPa)**										**Average (MPa)**
M-1	34	41	42	35	38	37	39	41	39	42	39
M-2	57	54	49	57	52	51	51	53	53	56	53
M-3	101	105	100	97	95	93	97	99	105	100	99
M-1F	48	50	43	43	45	42	46	44	43	44	45
M-2F	60	62	65	65	61	57	60	58	55	60	60
M-3F	105	102	104	102	115	118	110	114	111	115	110

Table A-B. Scattered Compressive Strength Results for concrete after Heating and Tested at Room Temperature, (MPa)

Concrete	Moisture	Maximum Temperature, (°C)																																				
Mixes	Content	25	105			Avg	200			Avg	300			Avg	400			Avg	600			Avg	800			Avg	1000			Avg	1100			Avg	1200			Avg
M-1	20%	-	38	39	42	40	37	37	40	38	36	36	37	36	30	32	34	32	20	25	26	24	12	14	15	14	5	8	6	6	4	6	5	5	11	10	11	11
	60%	-	35	37	38	37	35	35	35	35	34	31	36	34	30	29	30	30	21	18	25	21	13	11	12	12	6	6	7	6	5	5	4	5	10	10	10	10
	100%	39	32	35	38	35	30	32	33	32	29	30	30	30	25	30	29	28	15	19	21	18	10	10	9	10	5	3	4	4	4	3	5	4	5	6	6	6
M-2	20%	-	50	52	48	50	42	46	49	46	38	39	39	39	36	34	37	36	34	36	31	34	20	16	15	17	9	7	7	8	9	7	7	8	14	15	15	15
	60%	-	45	48	48	47	40	39	39	39	35	39	40	38	30	34	36	33	28	31	29	29	15	14	19	16	6	8	9	8	5	9	7	7	15	13	16	15
	100%	53	45	44	46	45	36	35	36	36	36	32	33	34	32	34	31	32	21	22	22	22	14	12	12	13	4	6	7	6	6	6	5	6	9	10	10	10
M-3	20%	-	103	101	100	101	99	98	101	99	92	98	97	96	94	92	96	94	52	58	57	56	32	33	34	33	13	12	11	12	12	11	10	11	19	19	18	19
	60%	-	99	95	100	98	96	97	97	97	95	95	90	93	89	85	86	87	55	51	61	56	28	27	34	30	13	13	11	12	10	13	11	11	17	18	19	18
	100%	99	94	98	96	96	94	96	96	95	90	89	90	90	80	88	86	85	50	48	52	50	24	28	25	26	8	7	9	8	17	19	20	19	14	15	15	15
M-1F	20%	-	44	46	47	46	42	43	40	42	37	38	38	38	33	32	40	35	32	32	32	32	18	15	16	16	7	7	9	8	7	6	7	7	13	15	13	14
	60%	-	41	42	43	42	37	38	38	38	34	36	38	36	32	32	33	32	25	20	26	24	11	18	13	14	6	9	6	7	6	6	5	6	13	12	13	13
	100%	45	41	41	40	41	34	34	34	34	30	33	33	32	29	31	29	30	16	24	20	20	12	15	10	12	5	6	4	5	5	4	5	5	8	8	7	8
M-2F	20%	-	60	59	61	60	56	58	59	58	52	56	55	54	50	49	52	50	35	40	36	37	18	19	19	19	7	8	8	8	8	9	10	9	19	20	16	18
	60%	-	53	52	54	53	49	50	50	50	47	47	46	47	42	45	44	44	34	38	36	36	15	18	20	18	8	6	9	8	7	7	9	8	17	18	15	17
	100%	60	50	51	50	50	49	49	47	48	43	45	46	45	40	40	41	40	30	35	35	33	16	19	17	17	6	6	5	6	6	9	8	8	14	13	14	14
M-3F	20%	-	110	112	113	112	105	106	106	106	102	101	104	102	99	101	100	100	69	70	67	69	35	38	37	37	15	13	14	14	11	11	13	12	19	19	18	19
	60%	-	106	105	109	107	104	104	105	104	96	96	97	96	93	94	96	94	71	67	69	69	32	30	36	33	12	14	15	14	10	11	13	11	19	20	18	19
	100%	110	100	100	101	100	96	96	98	97	92	95	94	94	85	96	90	90	61	67	66	65	27	26	30	28	10	15	11	12	10	8	11	10	15	19	17	17

Note: Control specimens at laboratory temperature about 25 °C

Table A-C. Scattered Flexural Strength Results for Concrete after Heating and Tested at Room Temperature, (MPa)

Temp. (°C)	M-1F			Avg.	M-2F			Avg.	M-3F			Avg.	M-1			Avg.	M-2			Avg.	M-3			Avg.
25	6.53	5.48	6.00	6.00	7.87	8.14	8.00	8.00	10.50	10.65	10.80	10.65	4.52	4.77	4.92	4.74	6.80	6.96	7.23	7.00	9.02	8.70	9.29	9.00
105	4.86	5.33	5.41	5.20	7.51	7.55	7.45	7.50	8.73	9.29	8.31	8.78	4.53	4.52	4.48	4.51	6.33	6.40	6.78	6.50	8.90	8.10	8.50	8.50
200	4.30	6.20	4.55	5.02	6.98	6.82	7.21	7.00	8.35	8.60	8.55	8.50	4.33	4.36	4.35	4.35	5.34	5.58	5.59	5.50	7.80	7.89	8.30	8.00
300	3.64	3.95	3.73	3.77	5.33	5.28	5.30	5.30	7.02	6.98	7.00	7.00	3.40	3.56	3.53	3.50	5.00	4.83	5.18	5.00	5.80	6.00	6.20	6.00
400	3.00	3.50	2.50	3.00	4.12	3.89	4.00	4.00	5.70	5.80	6.50	6.00	2.10	2.20	1.70	2.00	3.68	3.82	3.59	3.70	4.73	4.97	5.30	5.00
600	1.50	1.00	1.25	1.25	2.59	2.44	2.48	2.50	4.35	3.90	3.75	4.00	0.89	0.90	1.20	1.00	2.14	1.96	1.91	2.00	2.99	2.86	3.14	3.00
800	0.15	0.16	0.12	0.14	0.79	0.82	0.90	0.84	1.56	1.87	1.92	1.78	0.15	0.13	0.11	0.13	0.63	0.65	0.69	0.66	0.94	0.92	0.91	0.92
1000	0.16	0.19	0.17	0.17	0.26	0.23	0.24	0.24	0.42	0.43	0.40	0.42	0.08	0.10	0.11	0.10	0.21	0.21	0.19	0.20	0.26	0.29	0.28	0.28
1100	0.52	0.45	0.43	0.47	0.38	0.32	0.35	0.35	0.97	0.94	1.05	0.99	0.03	0.02	0.01	0.02	0.14	0.11	0.10	0.12	0.33	0.30	0.28	0.30

Note: Control specimens at laboratory temperature about 25 °C

Table A-D. Scattered Results of Static Modulus of Elasticity under Temperature Effect, (GPa).

Temperature (°C)	M-1			Average	M-1F			Average	M-3			Average	M-3F			Average
25	27	31	31	30	35	36	33	35	67	69	73	70	83	80	82	82
105	27	29	28	28	27	32	30	30	52	54	53	53	54	57	53	55
300	27	26	24	26	28	25	30	28	49	54	50	51	53	50	55	53
600	11	18	15	15	19	17	16	17	36	35	31	34	37	46	38	40
800	5	8	10	8	9	9	11	10	20	18	22	20	23	24	21	23
1100	2	2	2	2	2	2	2	2	4	5	5	5	6	8	6	7
1200	-	-	-	Immeasurable	-	-	-	Immeasurable	-	-	-	Immeasurable	-	-	-	Immeasurable

Table A-E. Scattered Results of Poison's Ratio under Temperature Effect

Temperature (°C)	M-1			Average	M-1F			Average	M-3			Average	M-3F			Average
25	0.15	0.14	0.16	0.15	0.2	0.2	0.2	0.16	0.20	0.21	0.21	0.21	0.23	0.21	**0.22**	0.22
105	0.10	0.14	0.15	0.13	0.1	0.1	0.2	0.14	0.17	0.18	0.21	0.19	0.21	0.20	0.21	0.21
300	0.12	0.10	0.11	0.11	0.1	0.1	0.1	0.13	0.17	0.17	0.15	0.16	0.18	0.18	0.20	0.19
600	0.06	0.06	0.07	0.06	0.1	0.1	0.1	0.07	0.06	0.09	0.11	0.09	0.10	0.09	0.11	0.10
800	0.02	0.06	0.04	0.04	0	0.1	0.1	0.05	0.07	0.06	0.07	0.07	0.09	0.06	0.08	0.08
1100	0.01	0.01	0.01	0.01	0	0	0	0.01	0.02	0.02	0.02	0.02	0.02	0.02	0.02	0.02

Table A-F. Scattered Results of Increase in Porosity Percentage of Concrete after Heating to Various Temperatures, per cent

Concrete Mixes	Moisture Content	Maximum Heating Temperature (°C)																	
		25			Average	105			Average	300			Average	800			Average	1000			Average
M-1	20%	-	-	-	-	9	10	10	10	19	18	20	19	23	22	21	22	18	19	18	18
	60%	-	-	-	-	17	15	18	17	20	20	21	20	23	23	24	23	20	20	20	20
	100%	13	14	13	13	22	20	23	22	24	24	27	25	31	29	30	30	19	19	21	20
M-3	20%	-	-	-	-	6	8	7	7	10	10	10	10	11	11	13	12	8	9	8	8
	60%	-	-	-	-	10	10	9	10	12	11	10	11	13	12	13	13	10	10	10	10
	100%	5	6	9	7	10	12	13	12	19	18	19	19	20	20	19	20	11	12	11	11
M-1F	20%	-	-	-	-	8	10	7	8	13	14	15	14	15	17	16	16	13	15	14	14
	60%	-	-	-	-	11	14	13	13	18	18	17	18	17	20	19	19	13	15	16	15
	100%	10	13	12	12	15	15	14	15	21	20	20	20	24	23	24	24	19	17	16	17
M-3F	20%	-	-	-	-	4	5	5	5	7	8	9	8	8	9	9	9	3	4	4	4
	60%	-	-	-	-	7	8	8	8	9	9	8	9	11	11	12	11	5	5	5	5
	100%	4	8	5	6	8	10	9	9	12	12	11	12	14	12	15	14	7	8	9	8

Note: Control specimens at the laboratory temperature about 25 °C

Table A-G. Scattered Results of Increase in Average Pore Diameter in Concrete after Heating to Various Temperatures, ($x10^{-6}$ m)

Concrete Mixes	Moisture Content	Maximum Heating Temperature (°C)																			
		25			Avg.	105			Avg.	300			Avg.	800			Avg.		1000		Avg.
M-1	20%	-	-	-	-	0.03	0.04	0.04	0.04	0.05	0.08	0.07	0.07	0.09	0.14	0.11	0.11	0.28	0.30	0.32	0.30
	60%	-	-	-	-	0.06	0.05	0.06	0.06	0.08	0.08	0.08	0.08	0.16	0.2	0.17	0.18	0.33	0.35	0.36	0.35
	100%	0.04	0.06	0.05	0.05	0.07	0.05	0.08	0.07	0.10	0.09	0.08	0.09	0.22	0.24	0.25	0.24	0.53	0.52	0.59	0.55
M-3	20%	-	-	-	-	0.02	0.02	0.02	0.02	0.06	0.05	0.06	0.06	0.10	0.09	0.11	0.10	0.15	0.14	0.17	0.15
	60%	-	-	-	-	0.04	0.05	0.05	0.05	0.06	0.06	0.07	0.06	0.12	0.10	0.11	0.11	0.19	0.18	0.15	0.17
	100%	0.03	0.04	0.04	0.04	0.05	0.06	0.07	0.06	0.08	0.07	0.07	0.07	0.13	0.12	0.13	0.13	0.40	0.48	0.44	0.44
M-1F	20%	-	-	-	-	0.03	0.02	0.04	0.03	0.05	0.06	0.06	0.06	0.12	0.13	0.14	0.13	0.20	0.22	0.23	0.22
	60%	-	-	-	-	0.05	0.05	0.06	0.05	0.08	0.08	0.09	0.08	0.14	0.15	0.15	0.15	0.29	0.31	0.30	0.30
	100%	0.04	0.05	0.07	0.05	0.07	0.08	0.07	0.07	0.07	0.08	0.08	0.08	0.16	0.16	0.17	0.16	0.52	0.45	0.49	0.49
M-3F	20%	-	-	-	-	0.03	0.03	0.03	0.03	0.04	0.04	0.04	0.04	0.07	0.07	0.07	0.07	0.10	0.09	0.07	0.09
	60%	-	-	-	-	0.04	0.05	0.05	0.05	0.05	0.06	0.06	0.06	0.10	0.10	0.09	0.10	0.10	0.11	0.11	0.11
	100%	0.03	0.02	0.03	0.03	0.05	0.07	0.06	0.06	0.07	0.04	0.06	0.06	0.11	0.12	0.12	0.12	0.23	0.20	0.25	0.23

Note: Control specimens at the laboratory temperature about 25 °C

APPENDIX IX

GRAPHS

Fig. 3-1 Aggregate sieve analysis report: Grading of aggregate - 10mm

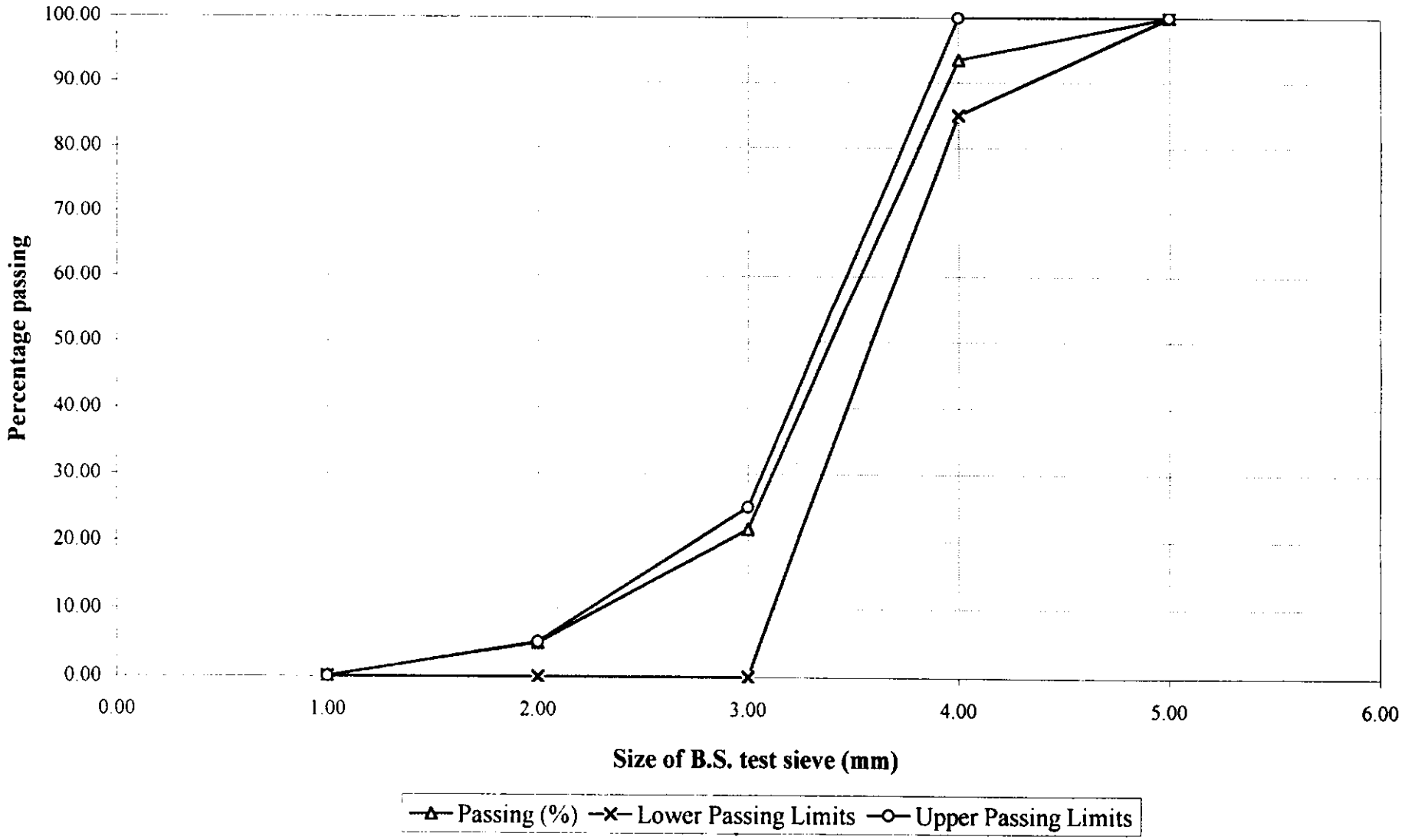

Fig. 3-2 Aggregate sieve analysis report: Grading of aggregate - 20mm

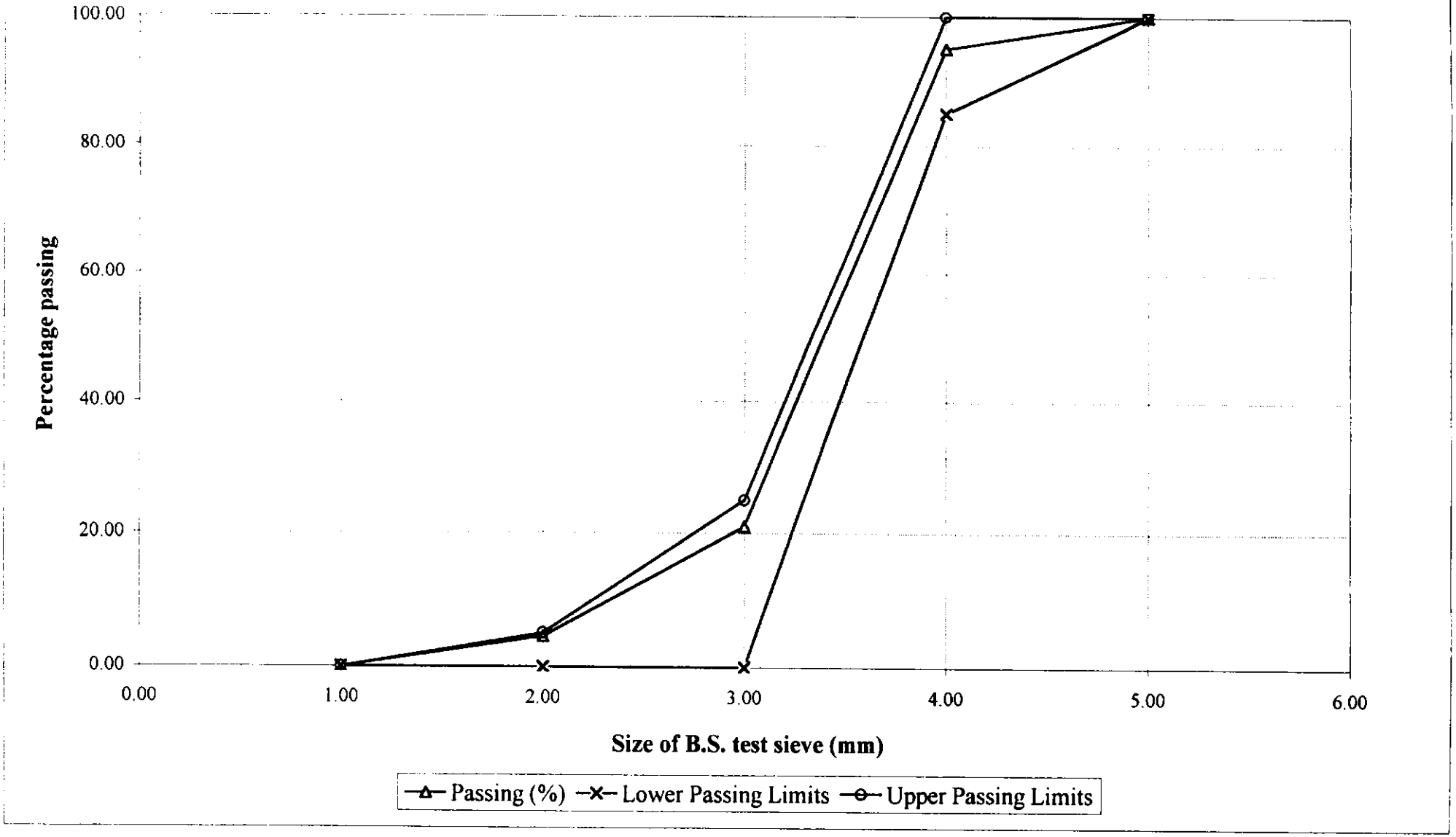

Fig. 3-3 Aggregate sieve analysis report: Grading of aggregate - Fine

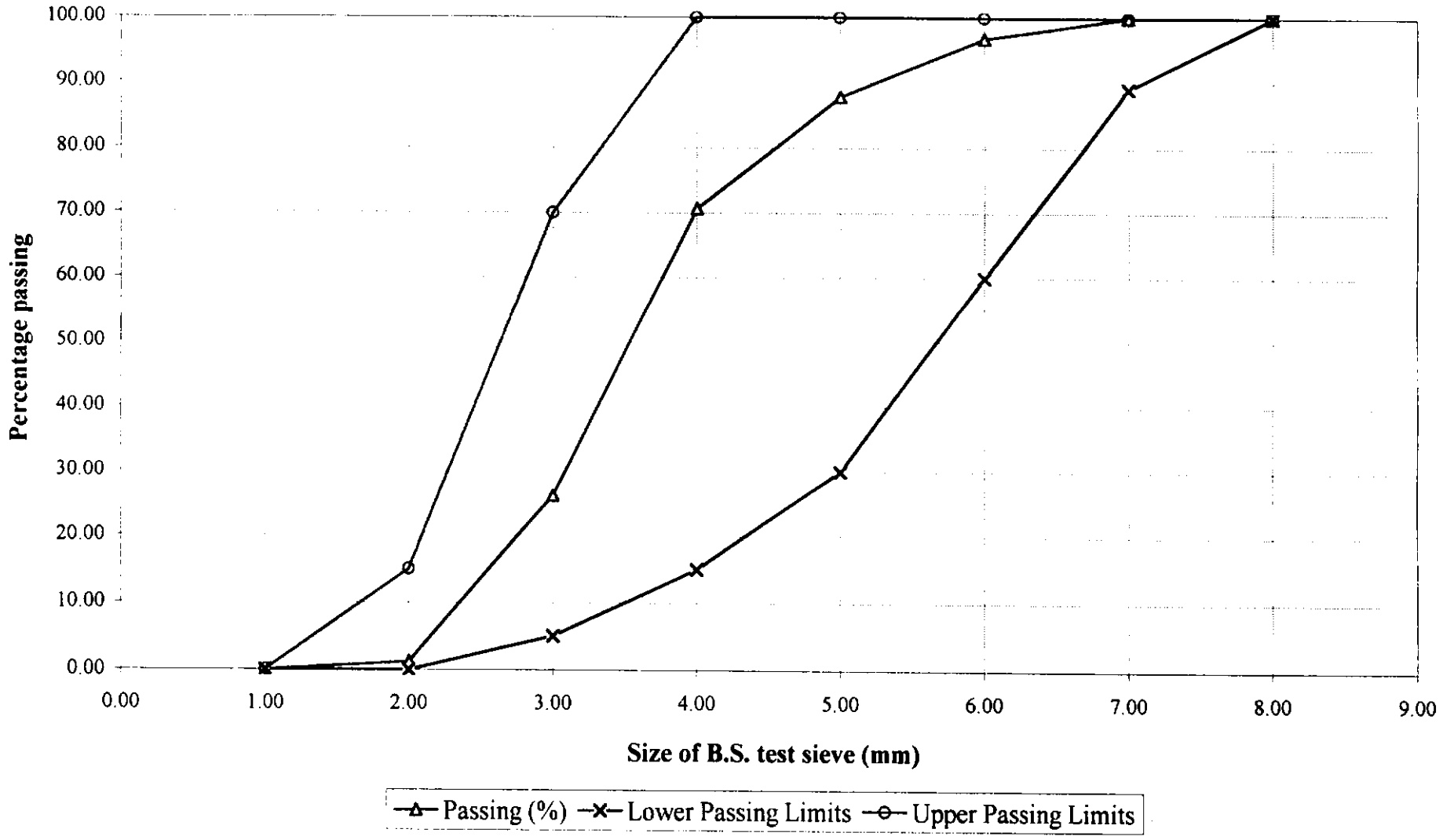

Fig. 3-4. Compressive Strength vs. Free W/C ratio for Control Mixes

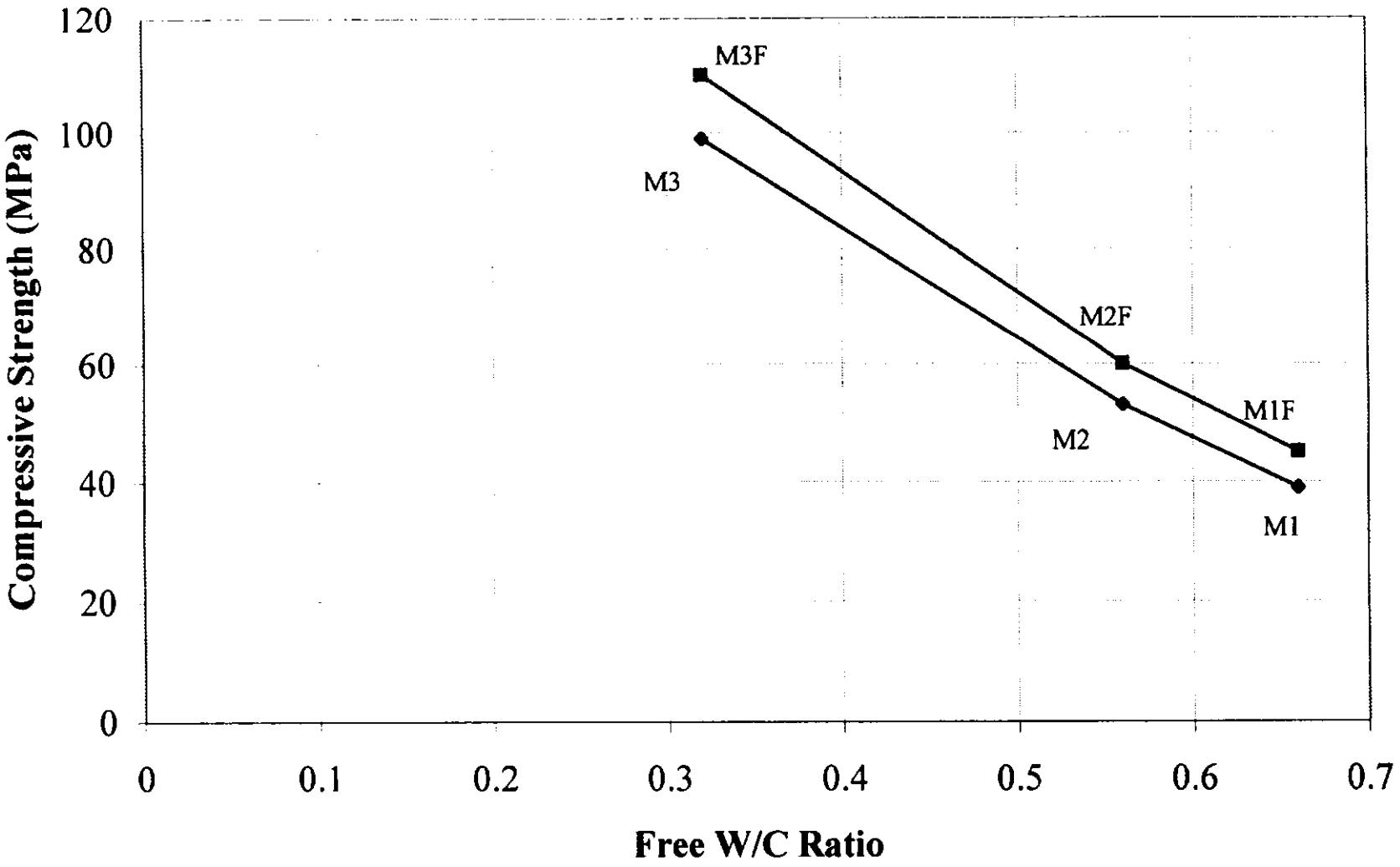

Fig. 3-5 28 days strength development of concrete mixes

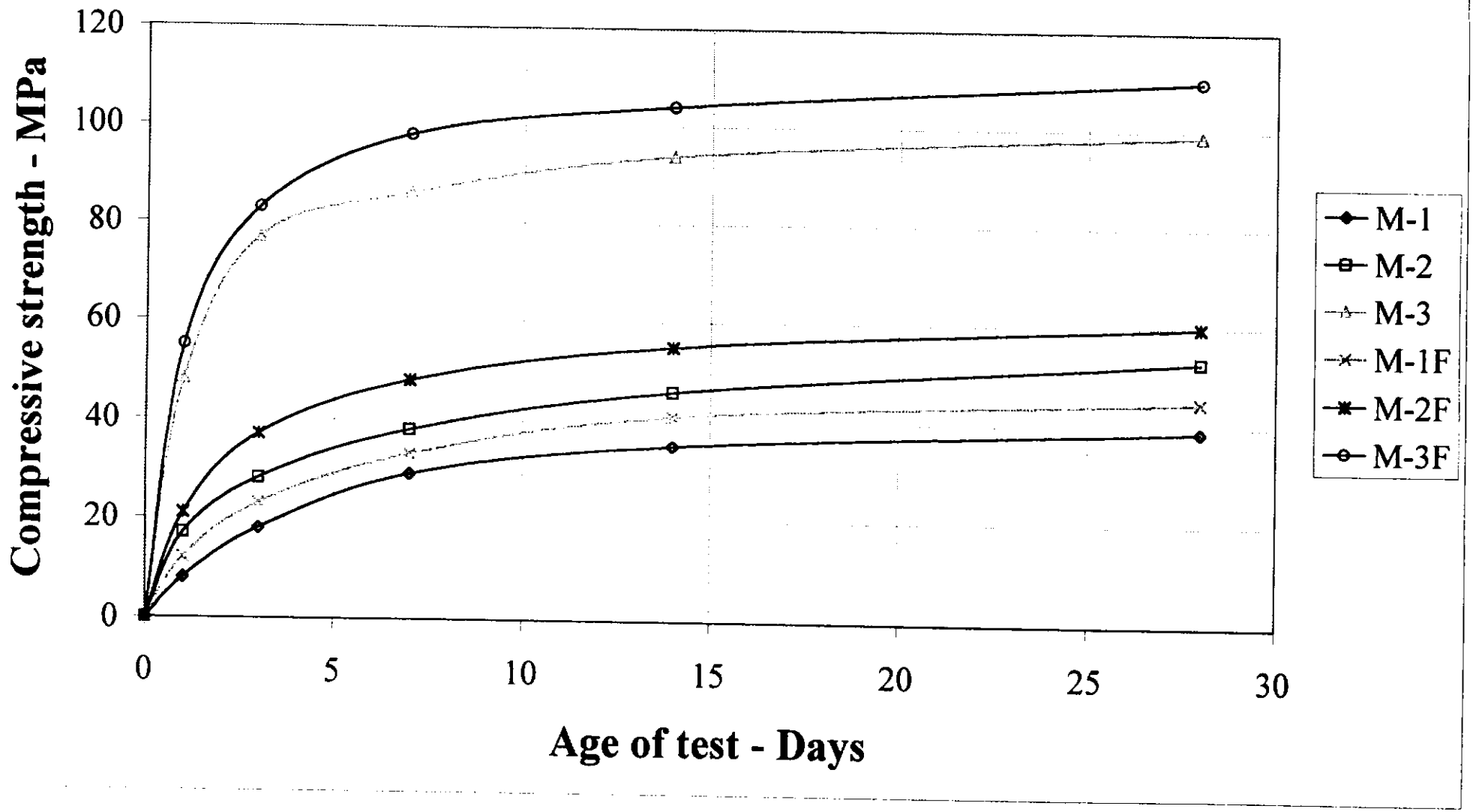

Fig. 4-1. Compressive Strength for Control Mixes

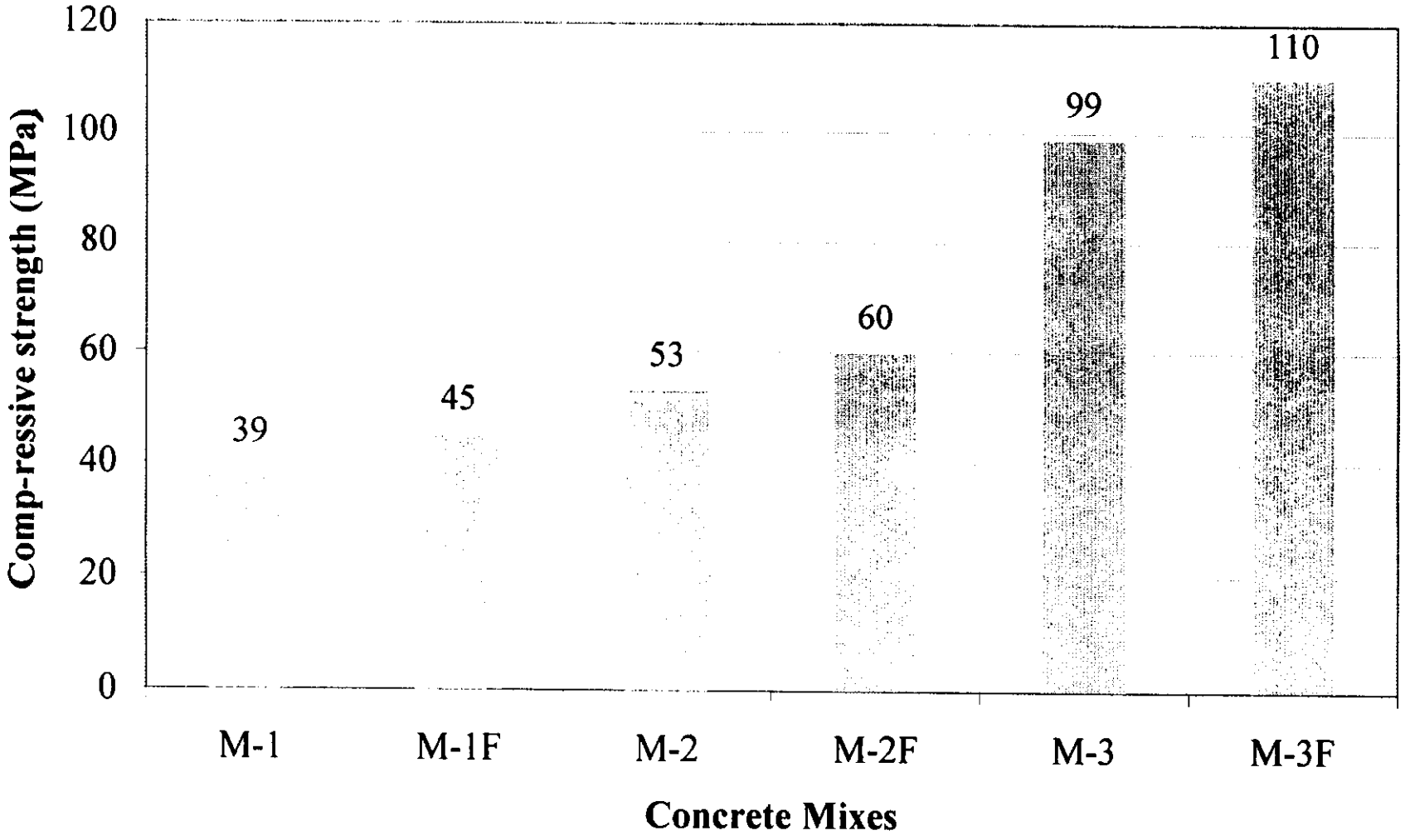

Fig. 4-2 Compressive Strength vs. Maximum Heating Temperature at Initial Moisture Content of 20%

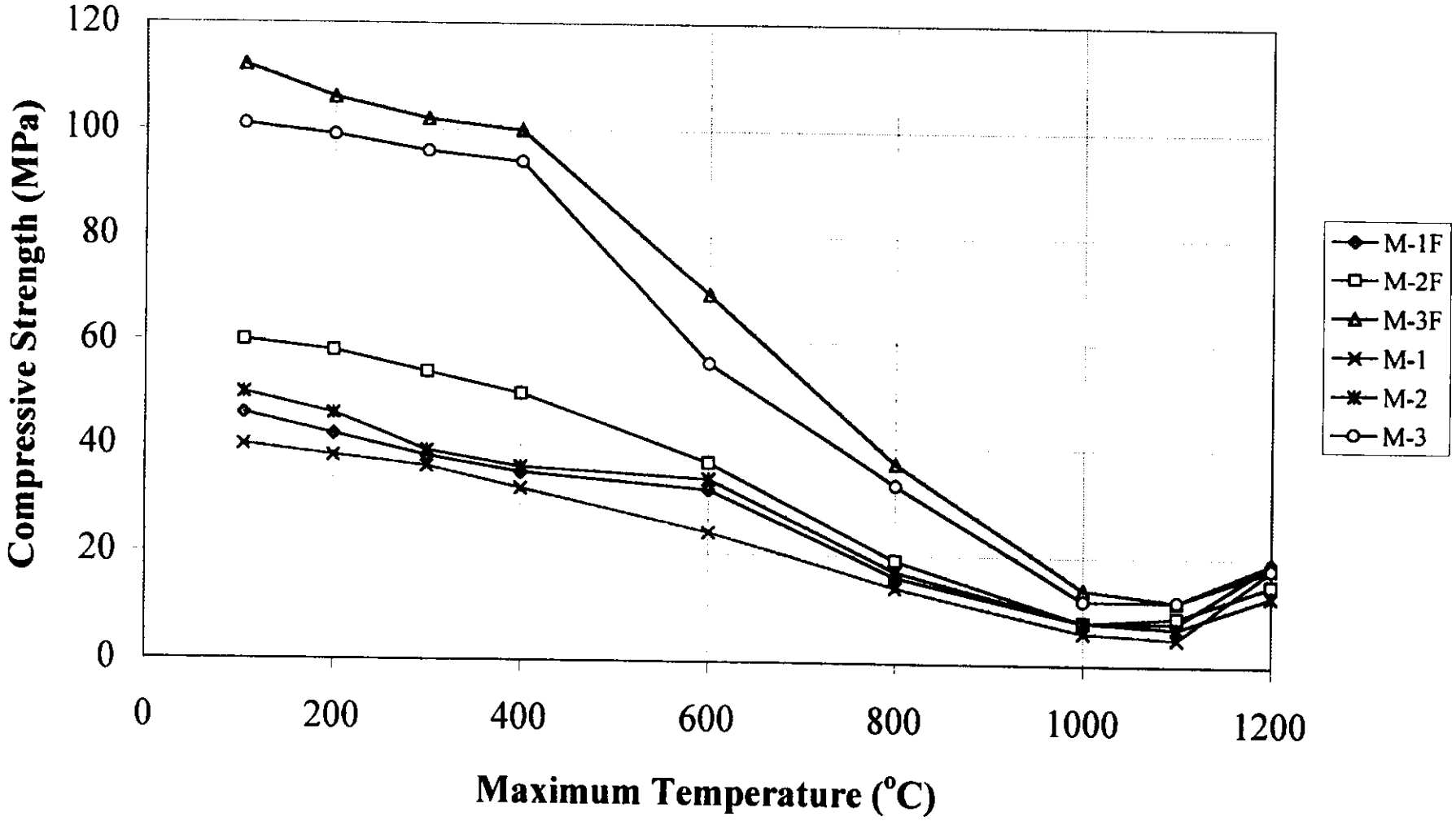

Fig. 4-3 Compressive Strength vs. Maximum Heating Temperature at Initial Moisture Content of 60%

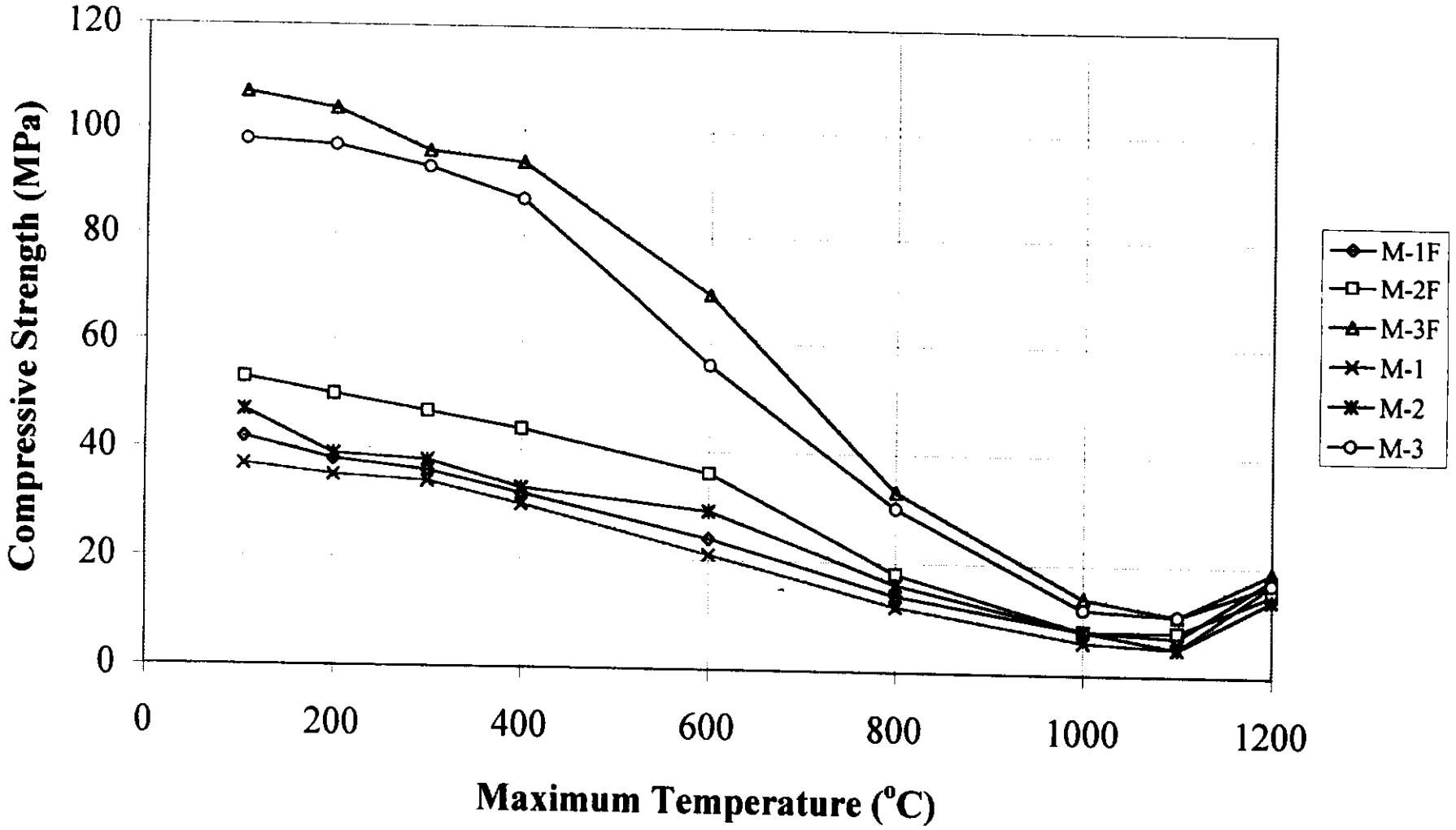

Fig. 4-4 Compressive Strength vs. Maximum Heating Temperature at Initial Moisture Content of 100%

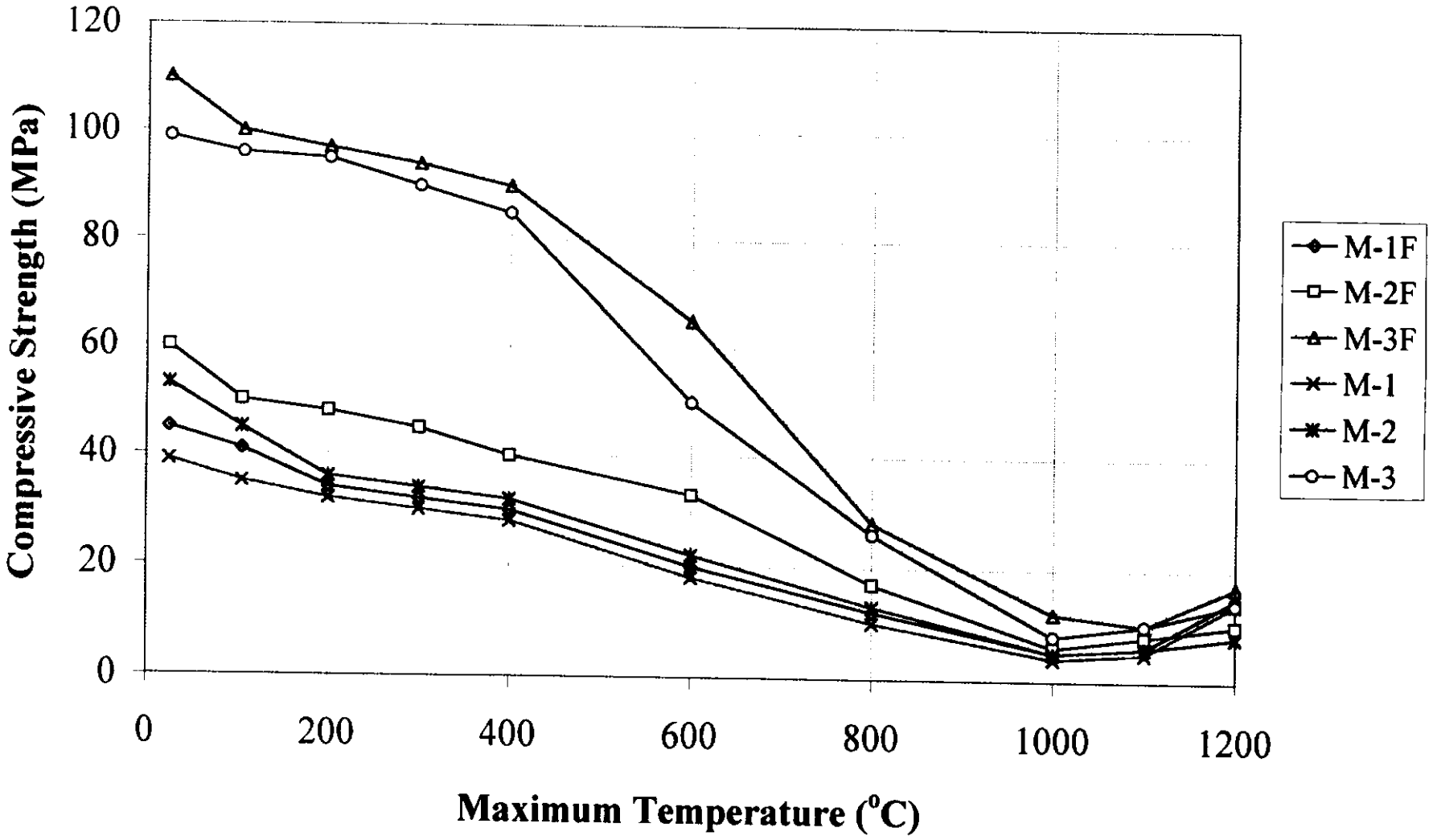

Fig. 4-5 Compressive Strength vs. Initial Moisture Content after Heating to a Maximum Temperature of 105 °C

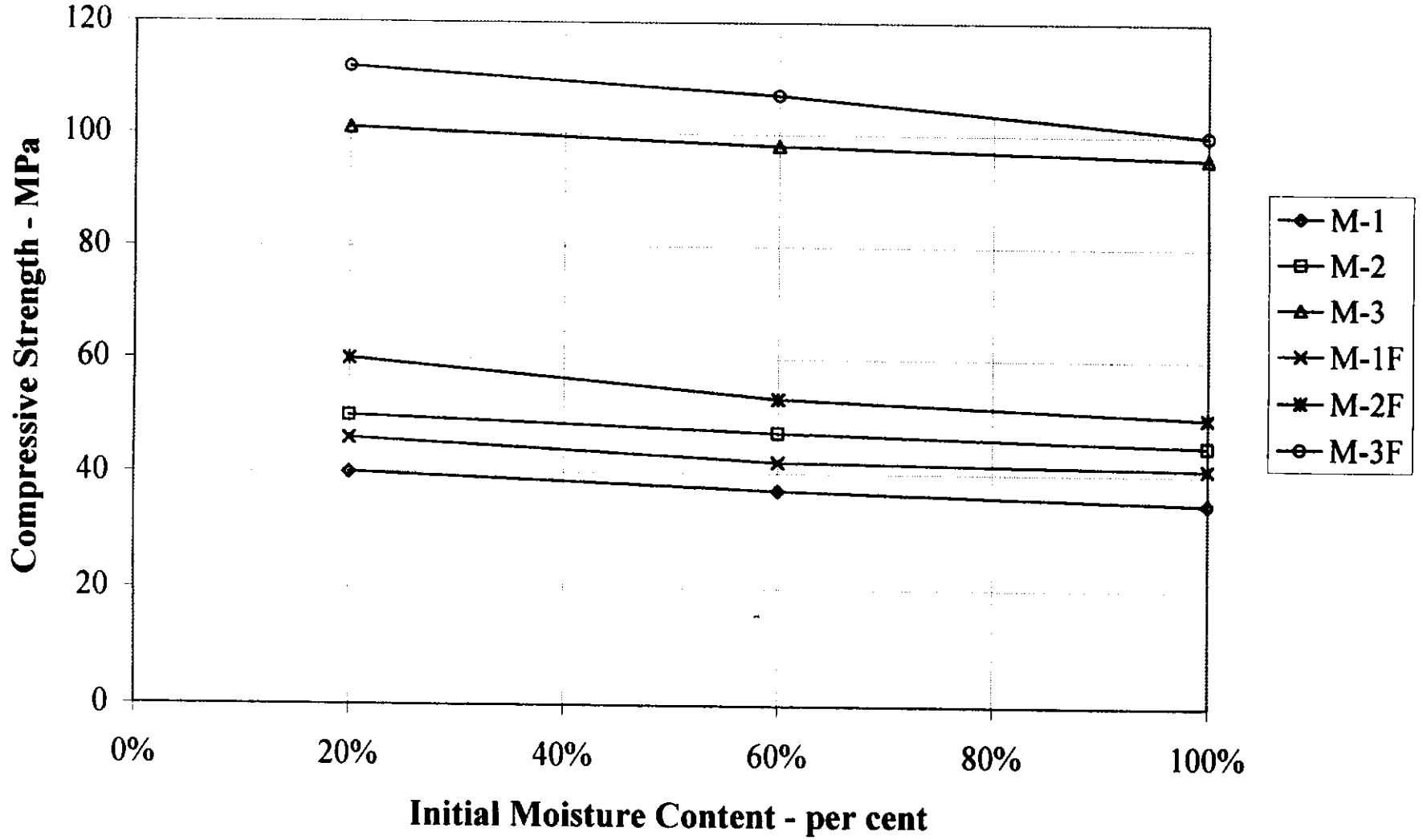

Fig. 4-6 Compressive Strength vs. Initial Moisture Content after Heating to a Maximum Temperature of 200 °C

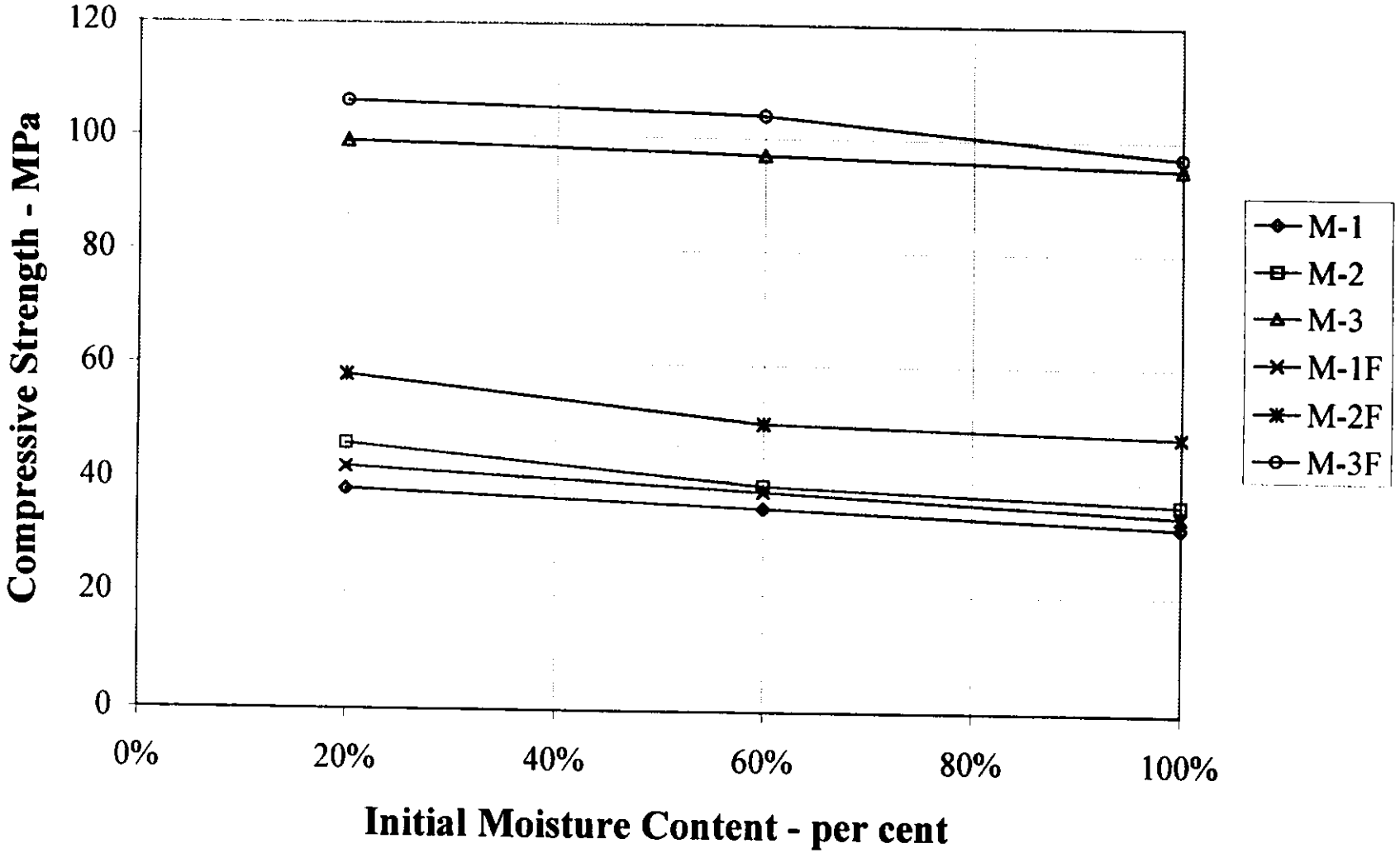

Fig. 4-7 Compressive Strength vs. Initial Moisture Content after Heating to a Maximum Temperature of 300 °C

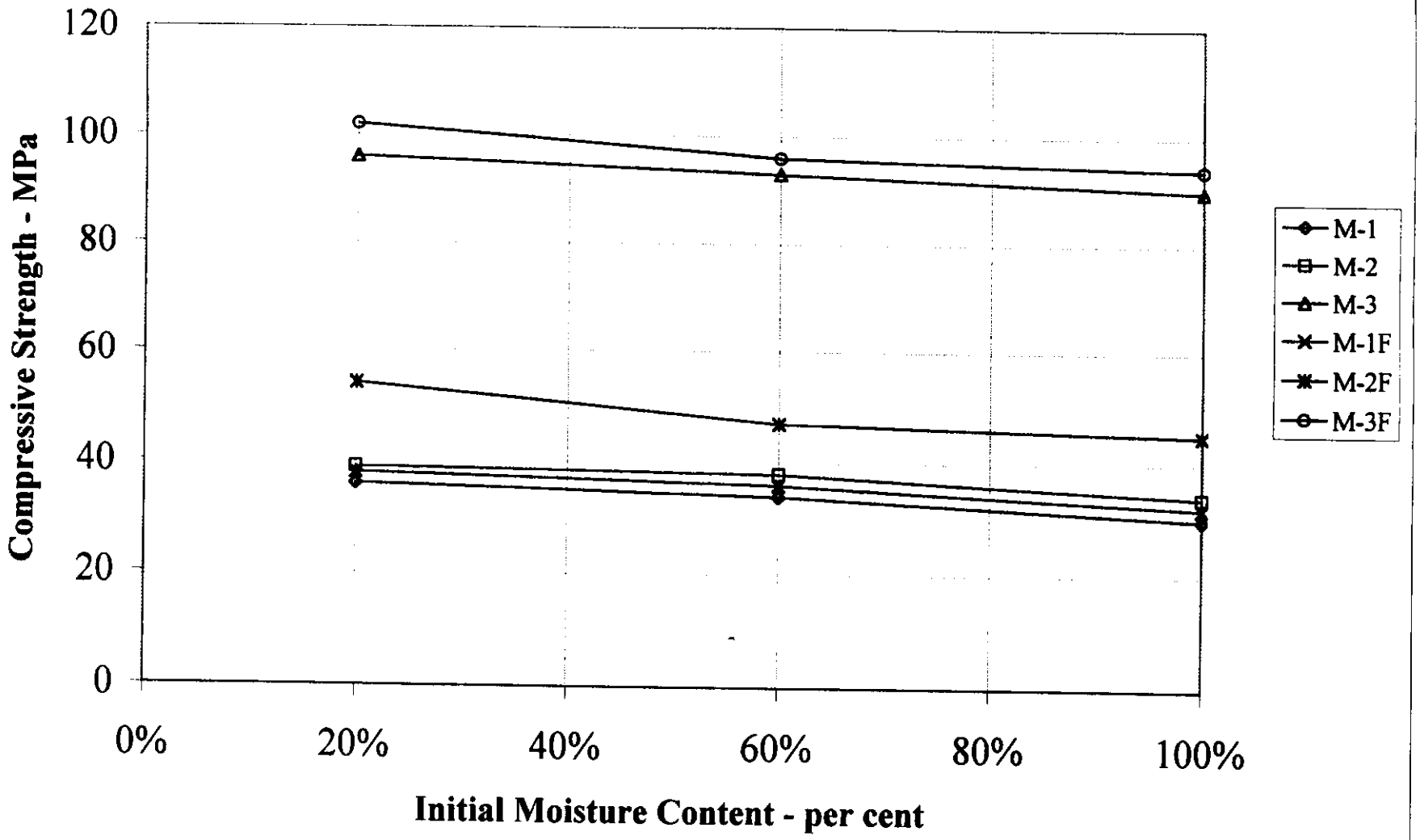

Fig. 4-8 Compressive Strength vs. Initial Moisture Content after Heating to a Maximum Temperature of 400 °C

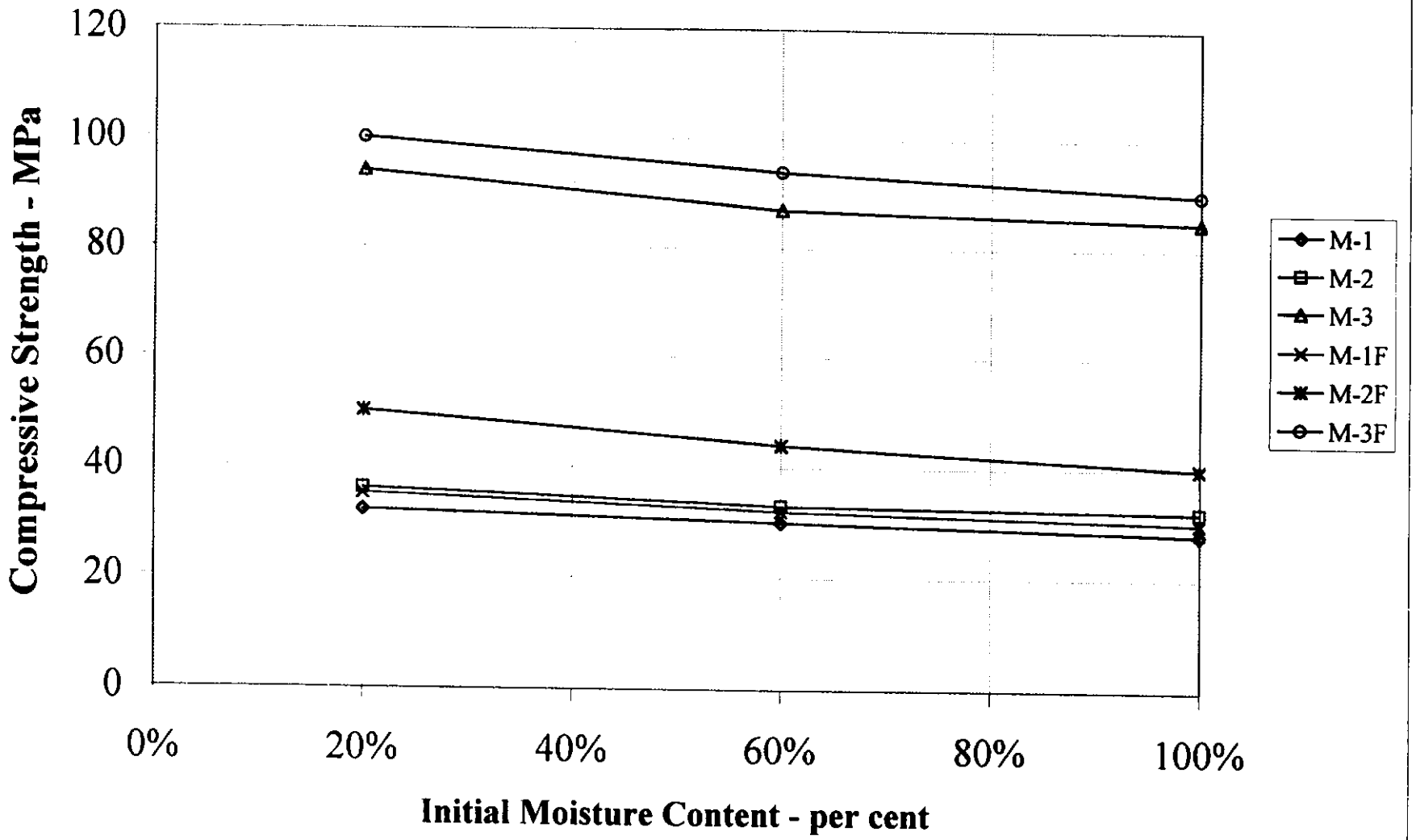

Fig. 4-9 Compressive Strength vs. Initial Moisture Content after Heating to a Maximum Temperature of 600 °C

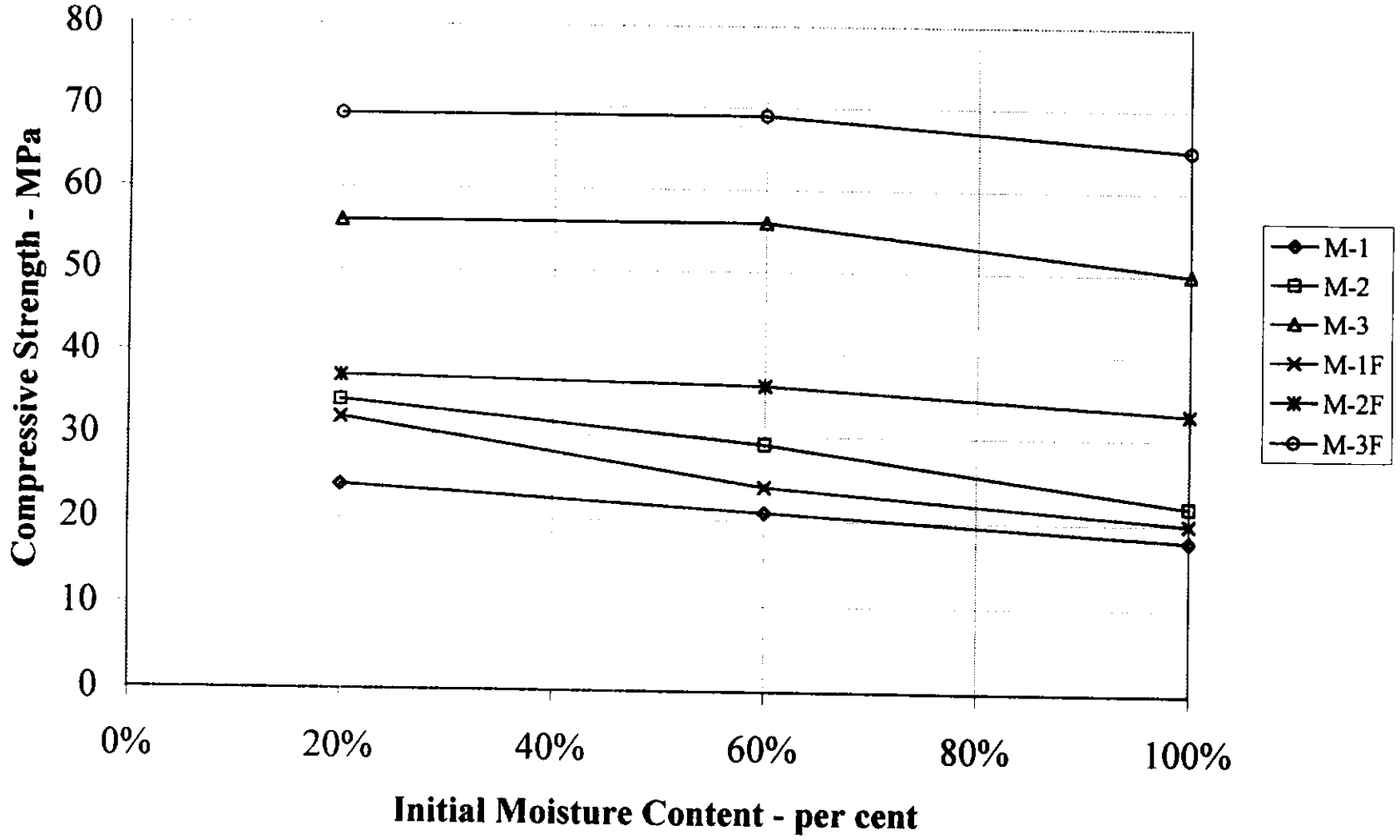

Fig. 4-10 Compressive Strength vs. Initial Moisture Content after Heating to a Maximum Temperature of 800 °C

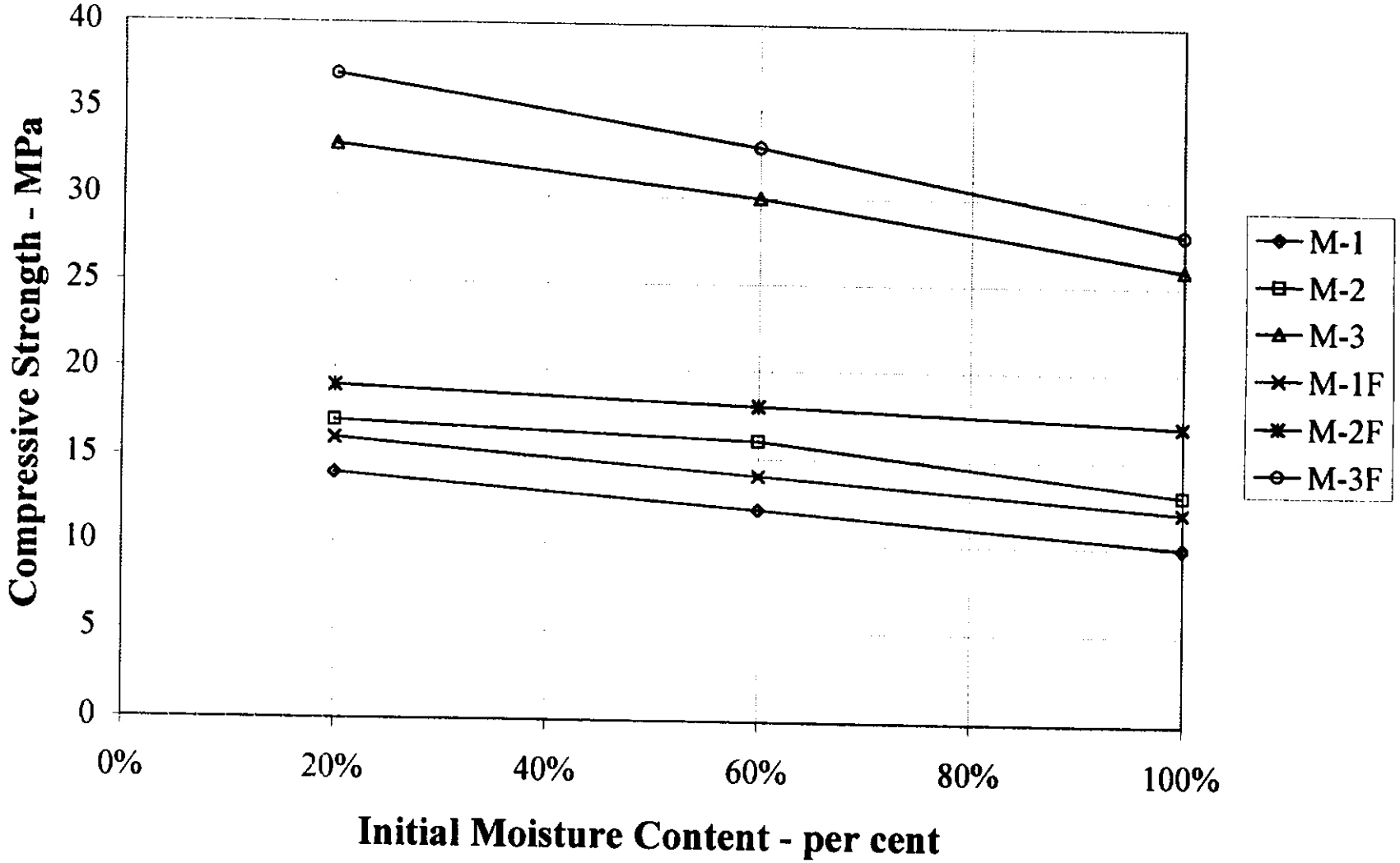

Fig. 4-11 Compressive Strength vs. Initial Moisture Content after Heating to a Maximum Temperature of 1000 °C

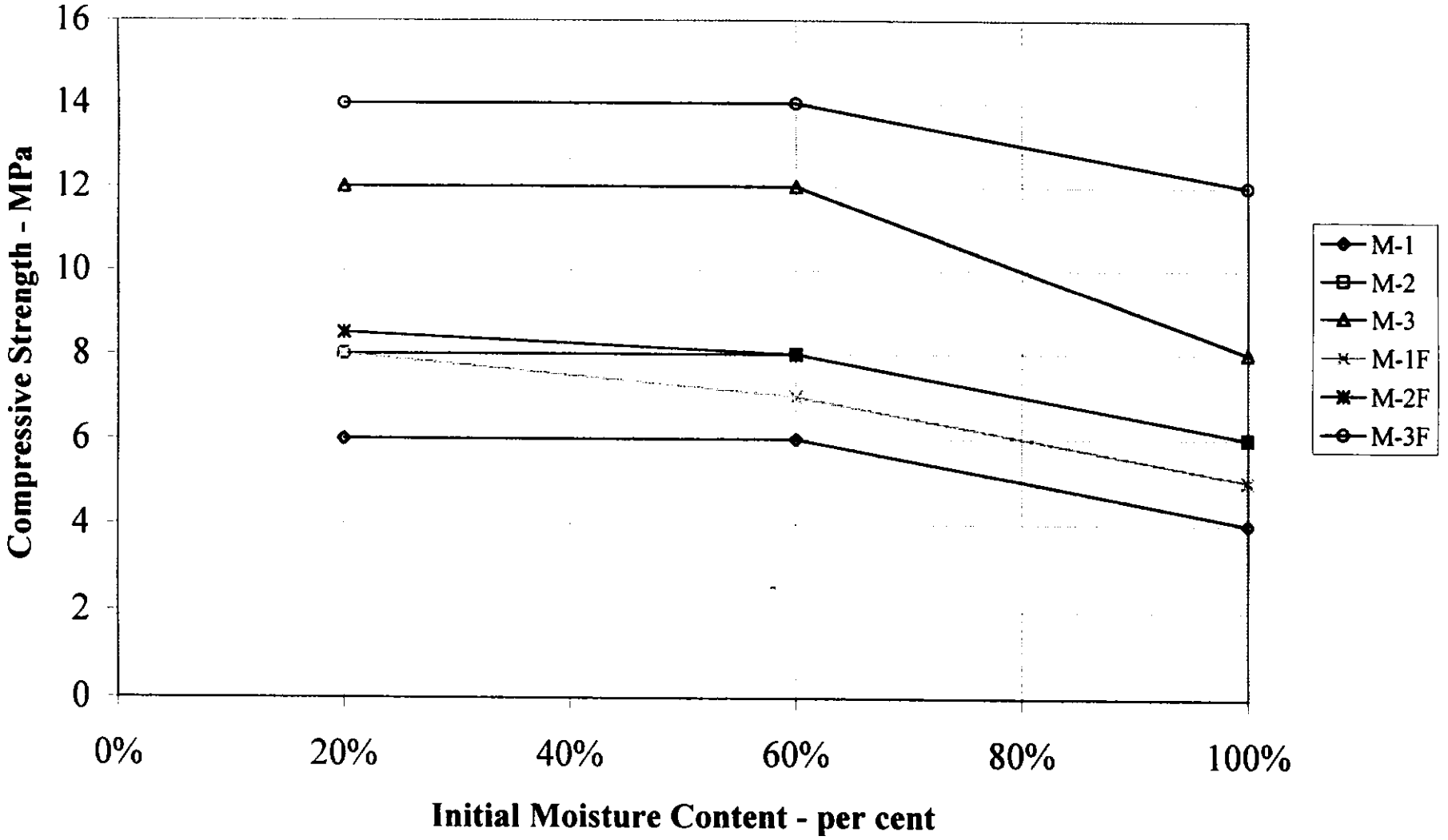

Fig. 4-12 Compressive Strength vs. Initial Moisture Content after Heating to a Maximum Temperature of 1100 °C

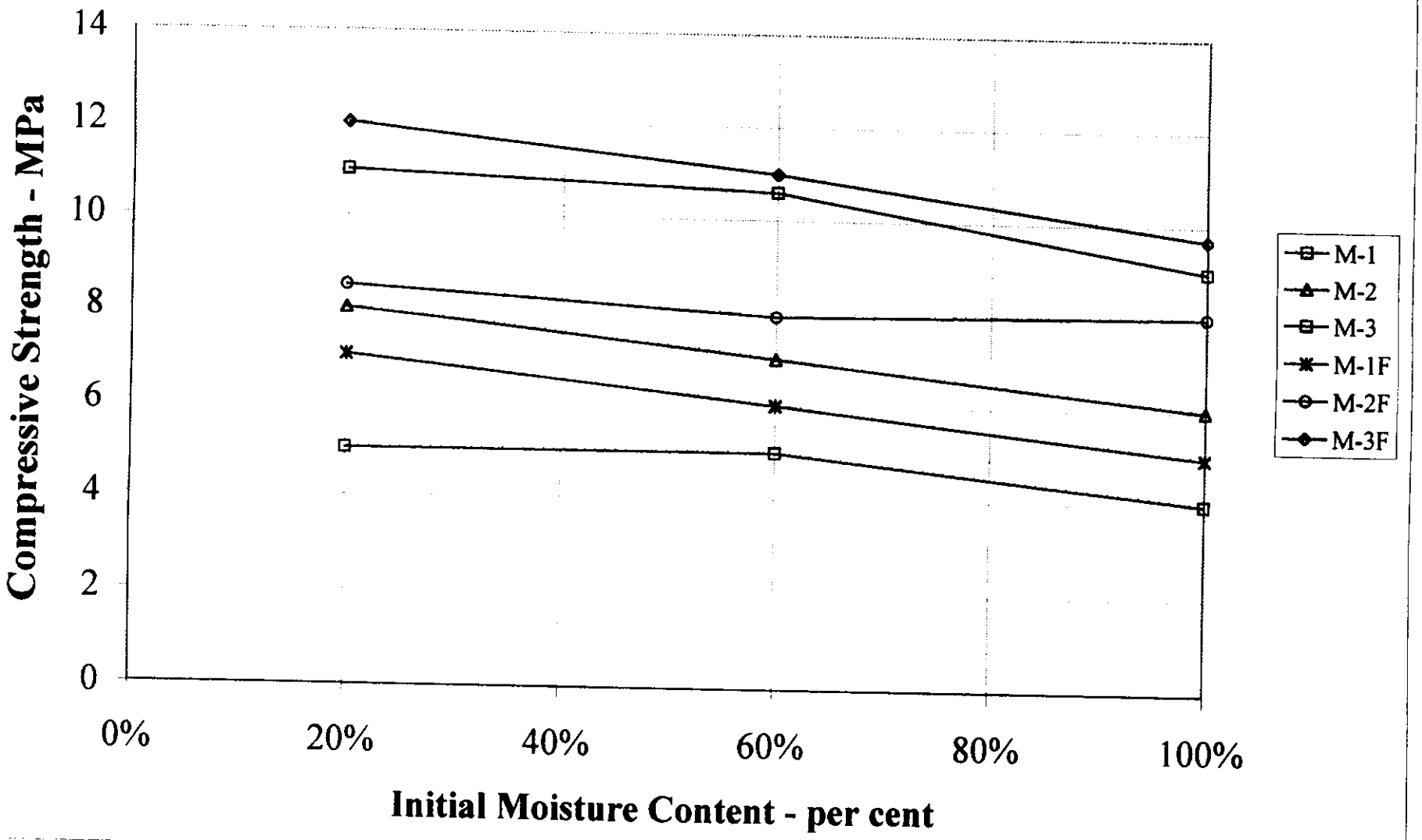

Fig. 4-13 Compressive Strength vs. Initial Moisture Content after Heating to a Maximum Temperature of 1200 °C

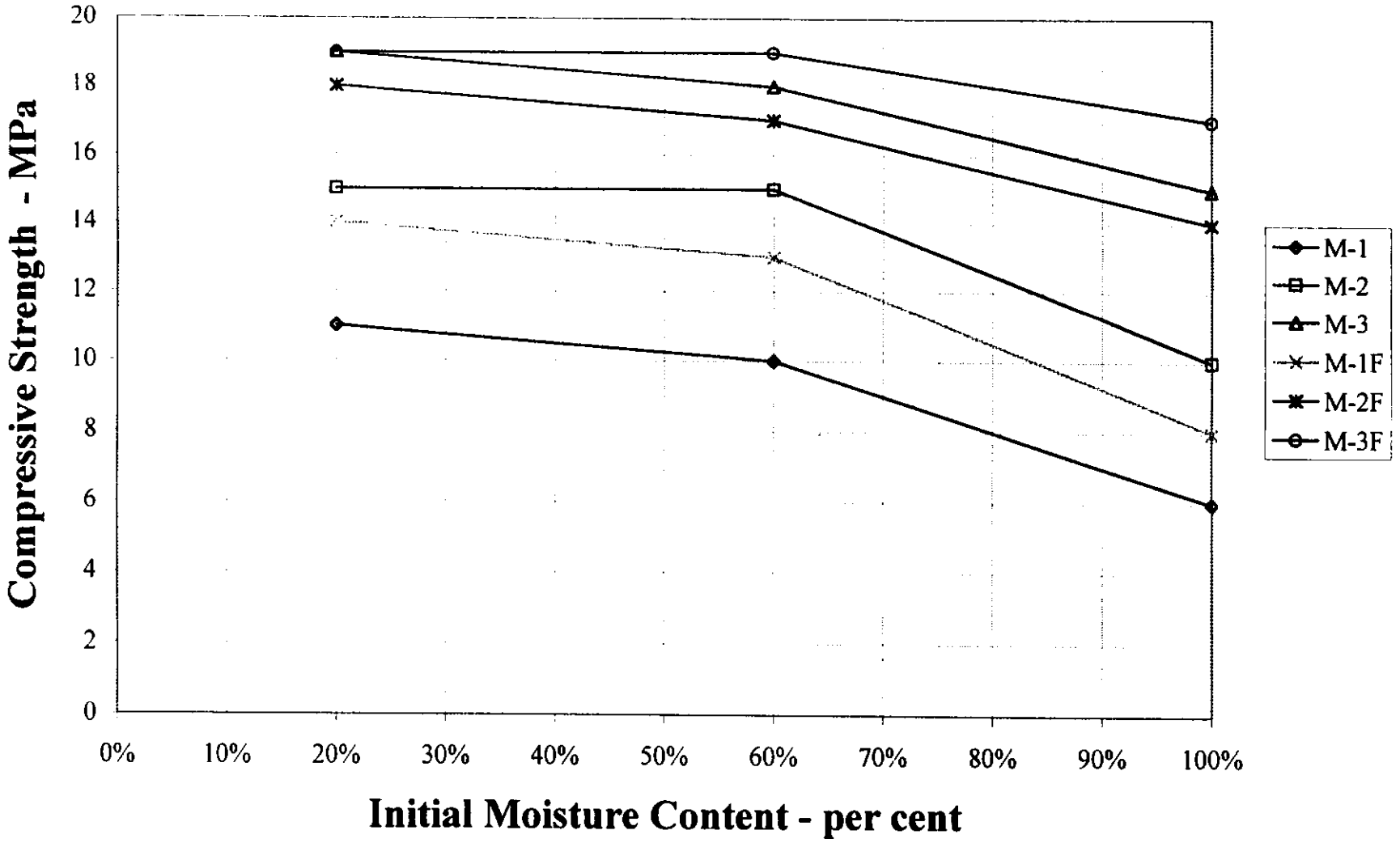

Fig. 4-14 Flexural Strength vs Maximum Heating Temperature at Initial Moisture Content of 100%

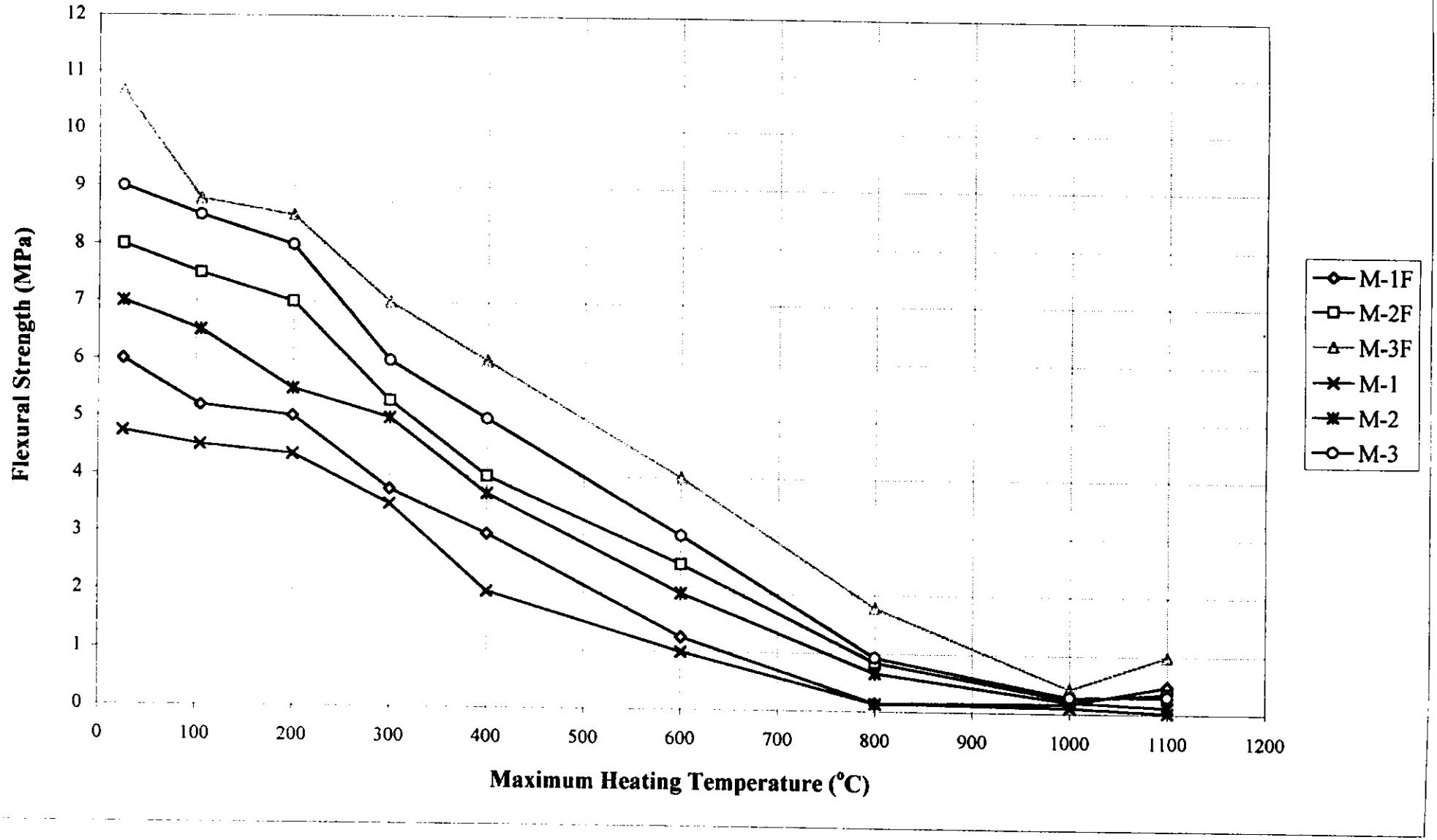

Fig. 4-15 Static Modulus of Elasticity vs Maximum Heating Temperatures

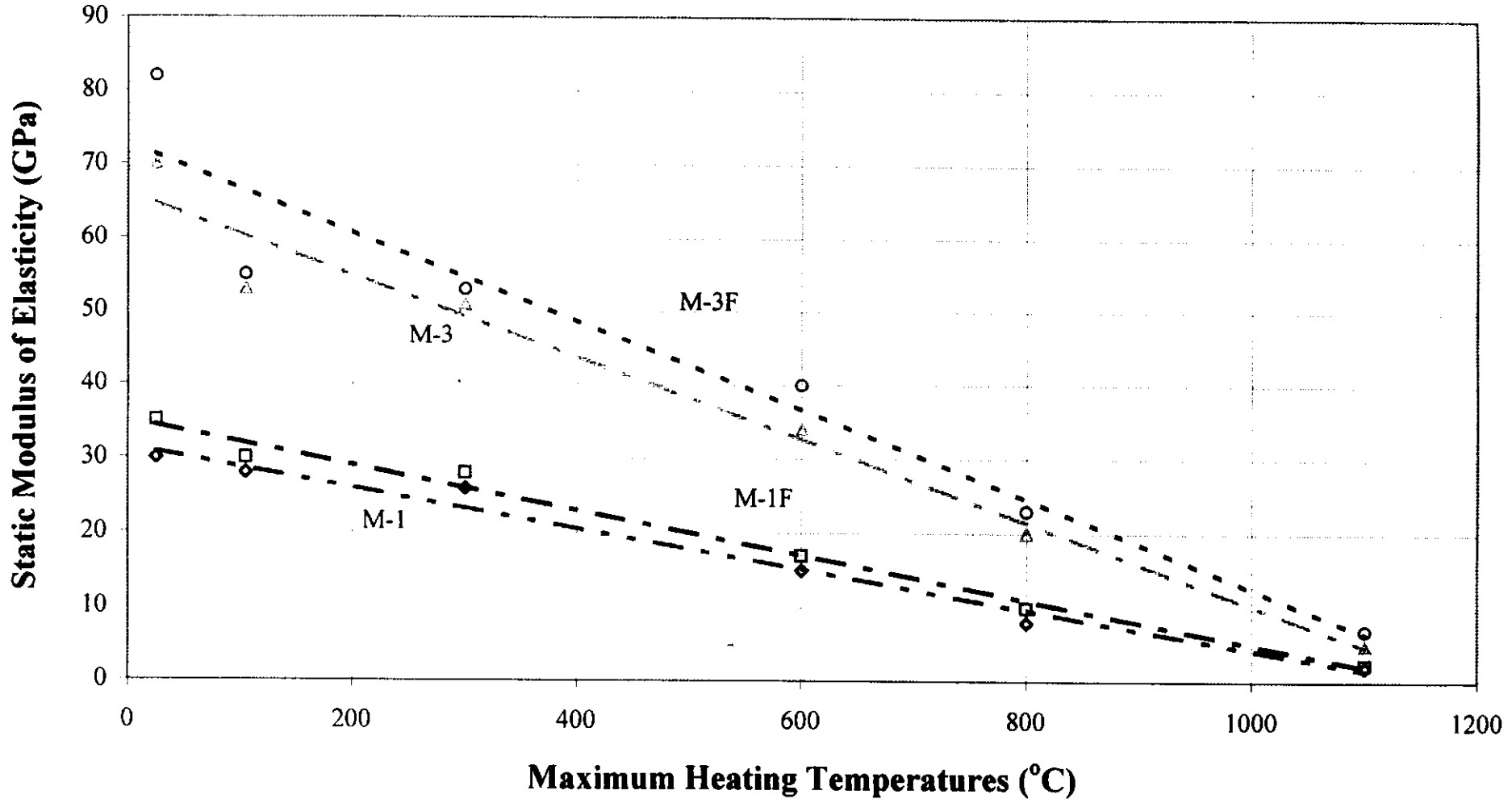

Fig. 4-16 Poisson's Ratio vs Maximum Heating Temperatures

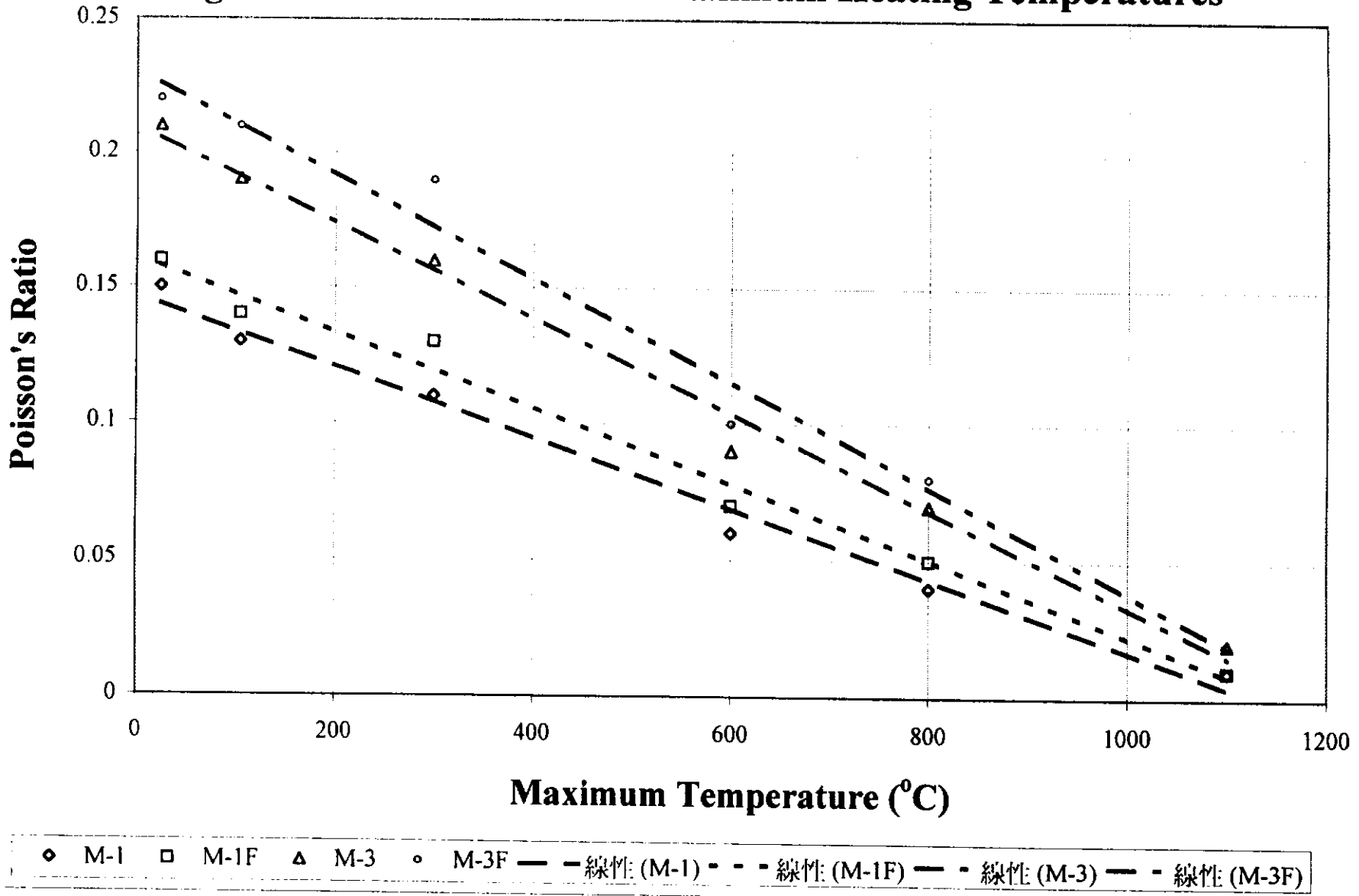

Fig. 4-17 Percentage of Porosity Distribution for Control Mixes

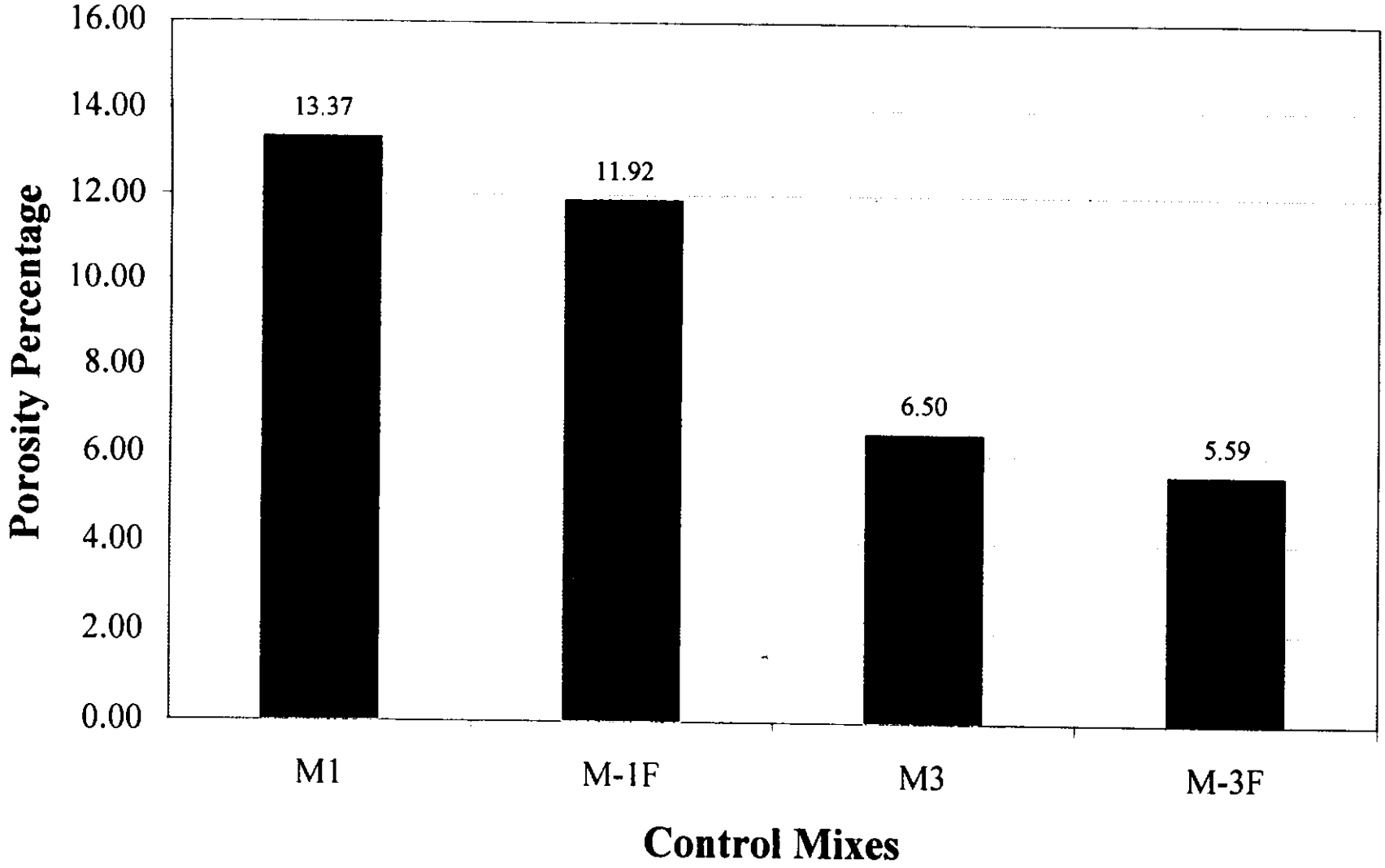

Fig. 4-18 Average Pore Diameter Distribution for Control Mixes

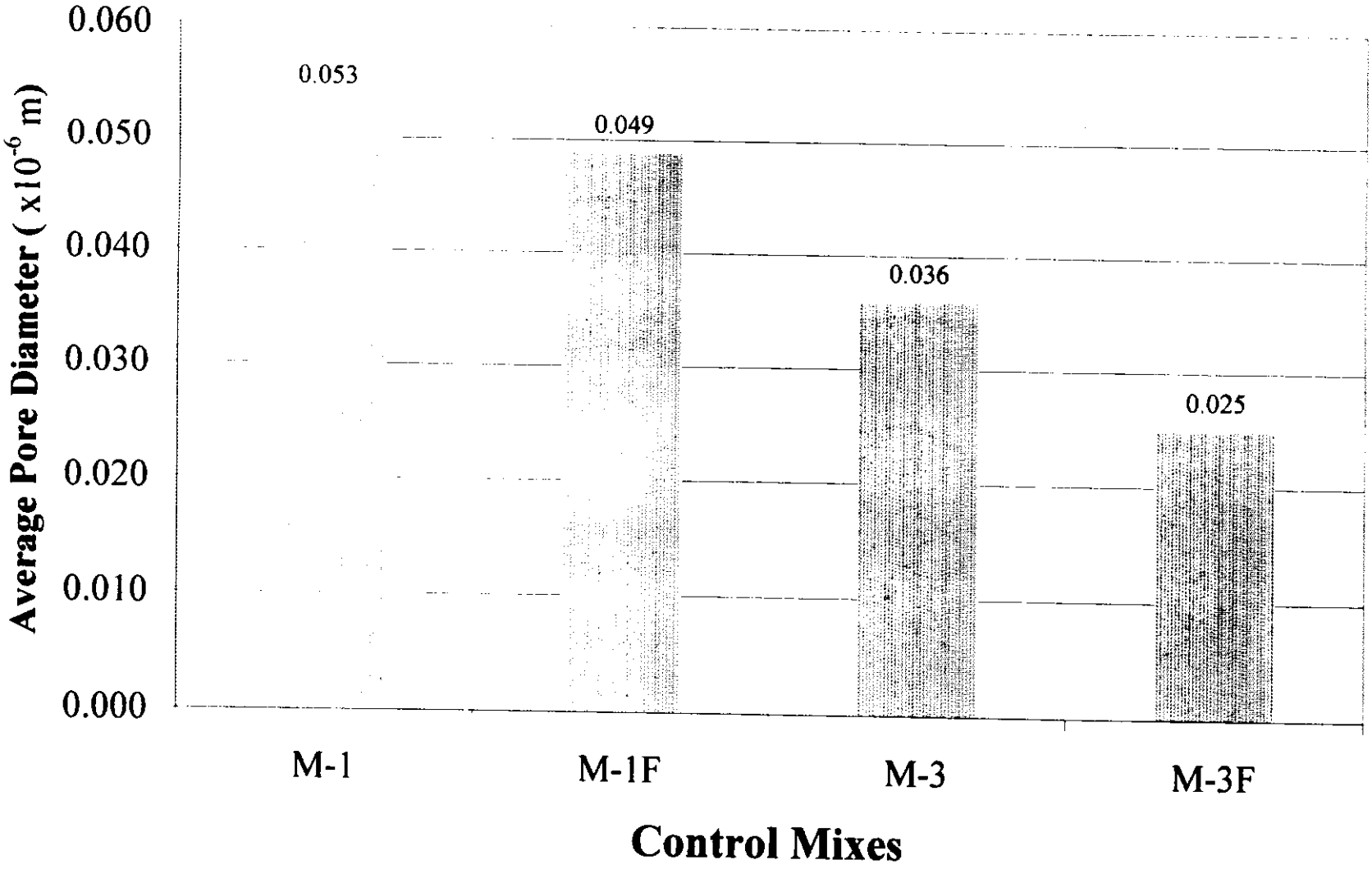

Fig. 4-19 Average Porosity Percentage vs. Maximum Heating Temperature at Initial Moisture Content of 20%

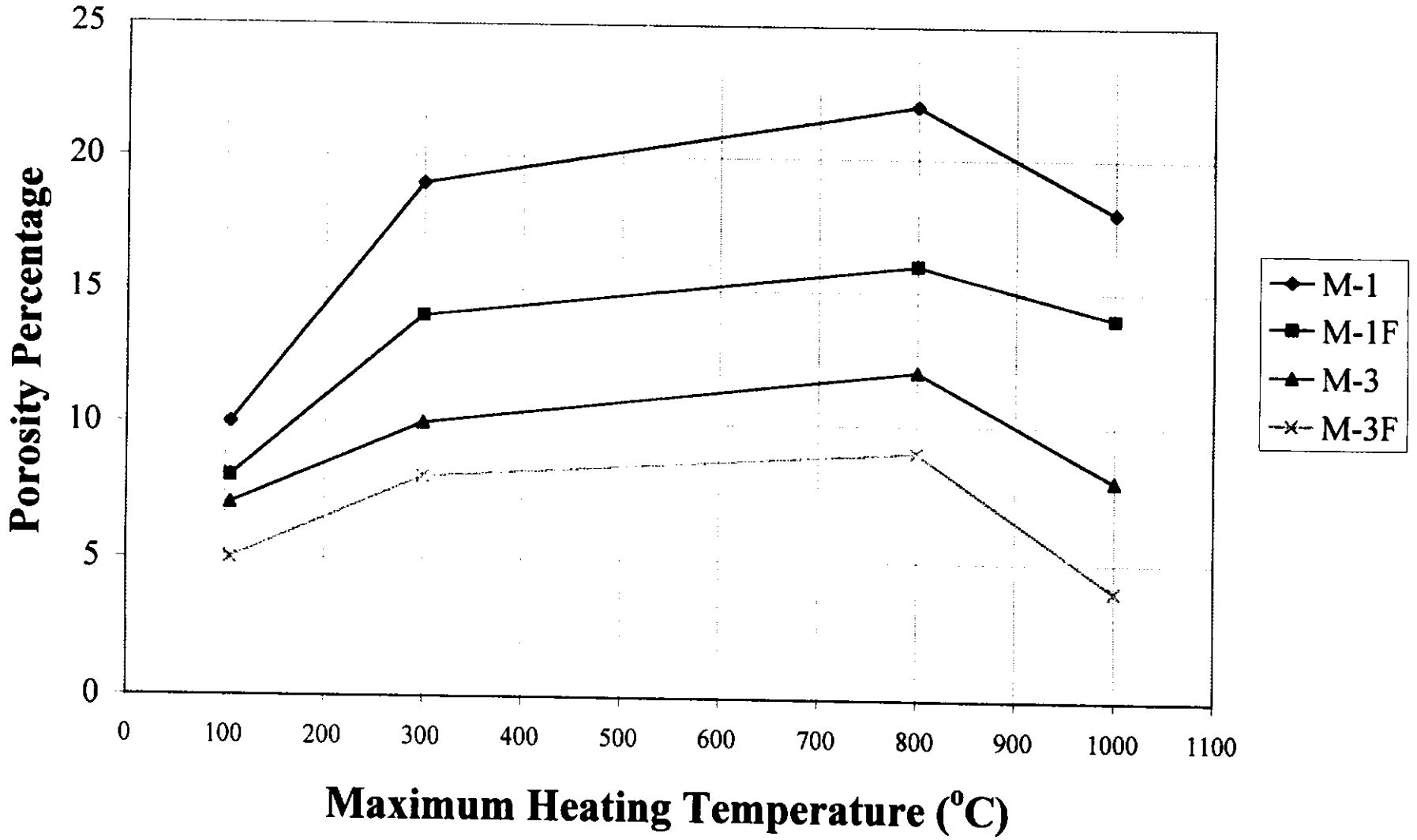

Fig. 4-20 Average Porosity Percentage vs. Maximum Heating Temperature at Initial Moisture Content of 60%

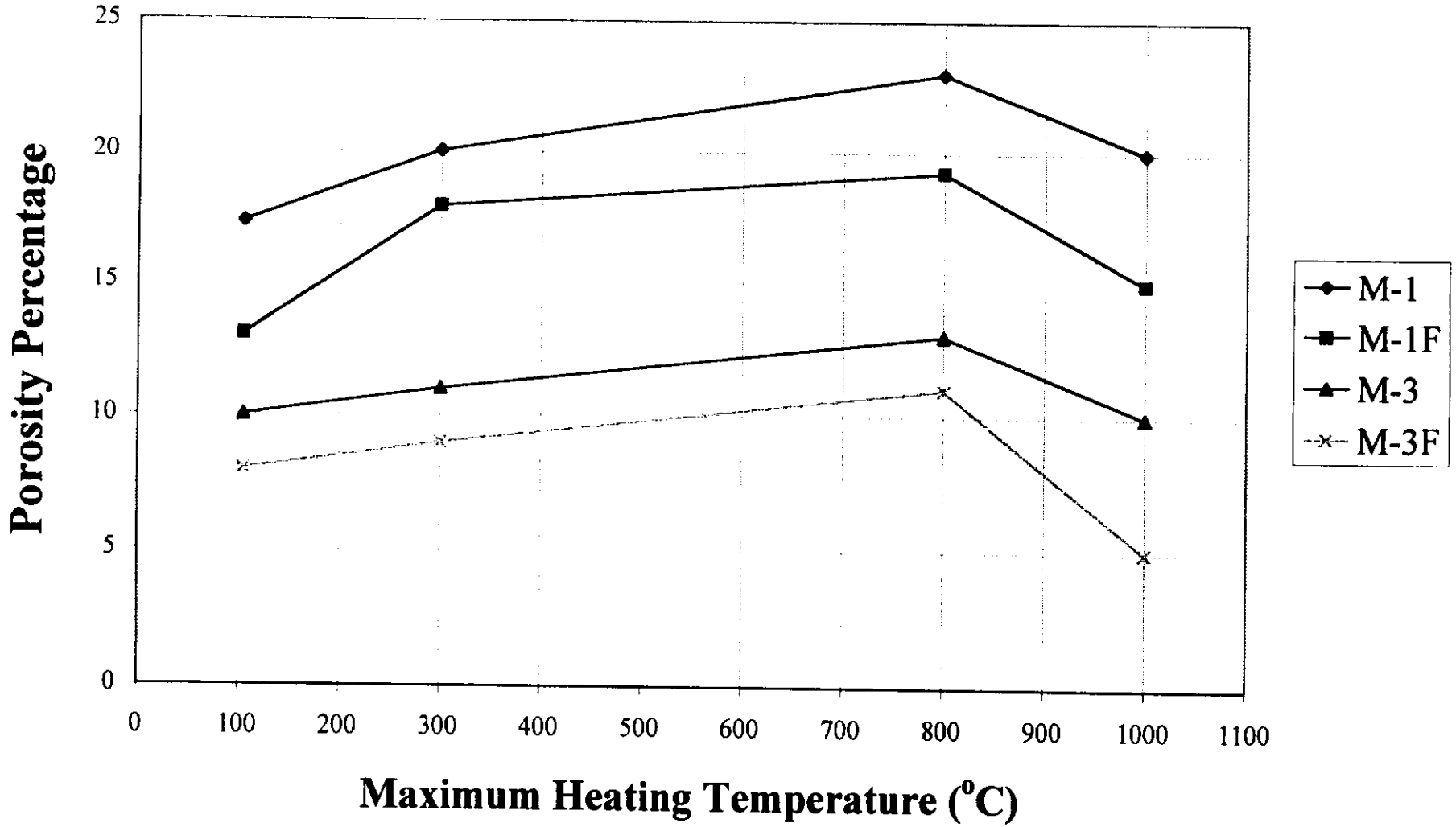

Fig. 4-21 Average Porosity Percentge vs. Maximum Heating Temperature at Initial Moisture Content of 100%

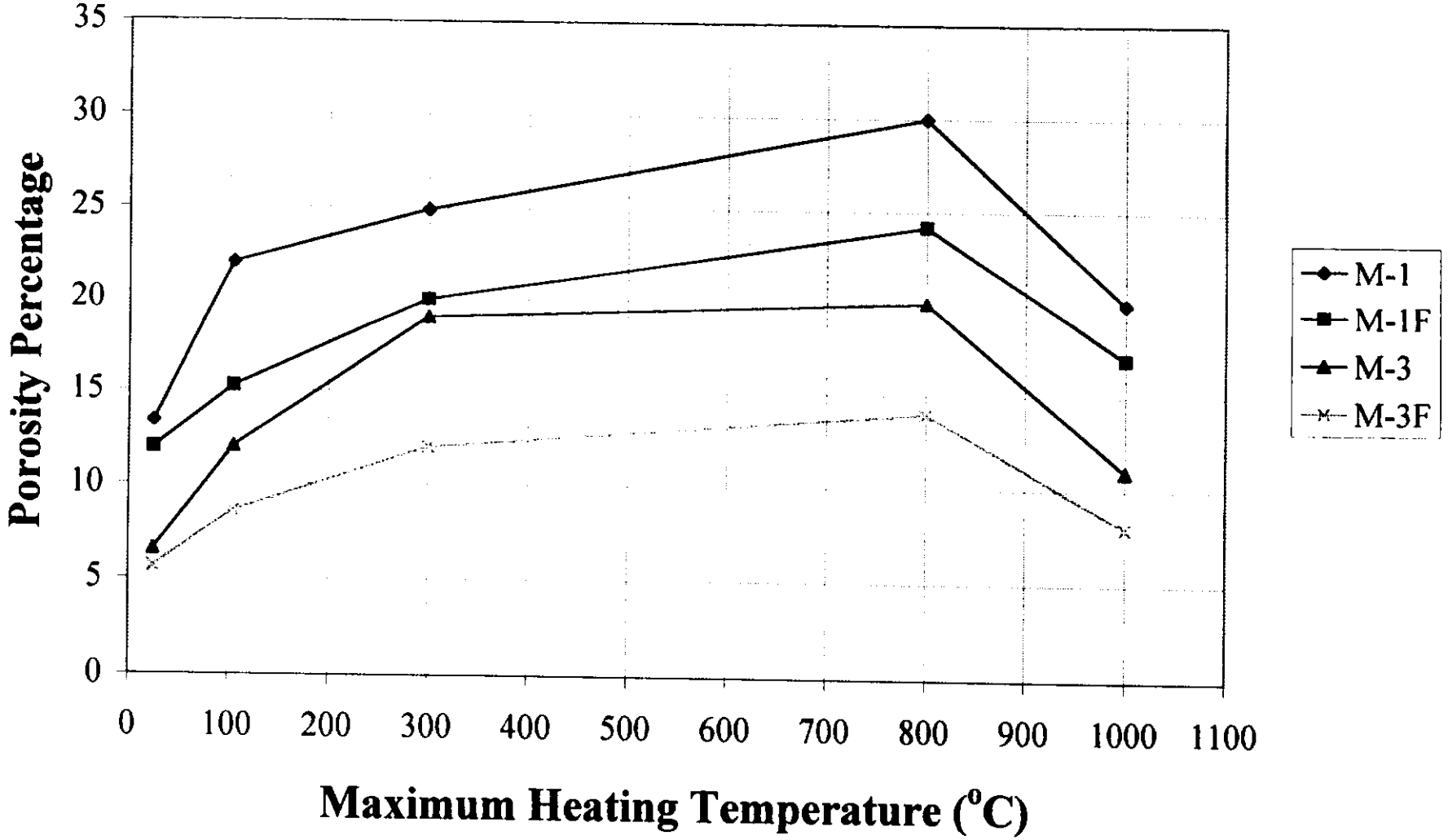

Fig. 4-22 Average Porosity Percentage vs. Initial Moisture Content after Heating to Maximum Temperature of 105°C

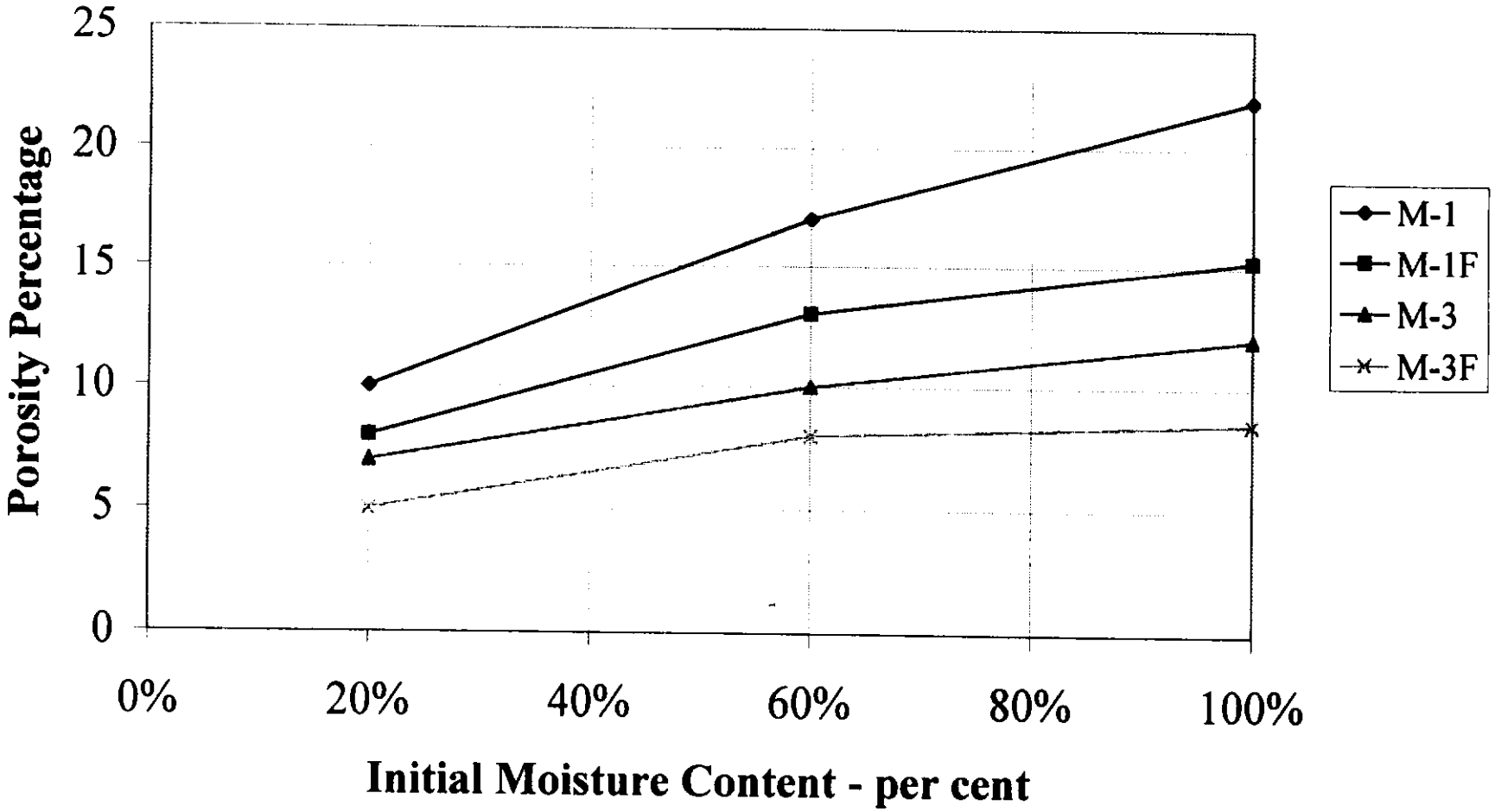

Fig. 4-23 Average Porosity Percentage vs. Initial Moisture Content after Heating to Maximum Temperature of 300°C

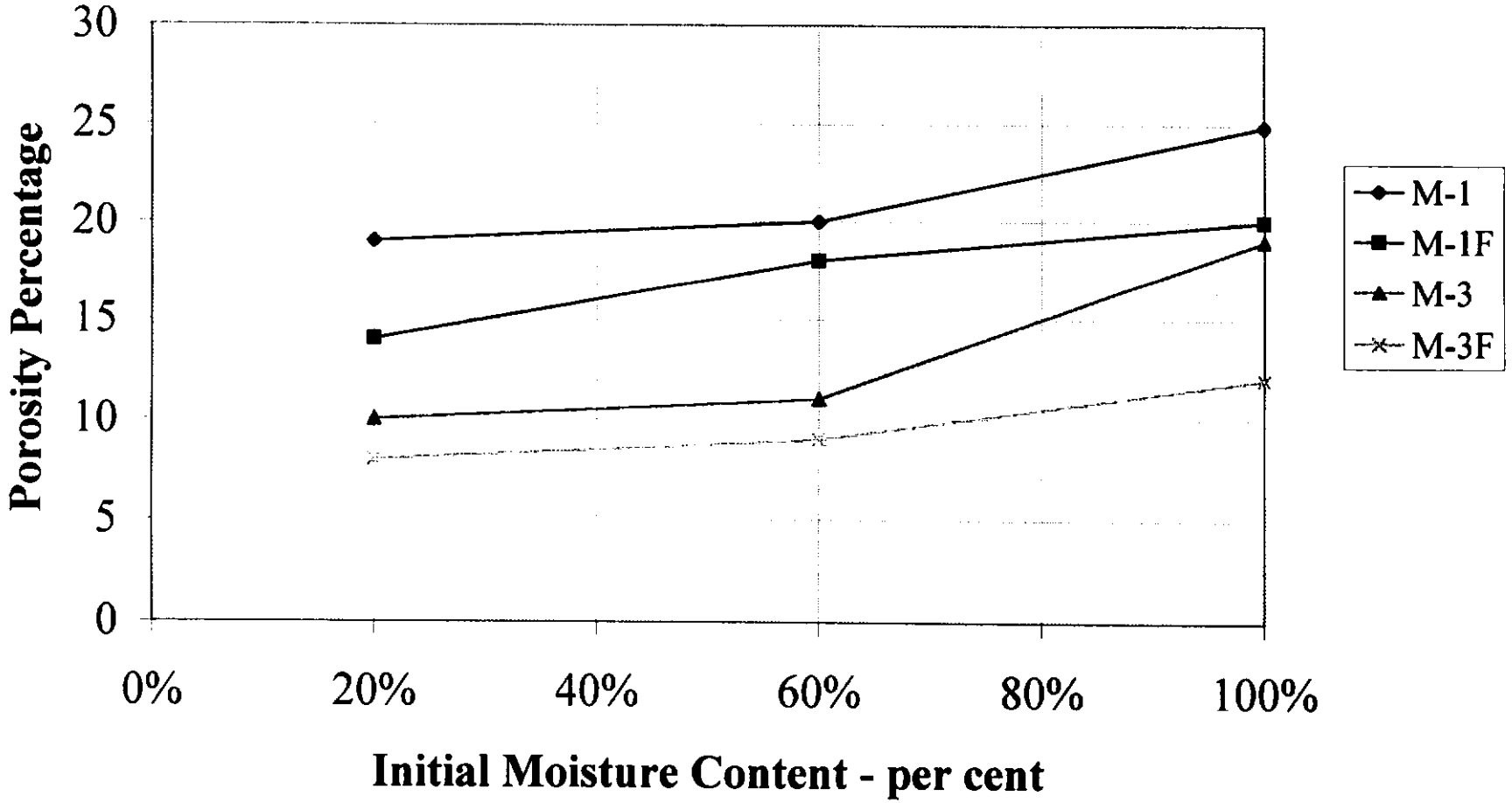

Fig. 4-24 Average Porosity Percentage vs. Initial Moisture Content after Heating to Maximum Temperature of 800°C

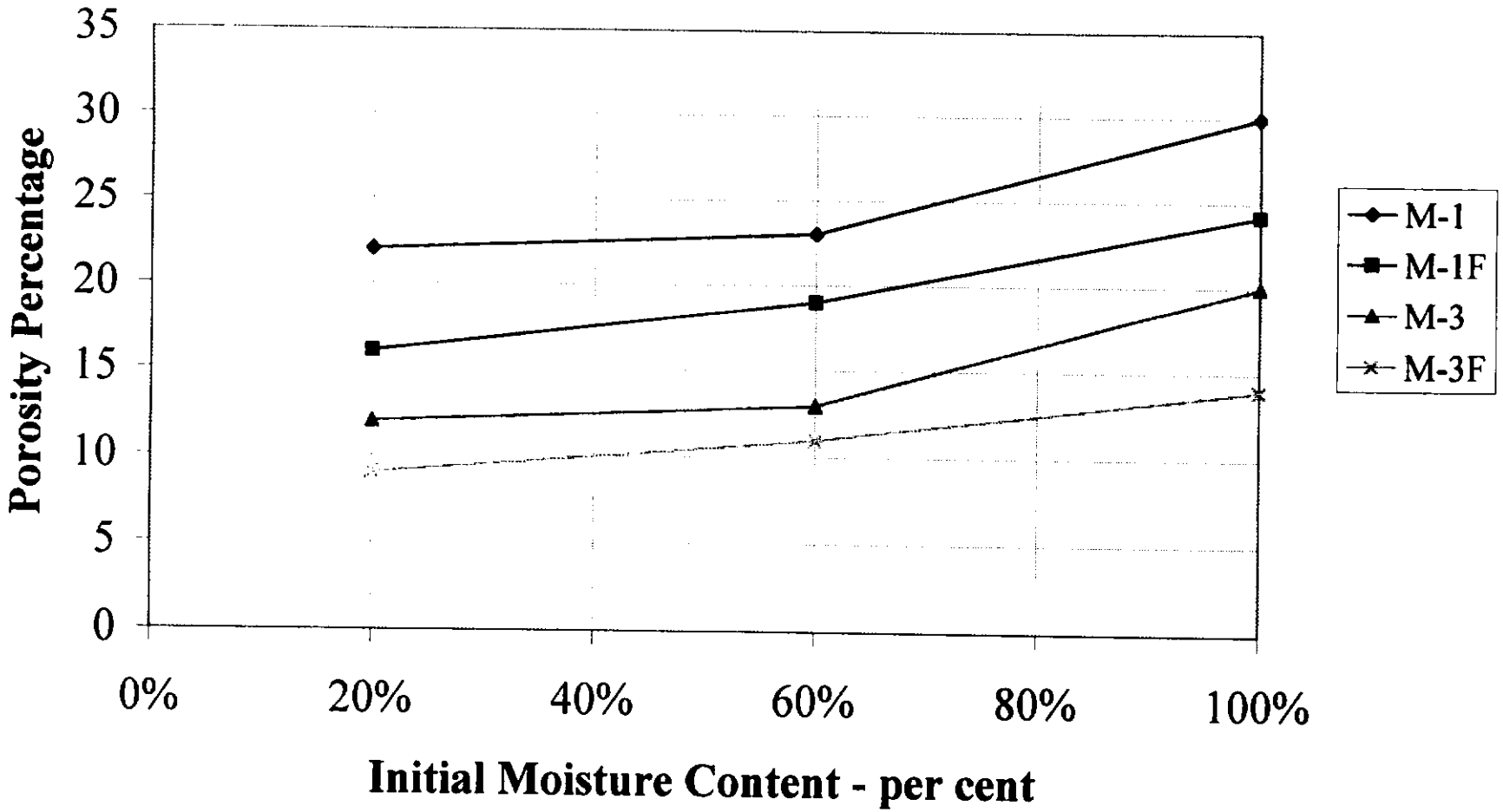

Fig. 4-25 Average Porosity Percentage vs. Initial Moisture Content after Heating to Maximum Temperature of 1000°C

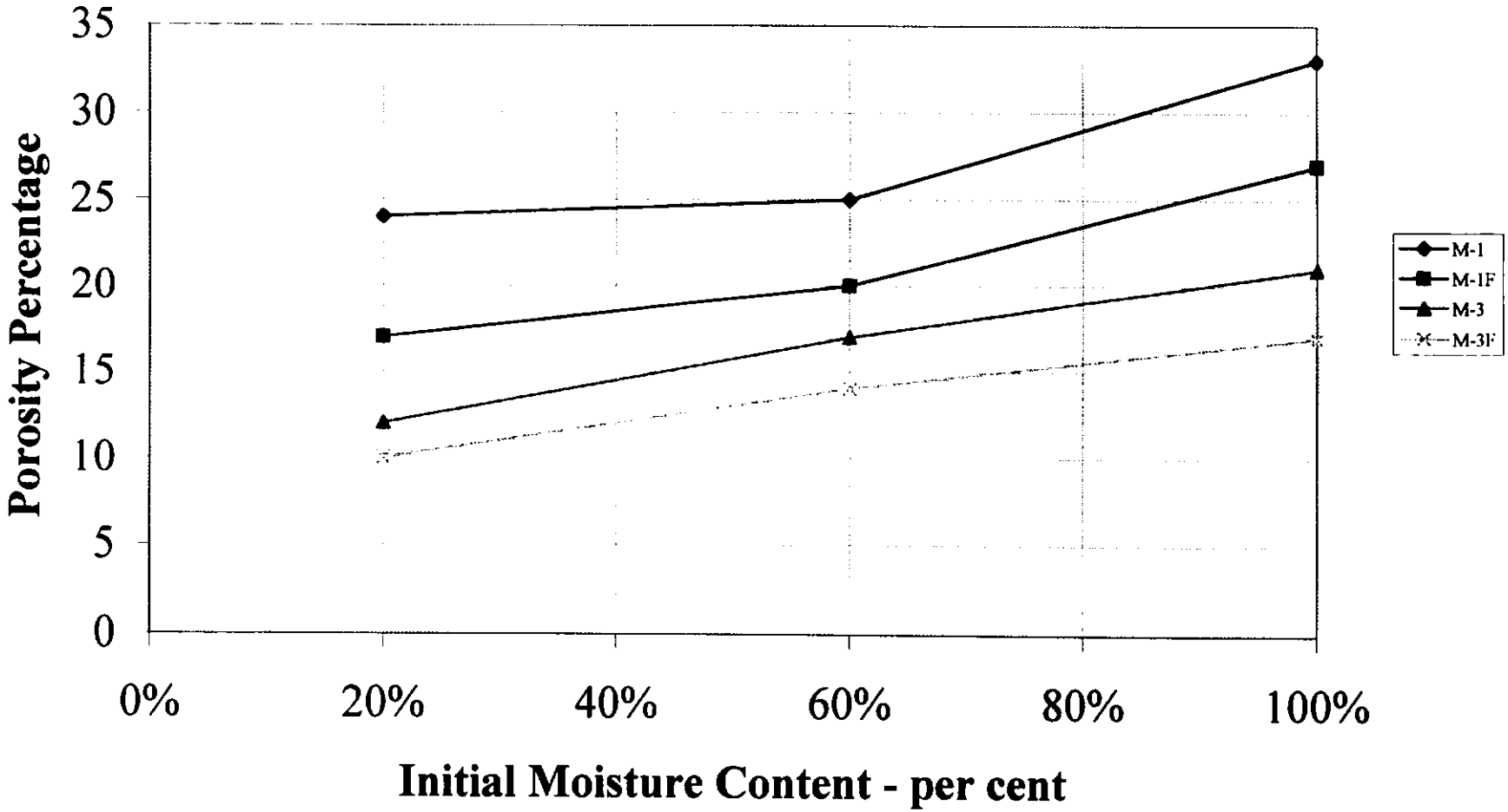

Fig. 4-26 Average Pore Diameter vs. Maximum Heating Temperature at Initial Moisture Content of 20%

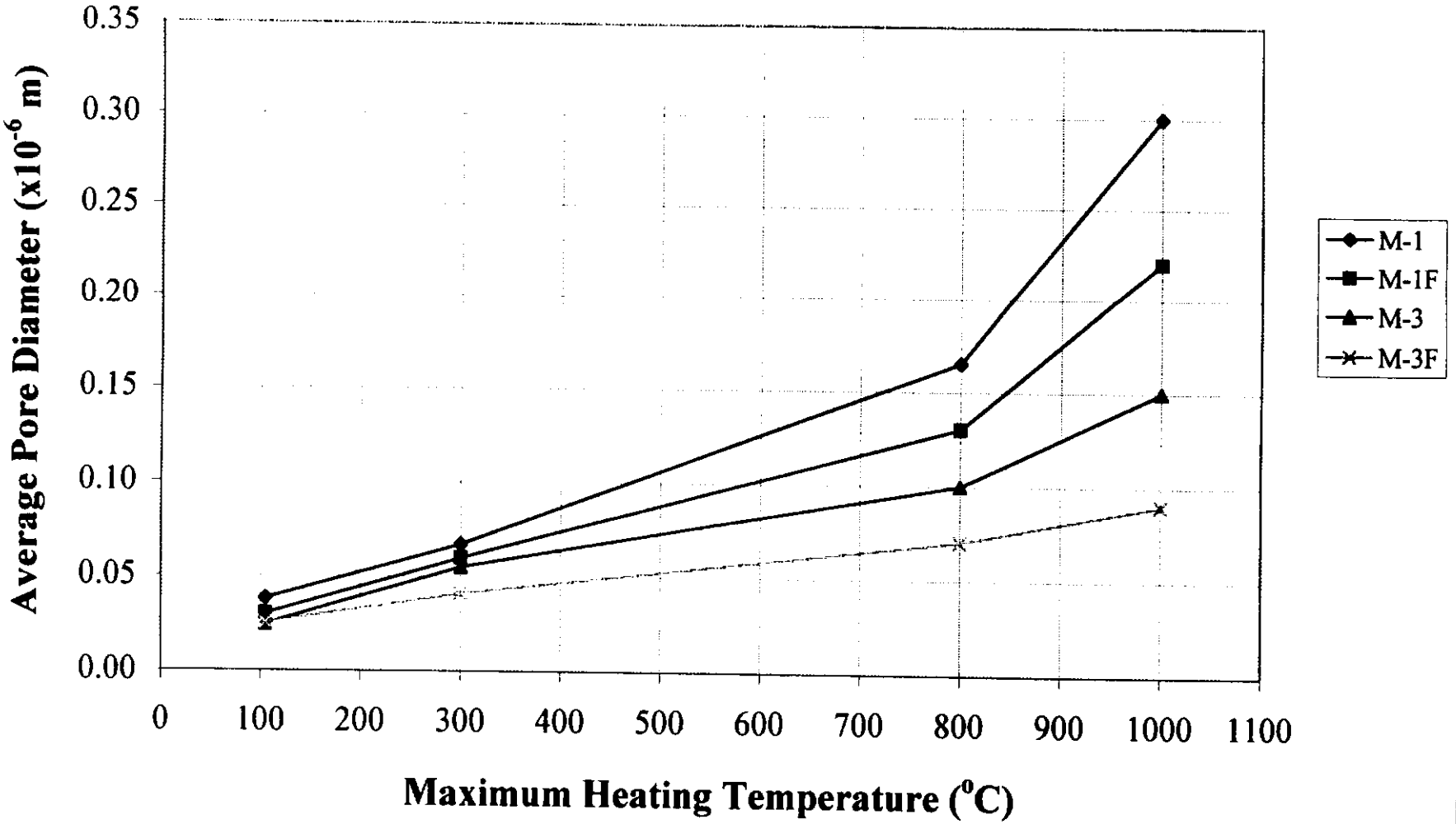

Fig. 4-27 Average Pore Diameter vs. Maximum Heating Temperature at Initial Moisture Content of 60%

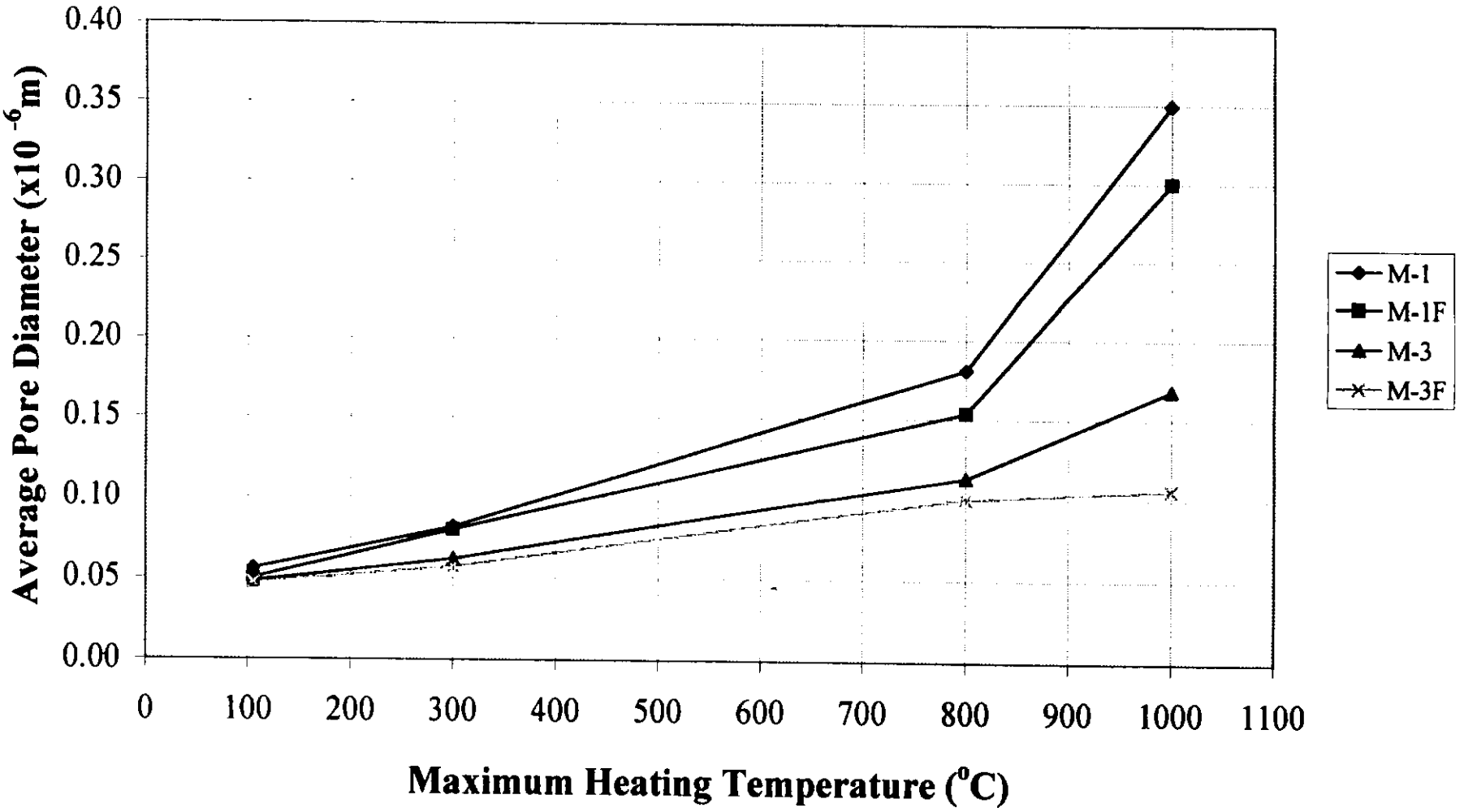

Fig. 4-28 Average Pore Diameter vs. Maximum Heating Temperature at Initial Moisture Content of 100%

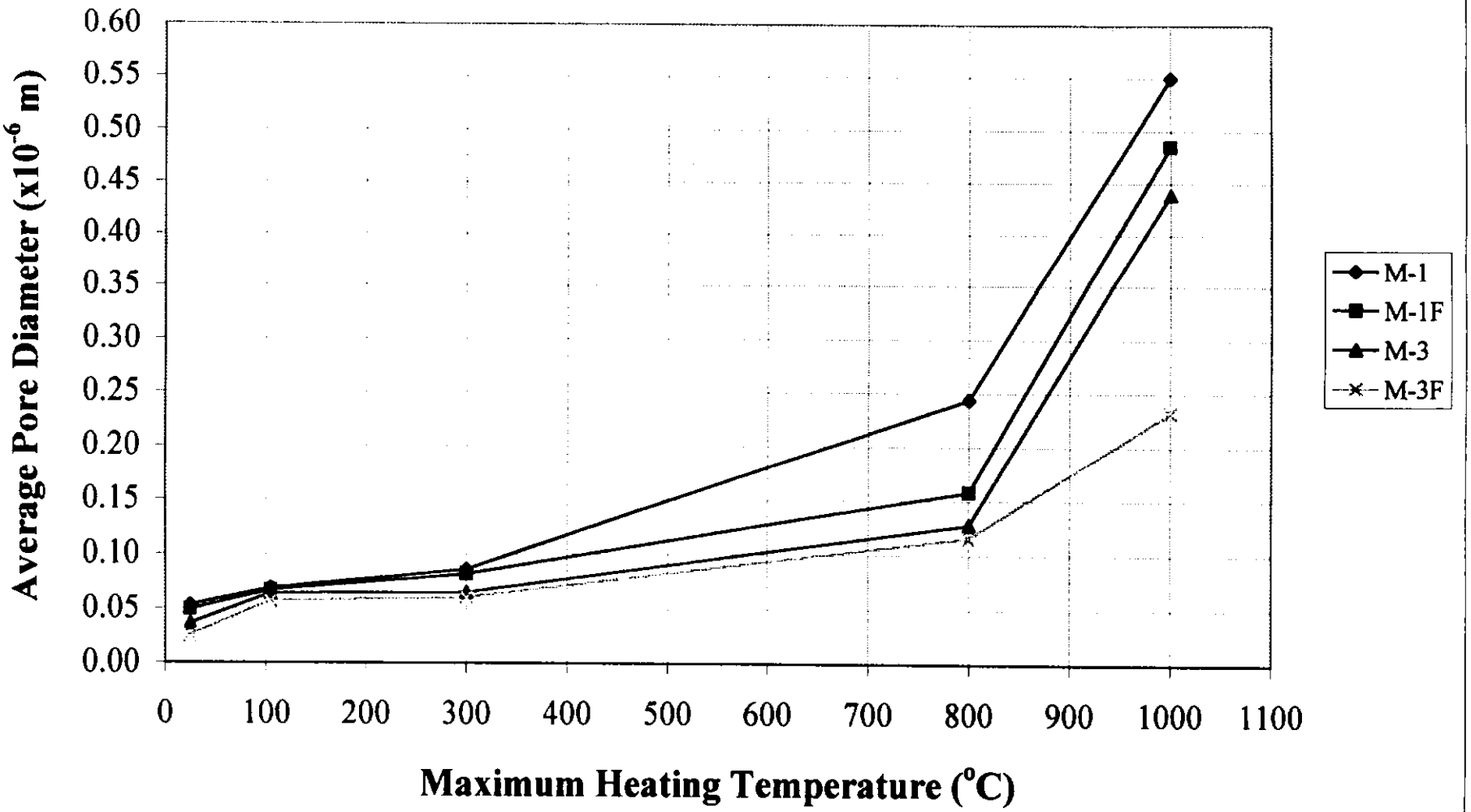

Fig. 4-29 Cumulative Intrusion Volume vs. Pore Diameter
(M-1 specimens initially at moisture content of 20%)

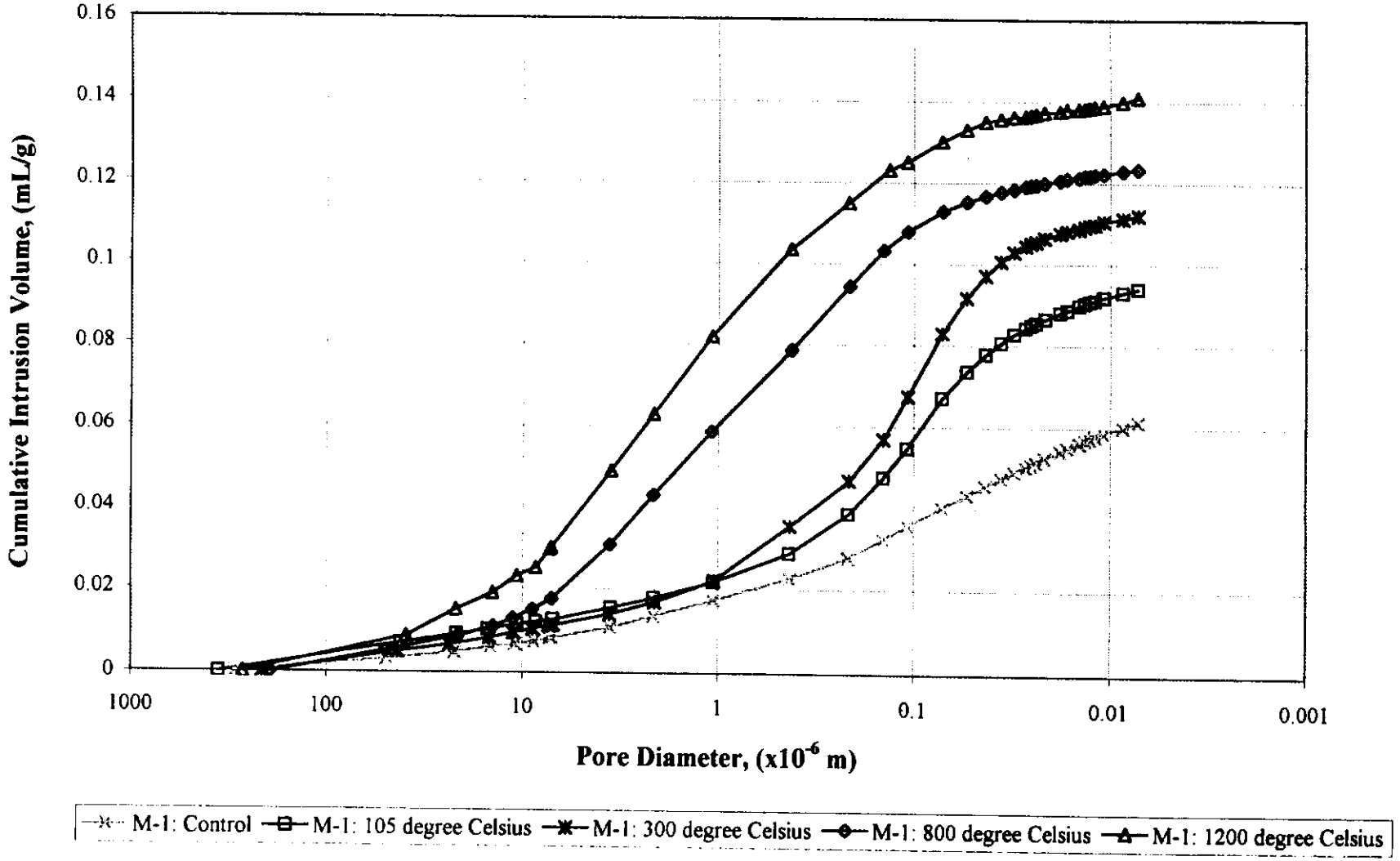

Fig. 4-30 Cumulative Intrusion Volume vs. Pore Diameter
(M-1 specimens initially at moisture content of 60%)

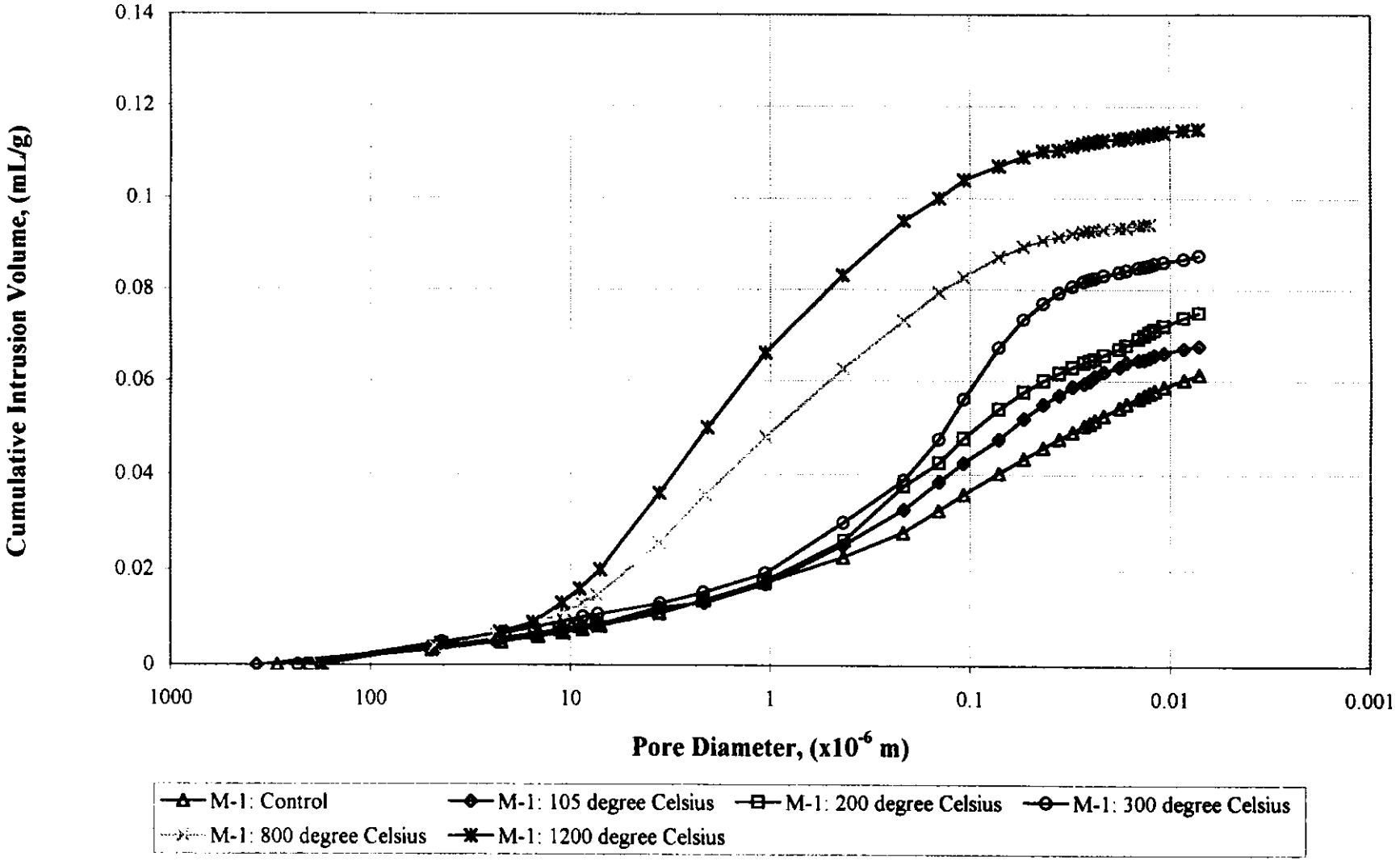

Fig. 4-31 Cumulative Intrusion Volume vs. Pore Diameter
(M-1 specimens initially at moisture content of 100%)

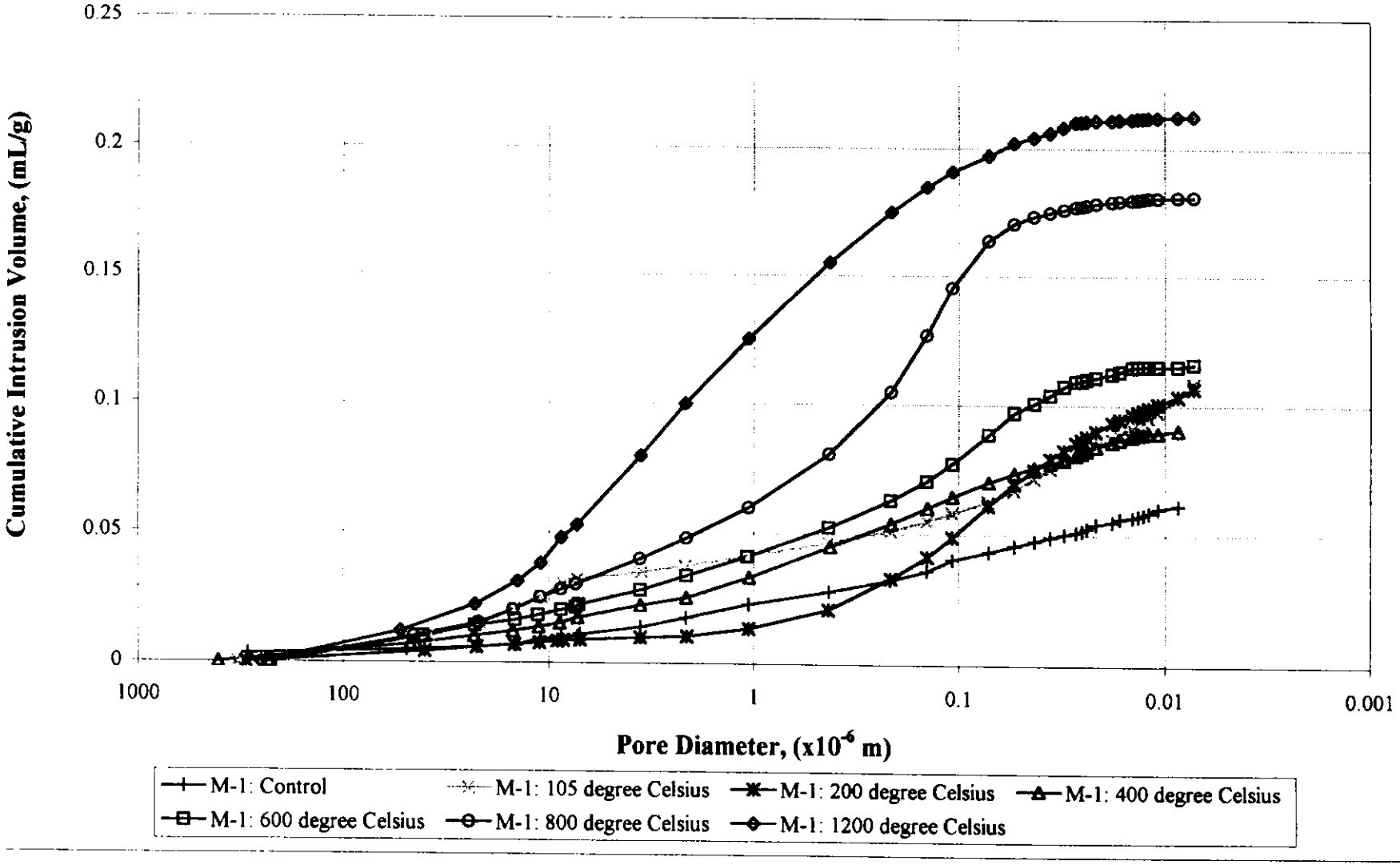

Fig. 4-32 Cumulative Intrusion Volume vs. Pore Diameter
(M-3 specimens initially at moisture content of 20%)

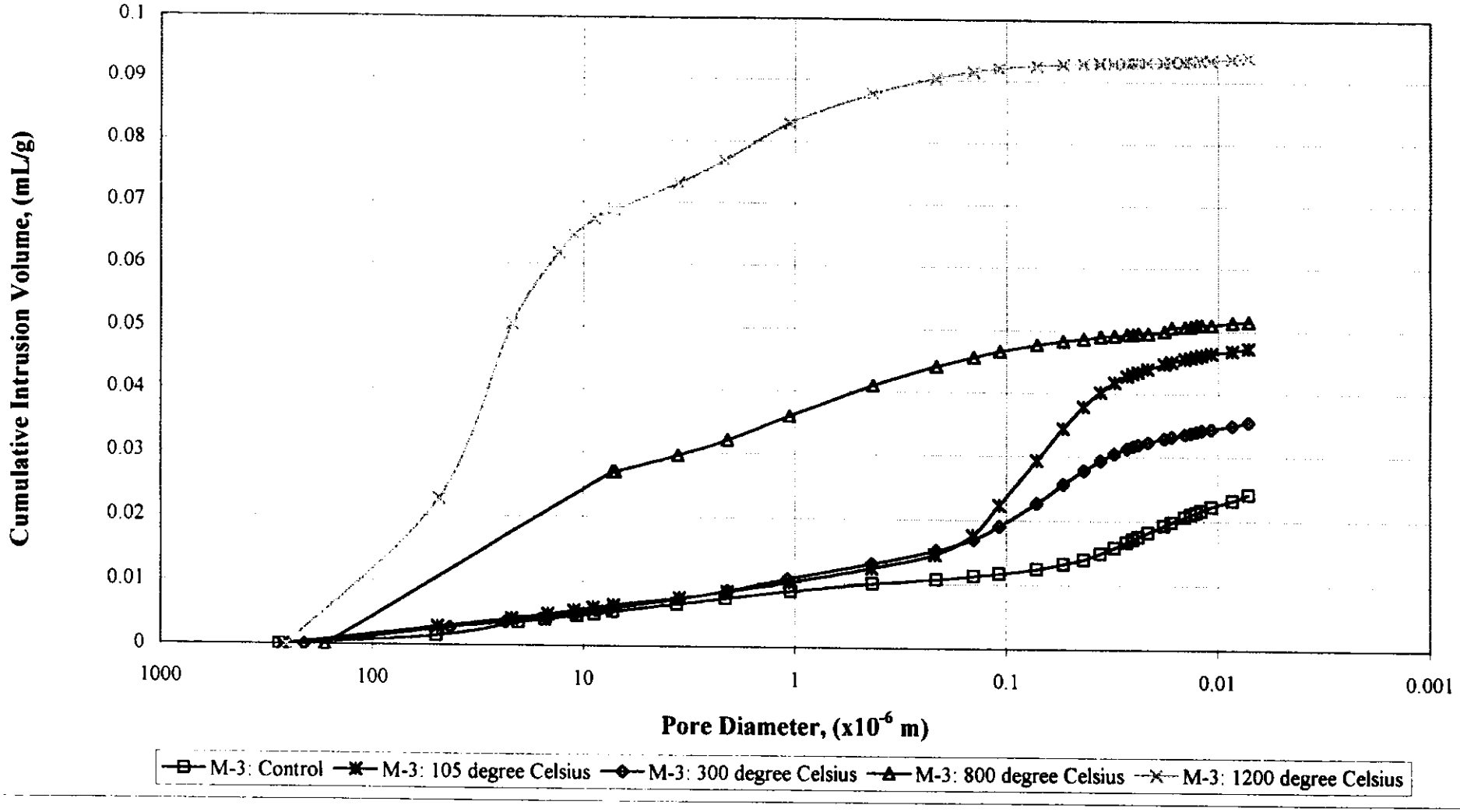

Fig. 4-33 Cumulative Intrusion Volume vs. Pore Diameter
(M-3 specimens initially at moisture content of 60%)

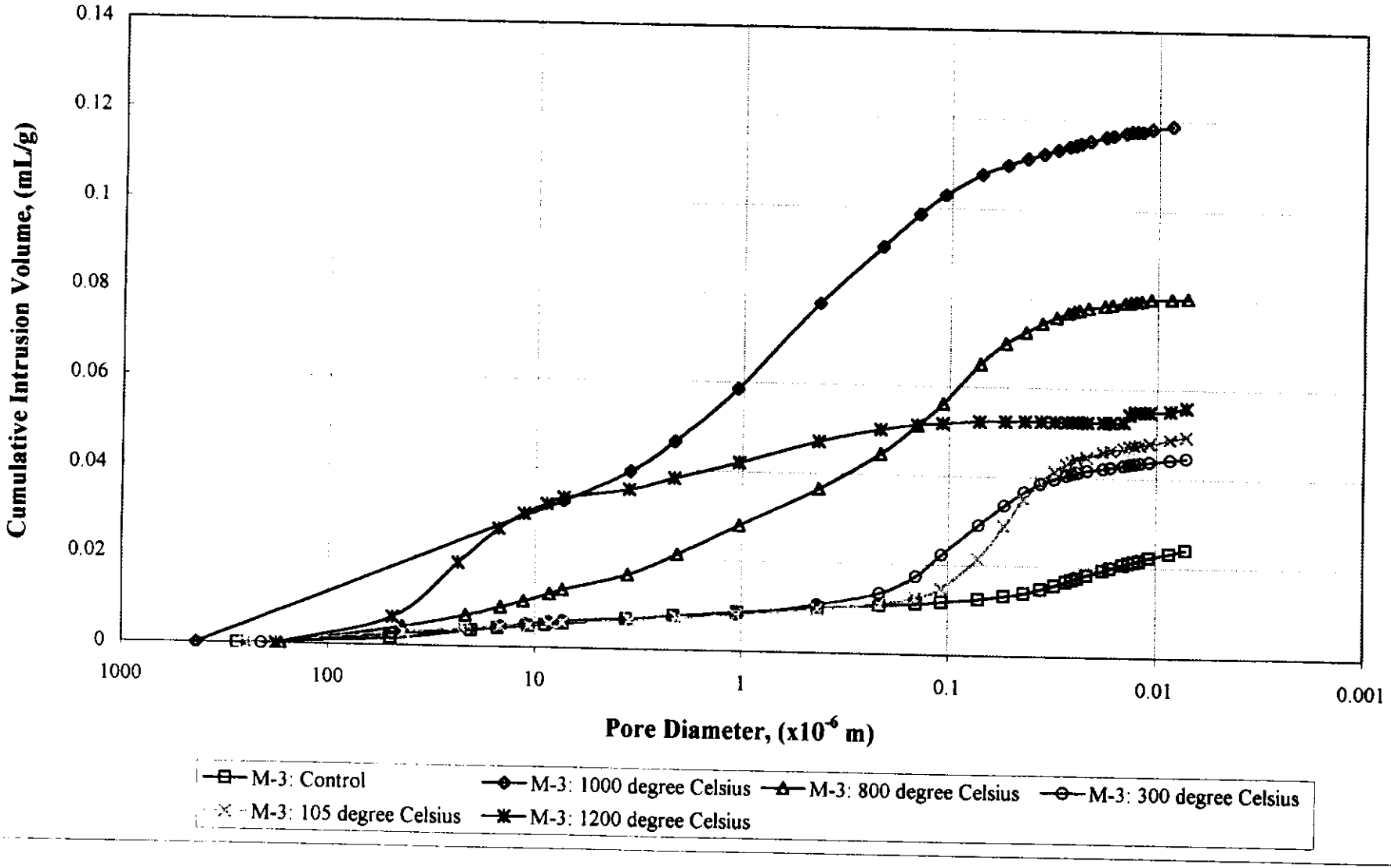

Fig. 4-34 Cumulative Intrusion Volume vs. Pore Diameter
(M-3 specimens initially at moisture content of 100%)

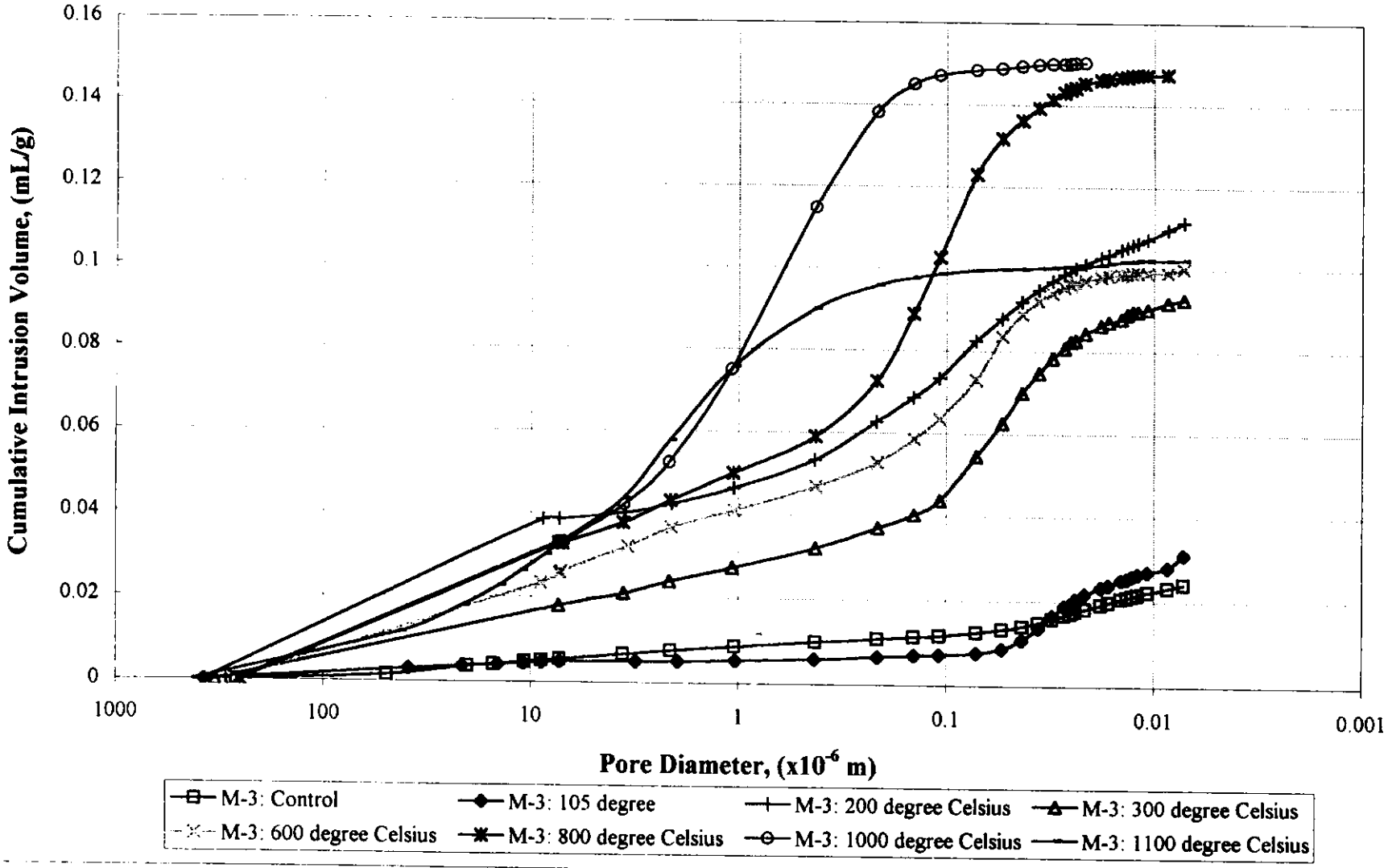

Fig. 4-35 Cumulative Intrusion Volume vs. Pore Diameter
(M-1F specimens initially at moisture content of 20%)

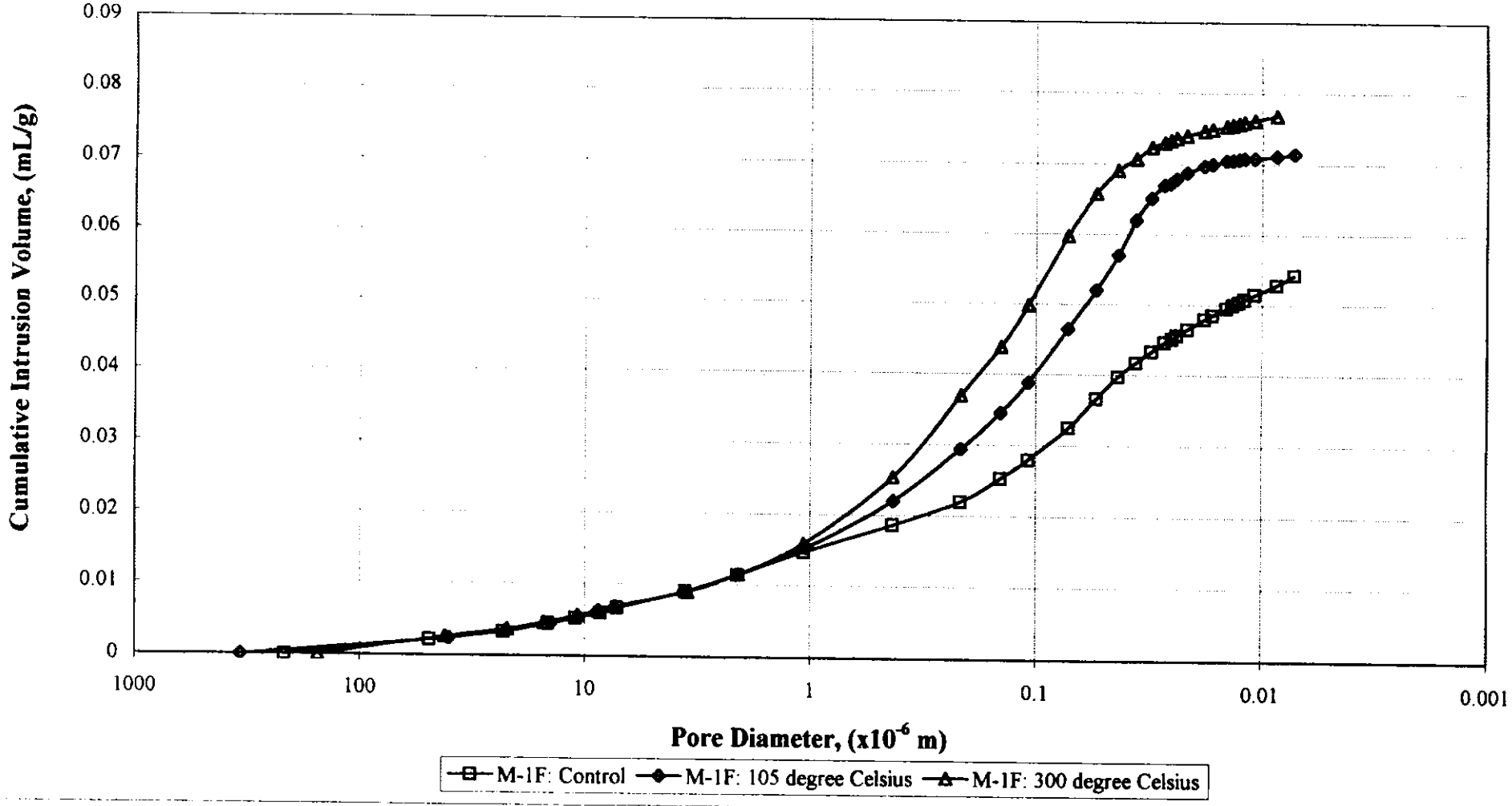

Fig. 4-36 Cumulative Intrusion Volume vs. Pore Diameter
(M-1F specimens initially at moisture content of 60%)

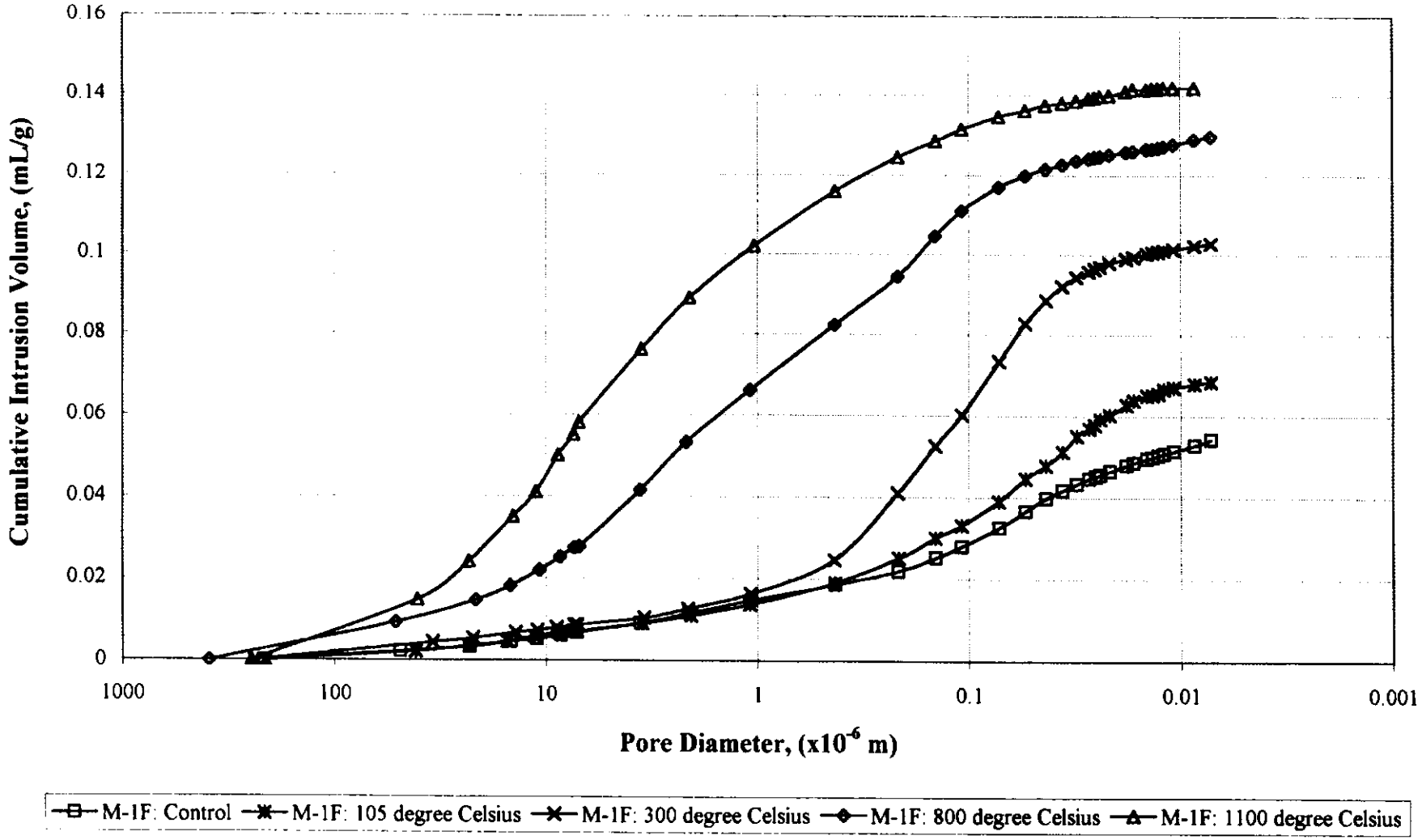

Fig. 4-37 Cumulative Intrusion Volume vs. Pore Diameter
(M-1F specimens initially at moisture content of 100%)

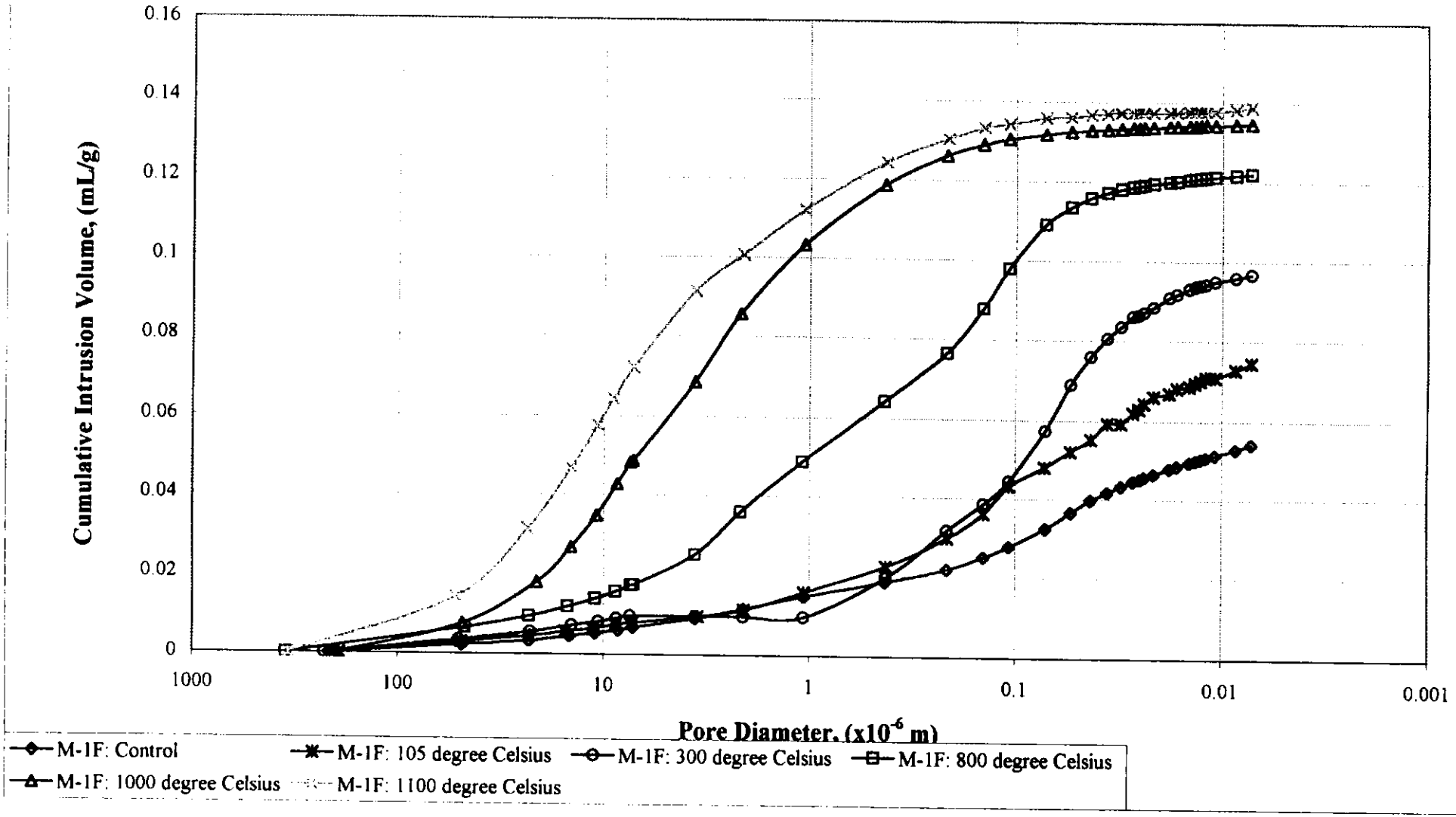

Fig. 4-38 Cumulative Intrusion Volume vs. Pore Diameter
(M-3F specimens initially at moisture content of 20%)

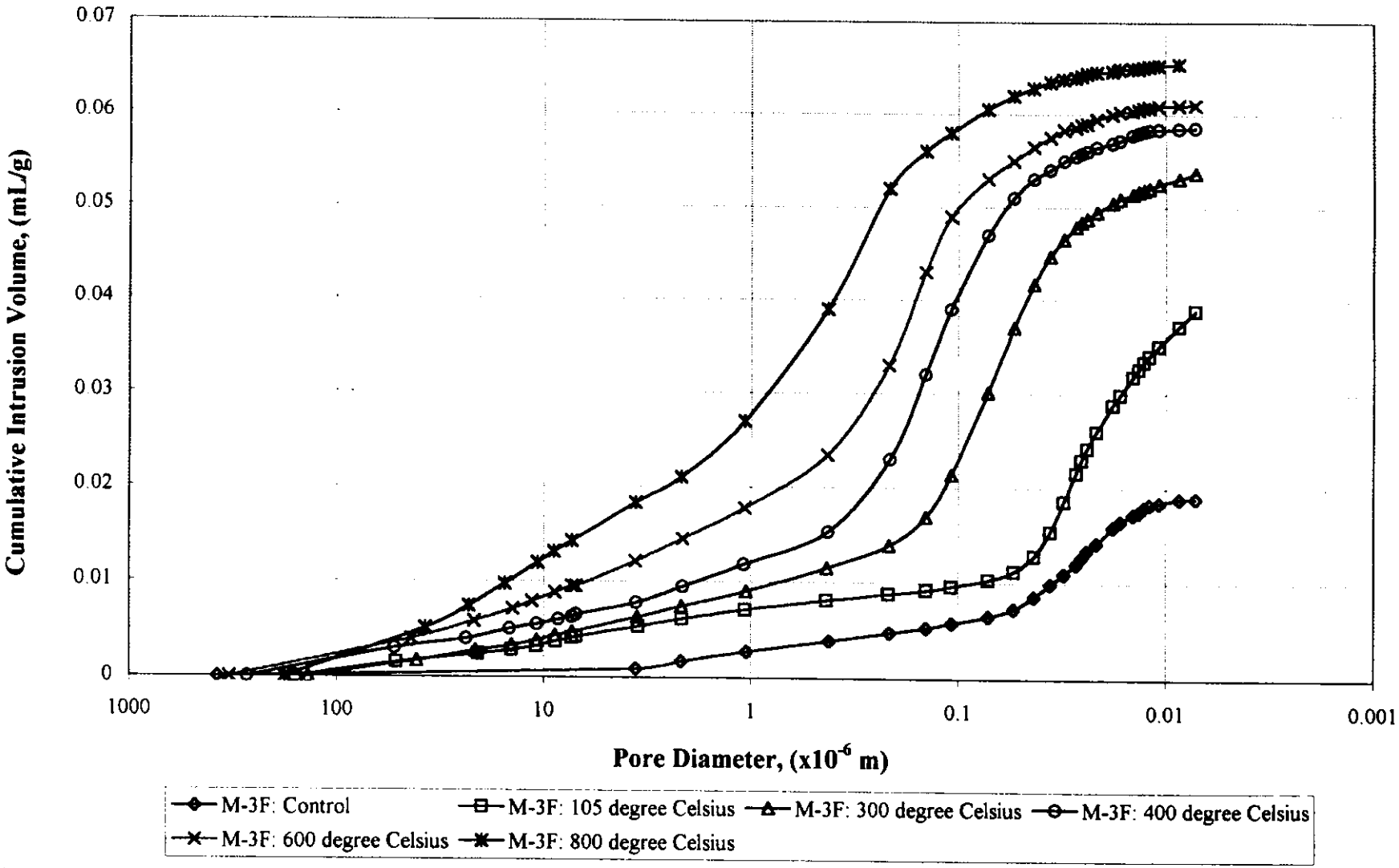

Fig. 4-39 Cumulative Intrusion Volume vs. Pore Diameter
(M-3F specimens initially at moisture content of 60%)

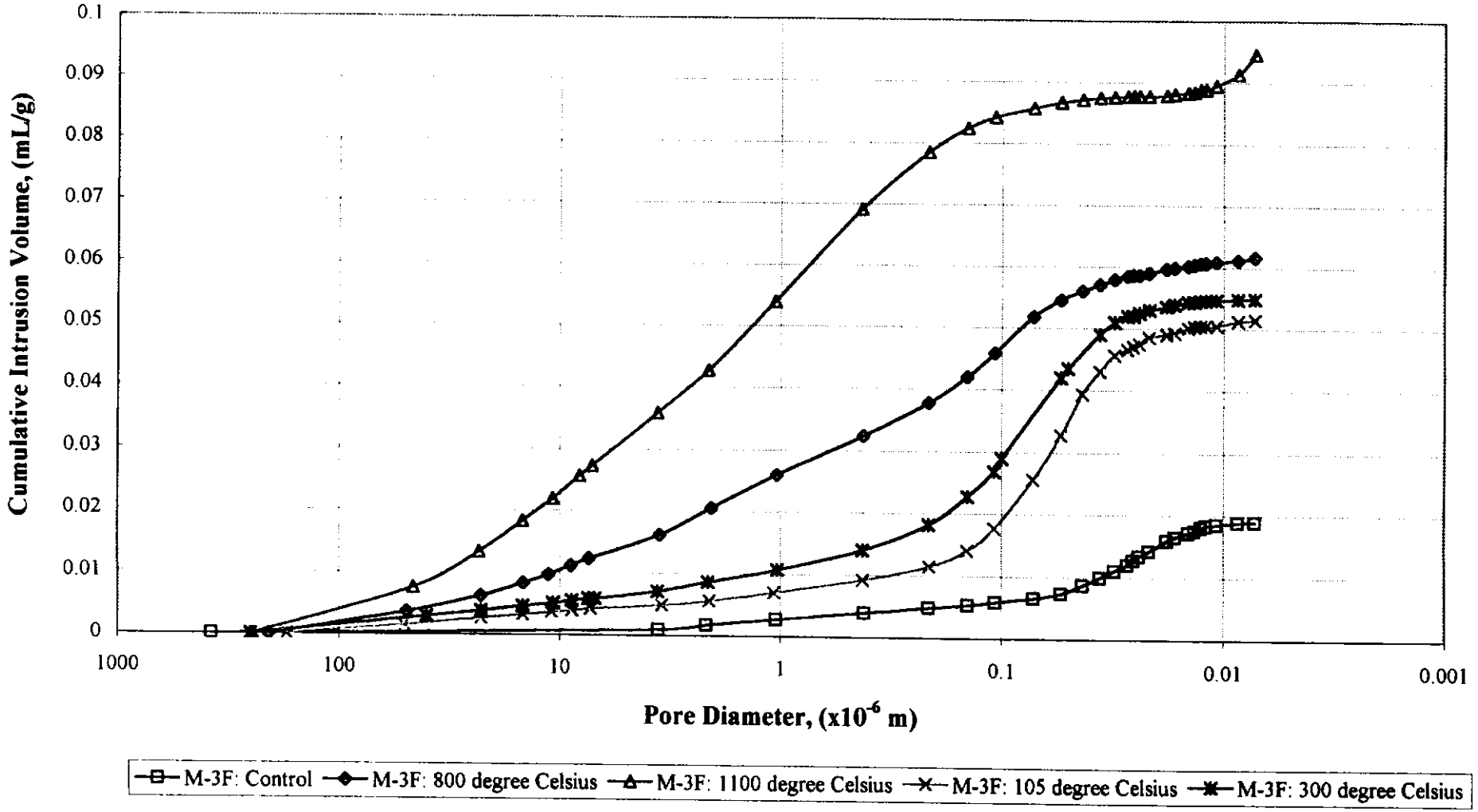

Fig. 4-40 Cumulative Intrusion Volume vs. Pore Diameter
(M-3F specimens initially at moisture content of 100%)

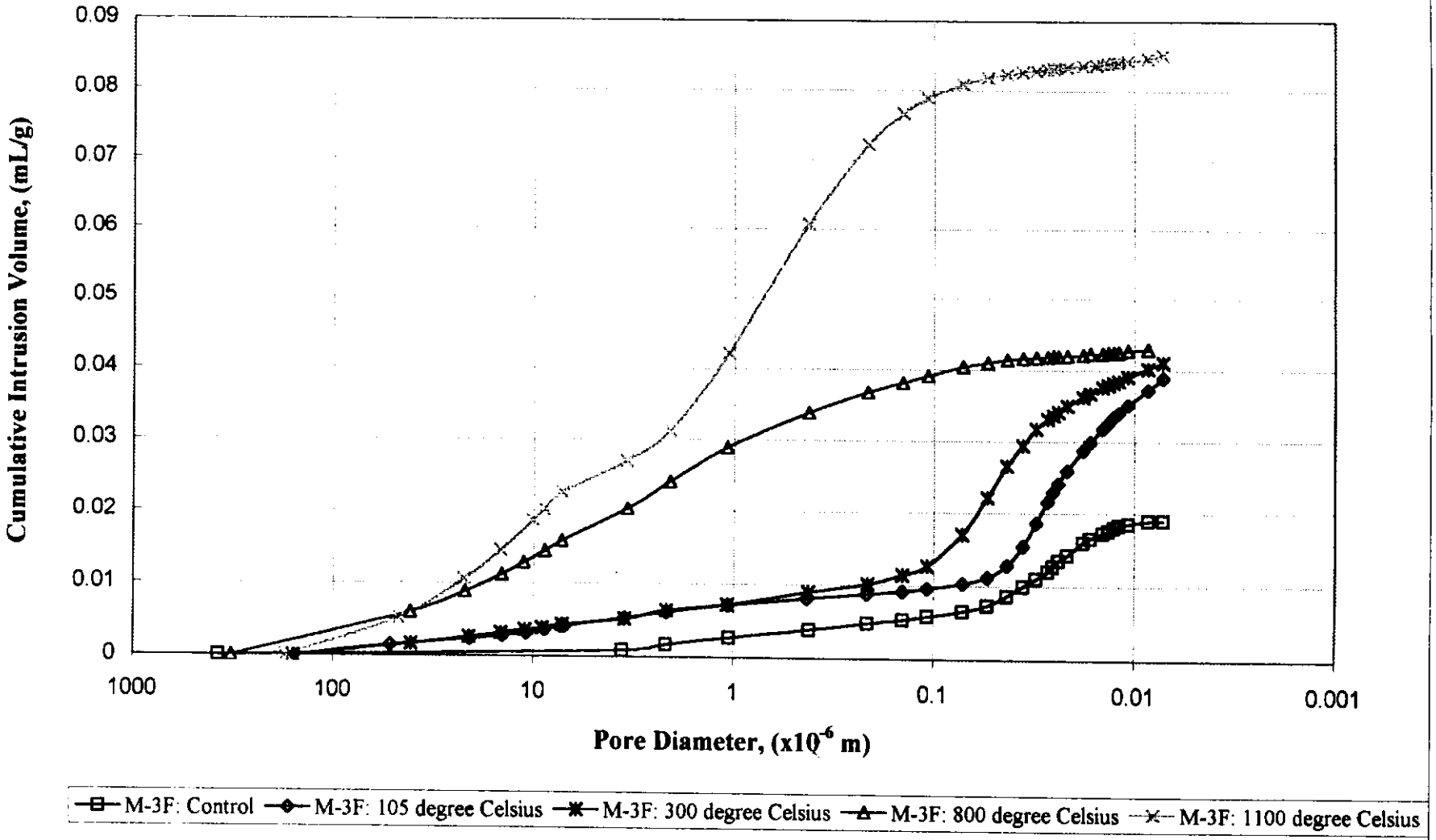

Fig. 4-41 Cumulative pore volume for concrete mixes with diameter ≥ 0.1×10^{-6}m at 20% initial moisture content

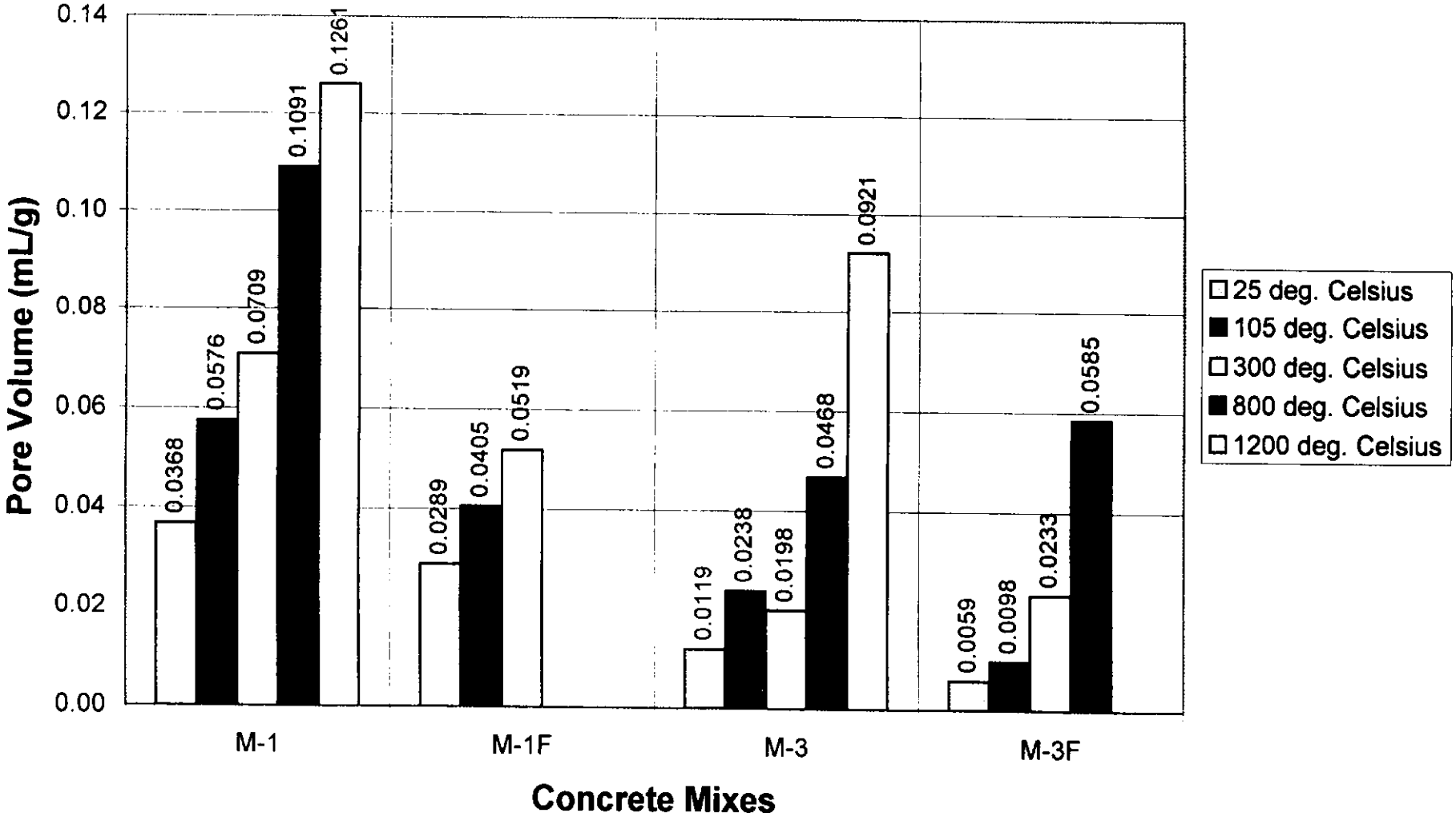

Fig. 4-42 Cumulative pore volume for concrete mixes with diameter ≥ 0.1×10^{-6}m at 60% initial moisture content

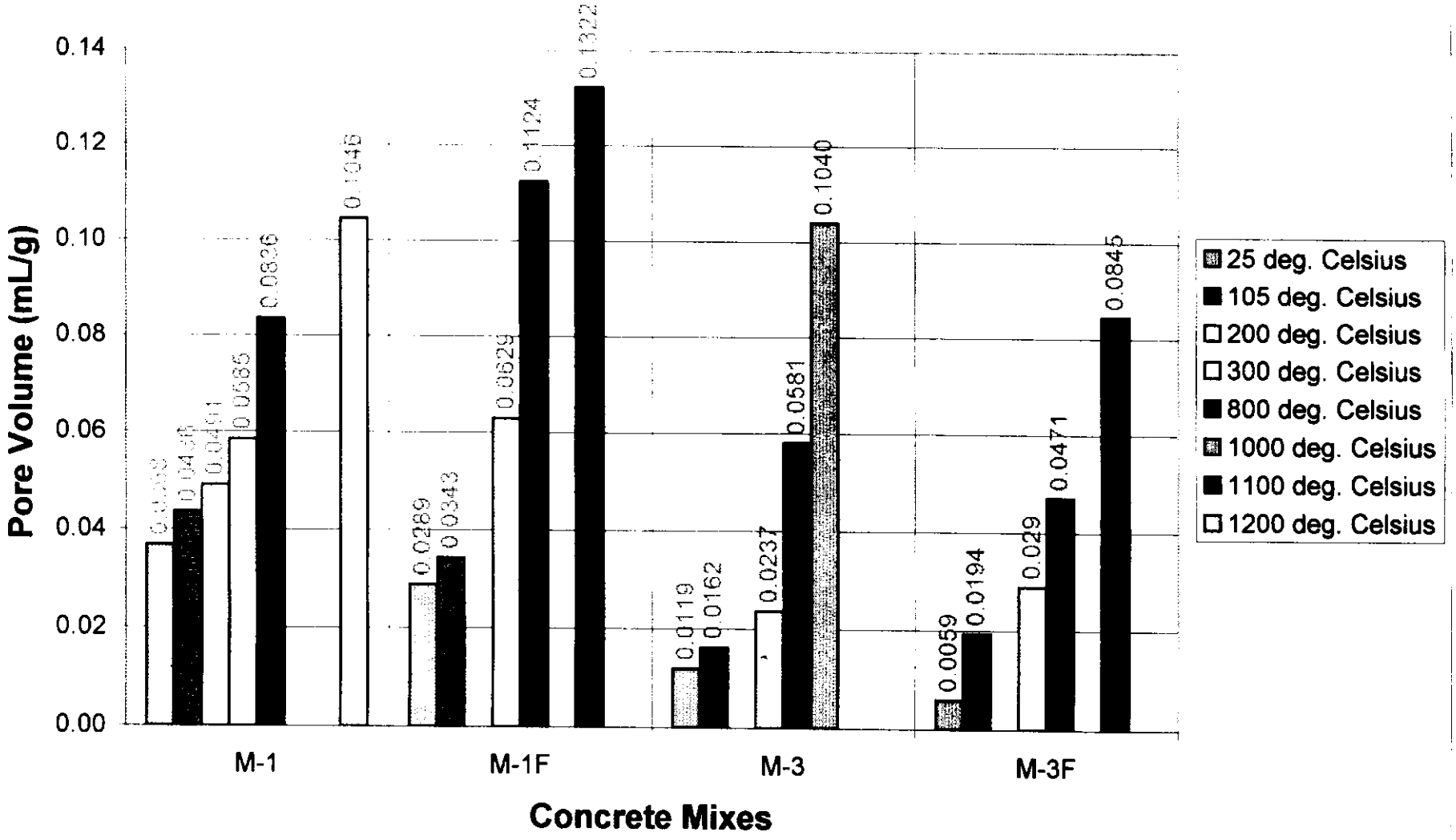

Fig. 4-43 Cumulative pore volume for concrete mixes with diameter ≥ 0.1×10^{-6}m at 100% initial moisture content

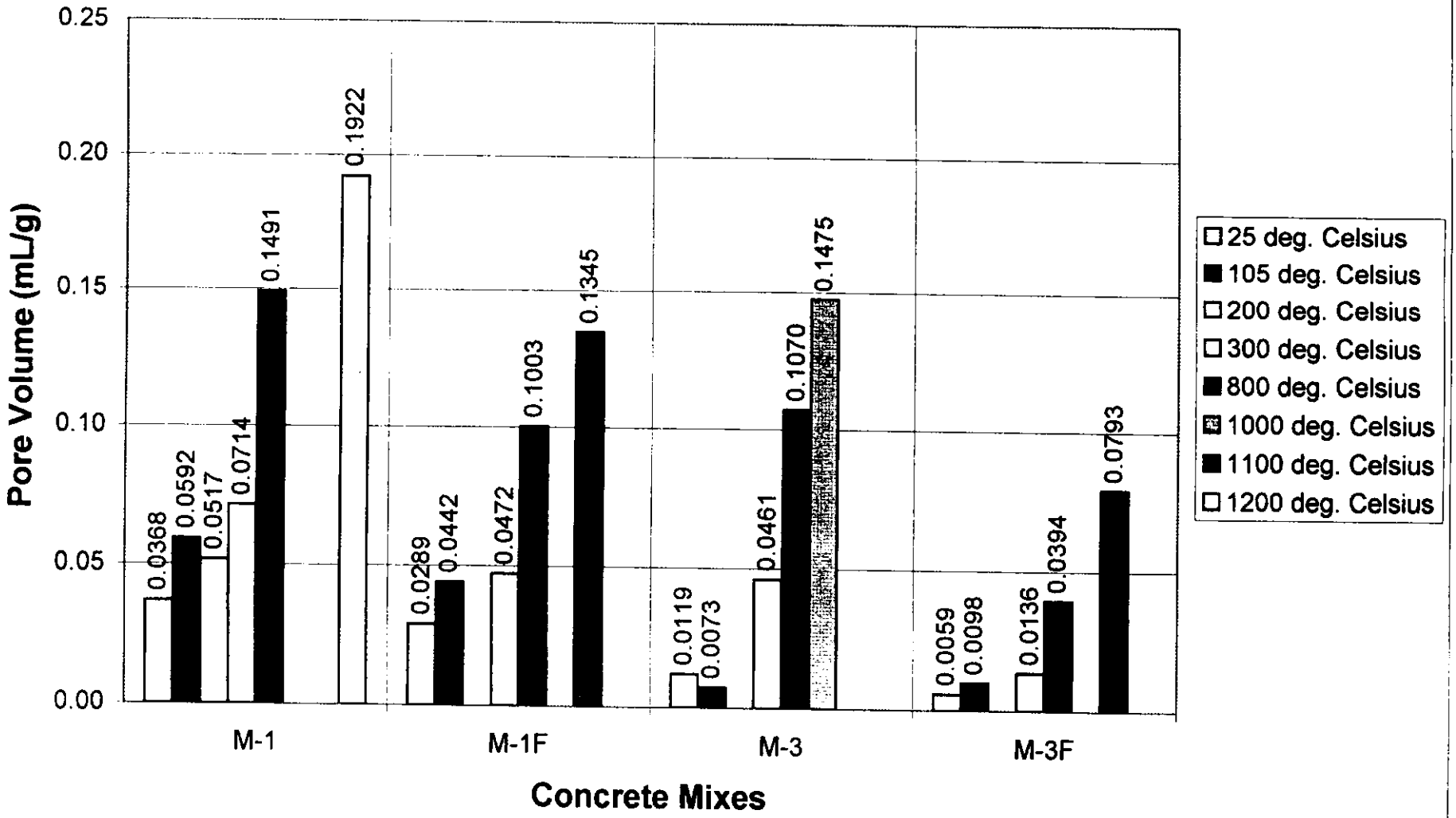

Fig. 4-44 Cumulative pore volume for concrete mixes with diameter ≥ 1.3×10^{-6}m at 20% initial moisture content

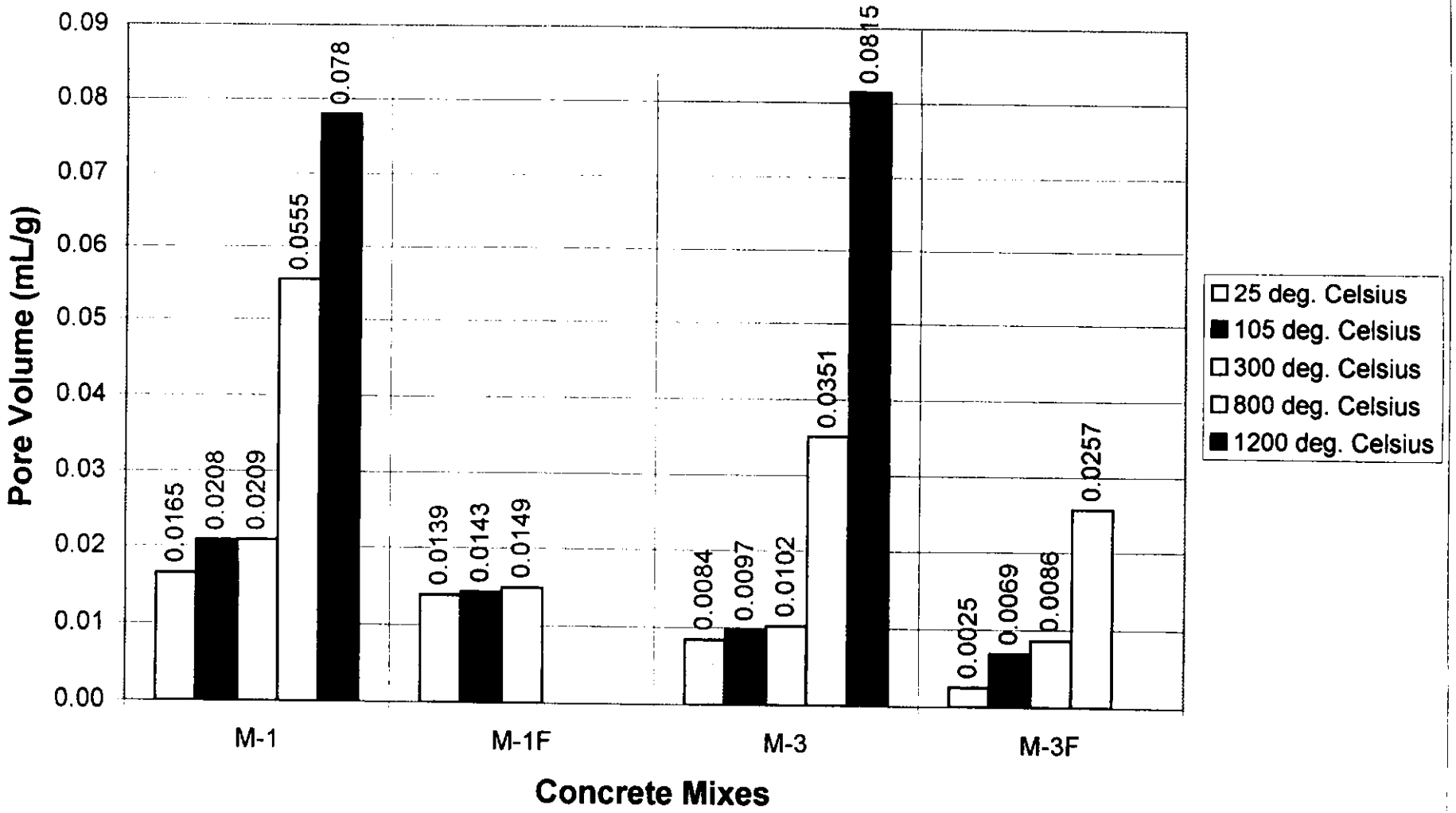

Fig. 4-45 Cumulative pore volume for concrete mixes with diameter ≥ 1.3×10^{-6}m at 60% initial moisture content

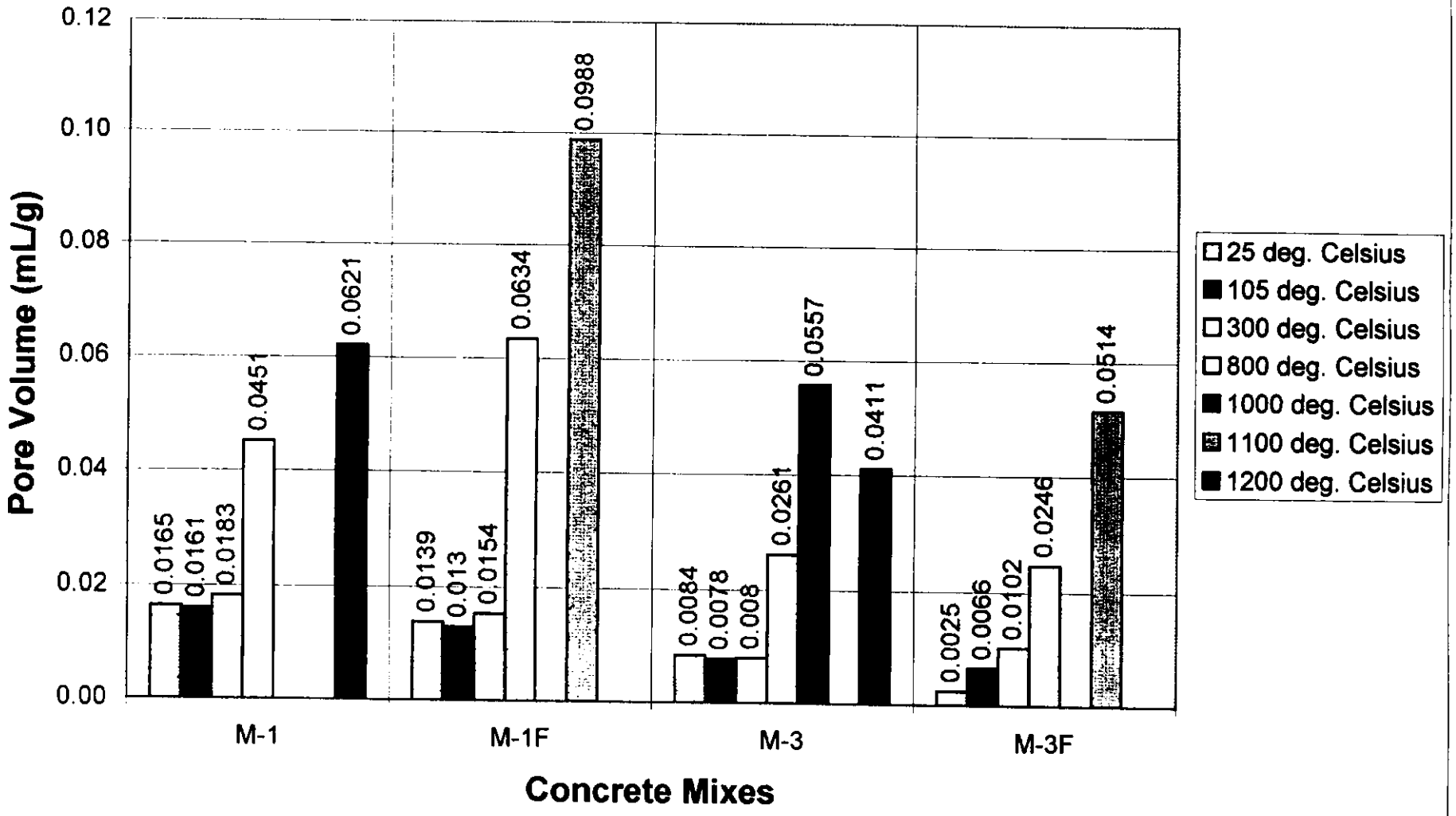

Fig. 4-46 Cumulative pore volume for concrete mixes with diameter $\geq 1.3 \times 10^{-6}$m at 100% initial moisture content

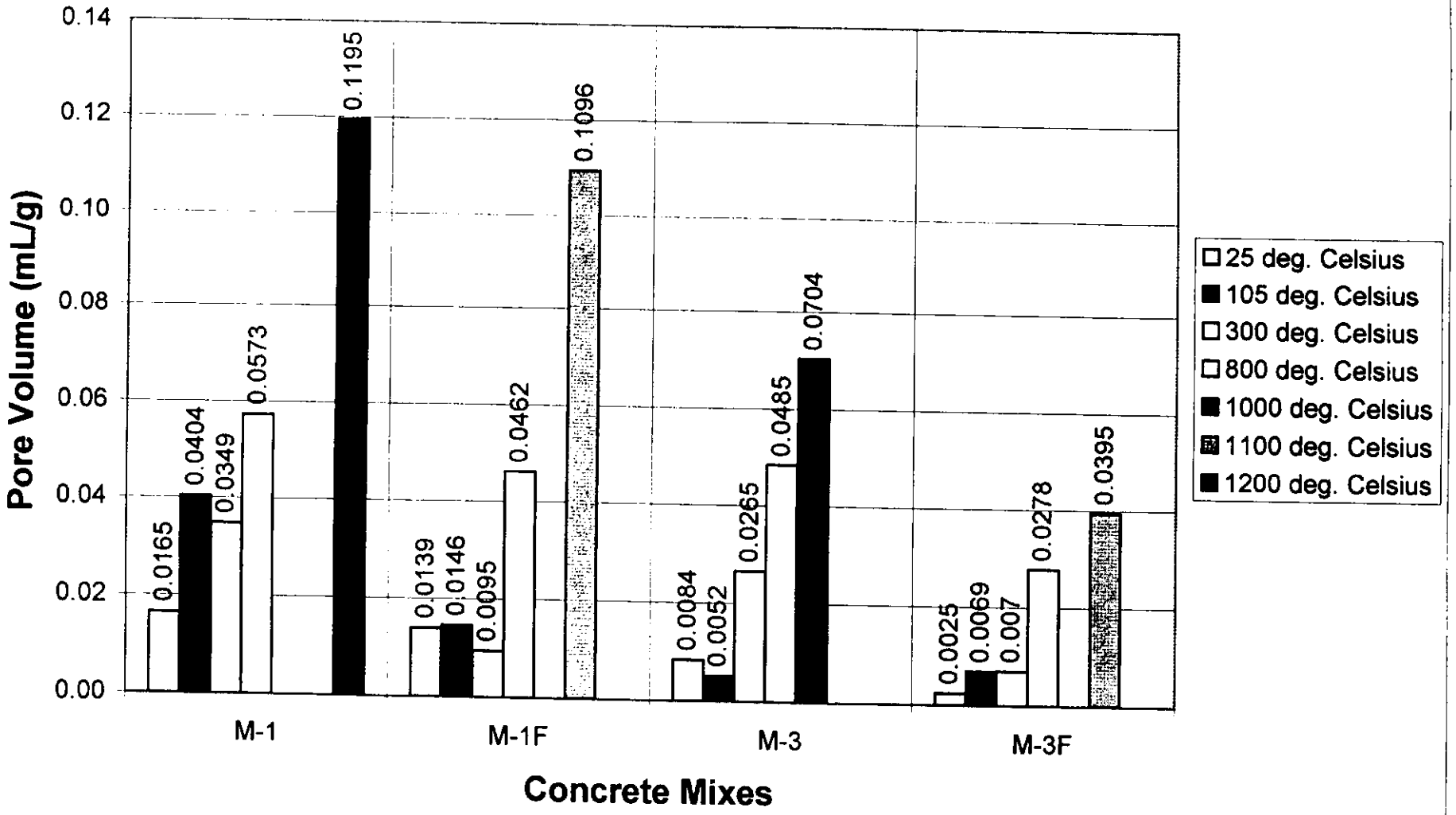

Fig. 4-47 Cumulative pore volume with diameter ≥ 0.1×10^{-6}m for concrete mix M-1

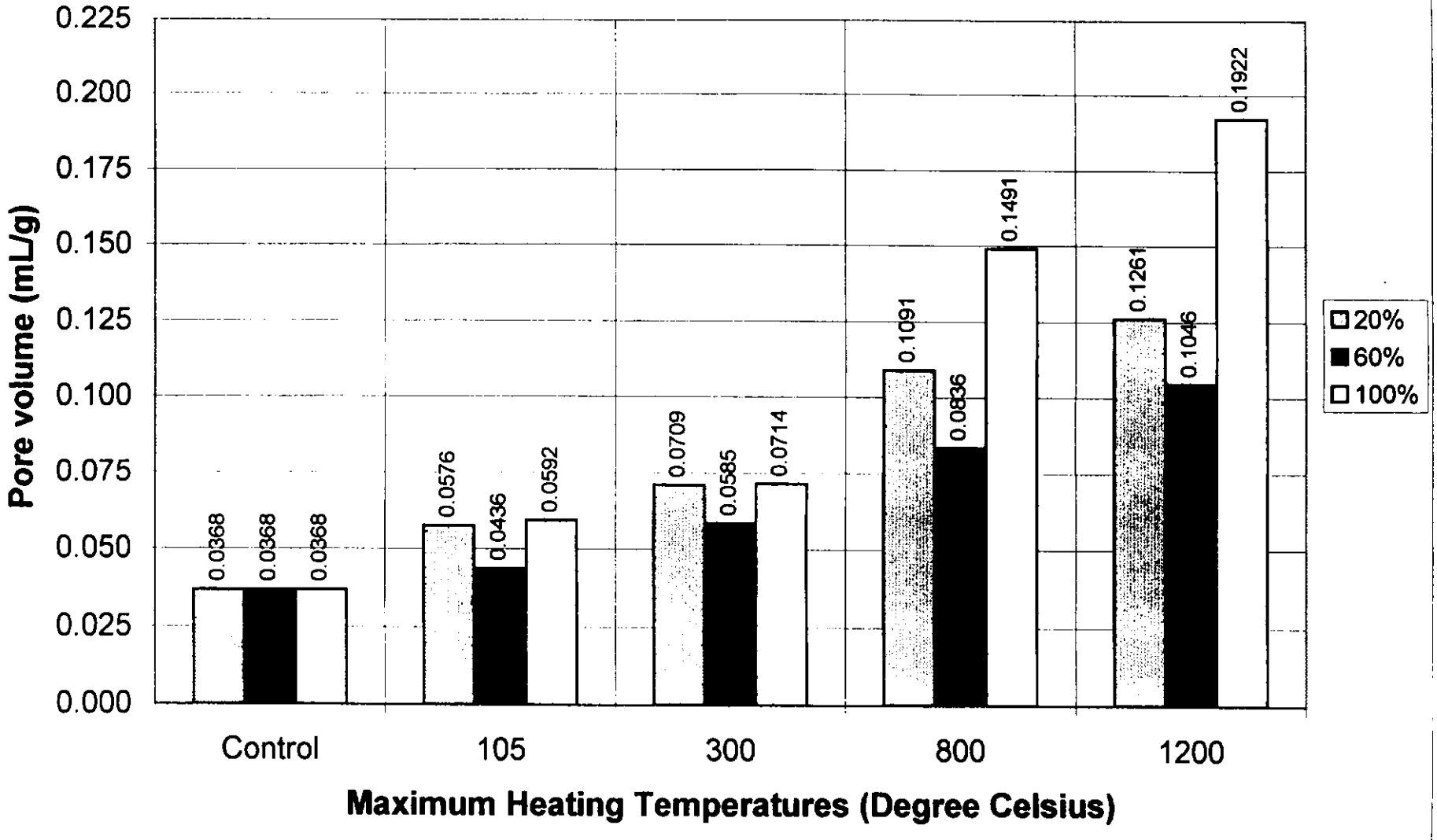

Fig. 4-48 Cumulative pore volume with diameter ≥ 1.3×10^{-6}m for concrete mix M-1

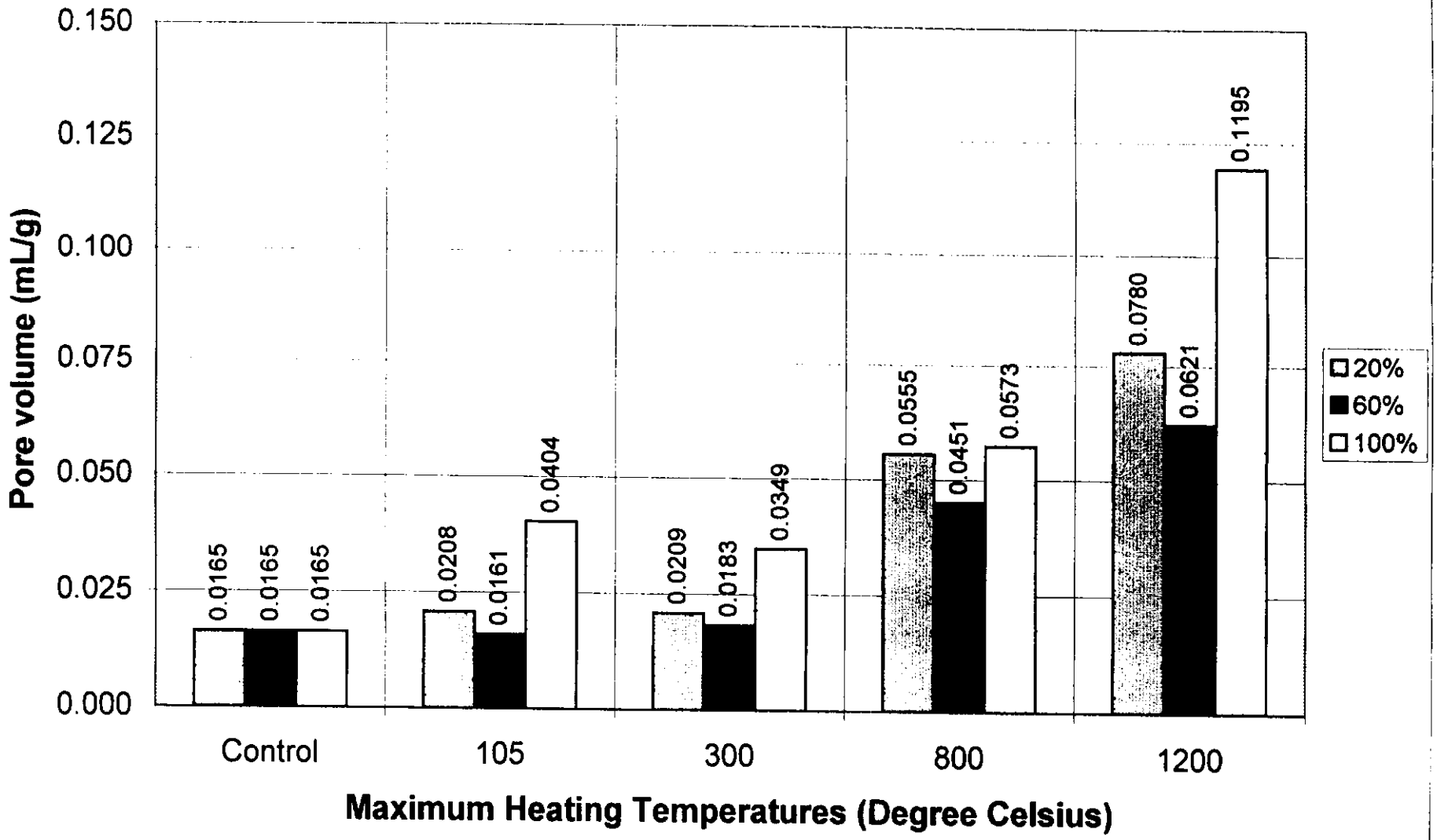

Fig. 4-49 Cumulative pore volume with diameter $\geq 0.1 \times 10^{-6}$m for concrete mix M-1F

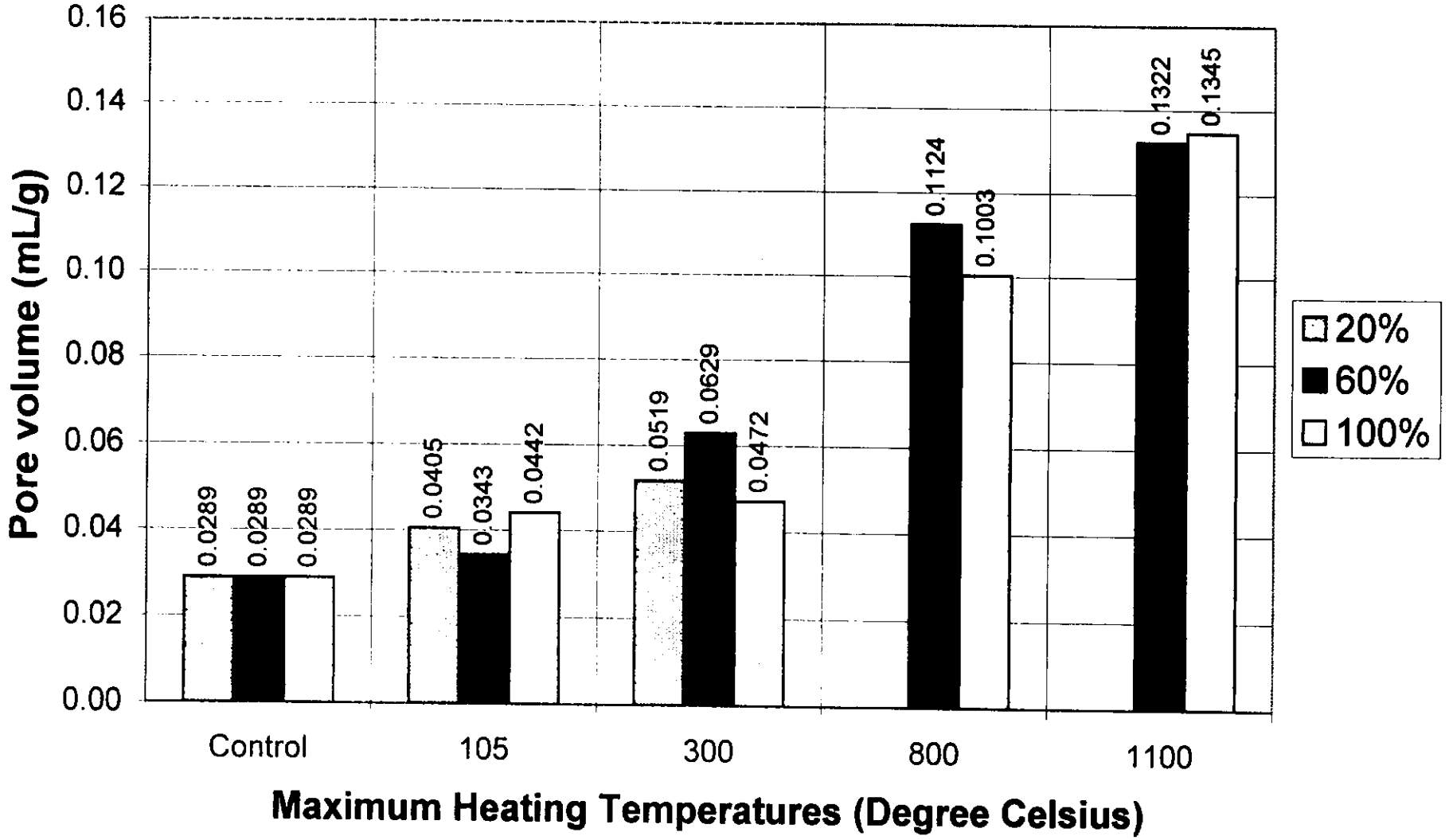

Fig. 4-50 Cumulative pore volume with diameter ≥ 1.3×10^{-6}m for concrete mix M-1F

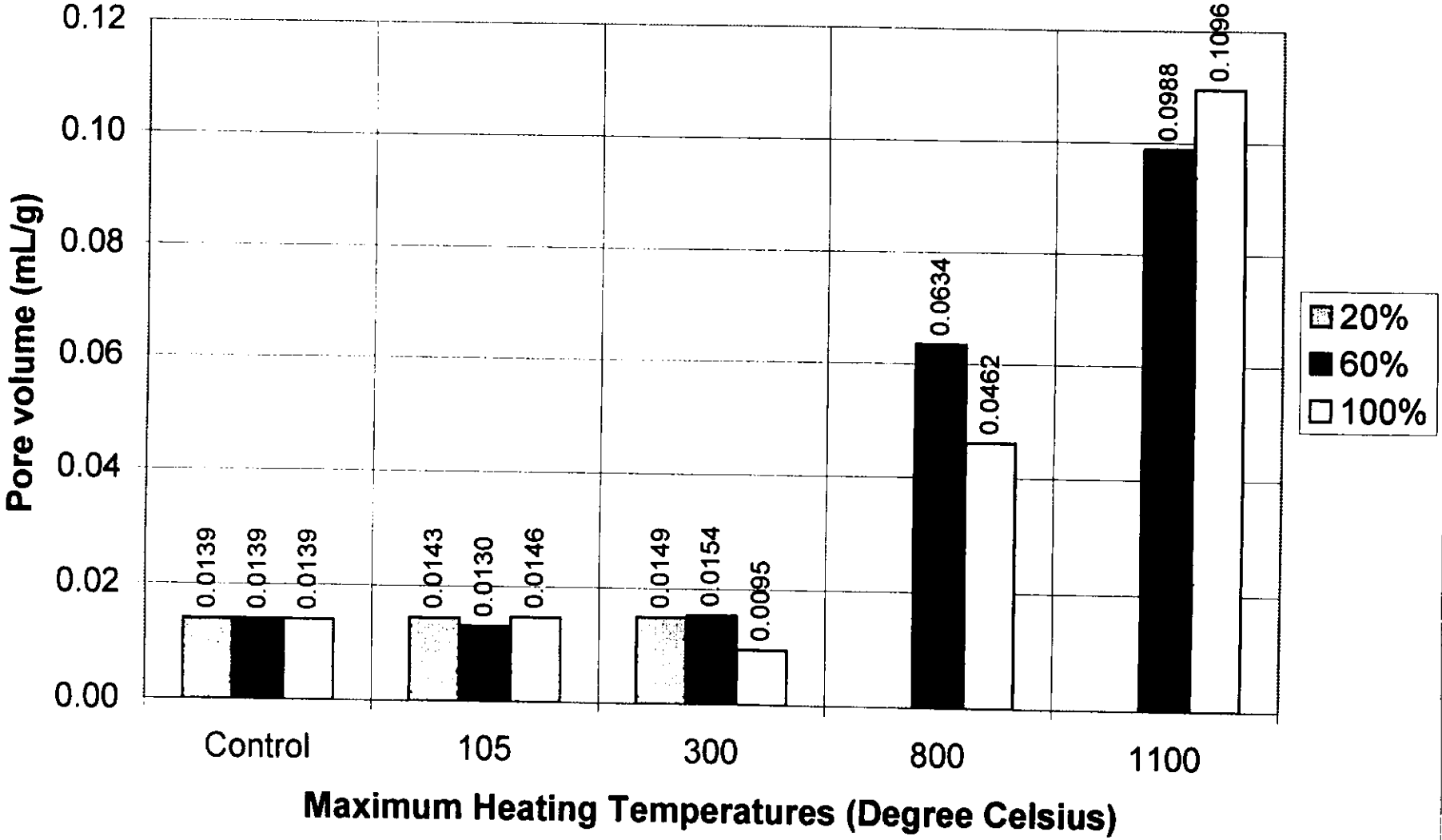

Fig. 4-51 Cumulative pore volume with diameter $\geq 0.1 \times 10^{-6}$m for concrete mix M-3

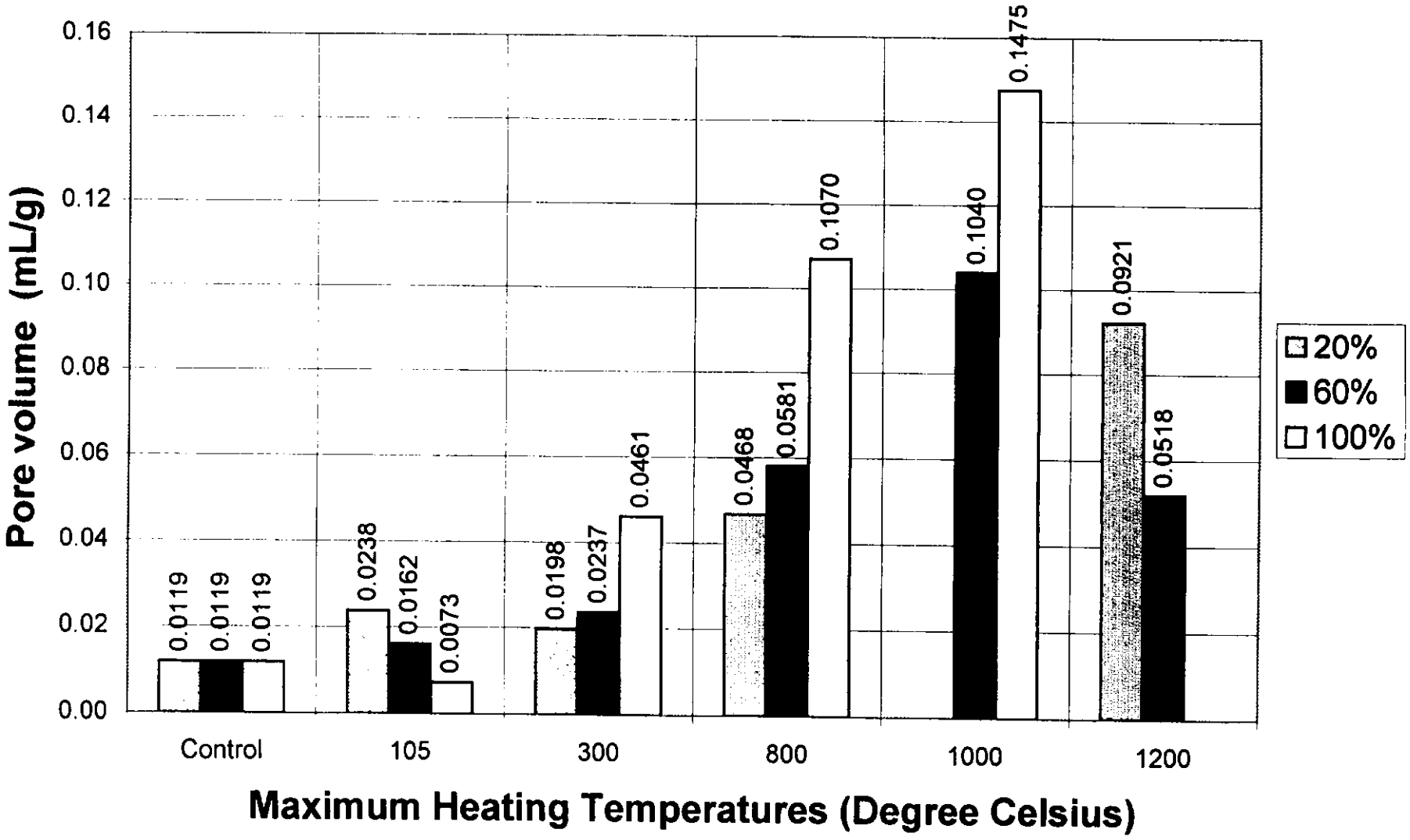

Fig. 4-52 Cumulative pore volume with diameter $\geq 1.3 \times 10^{-6}$m for concrete mix M-3

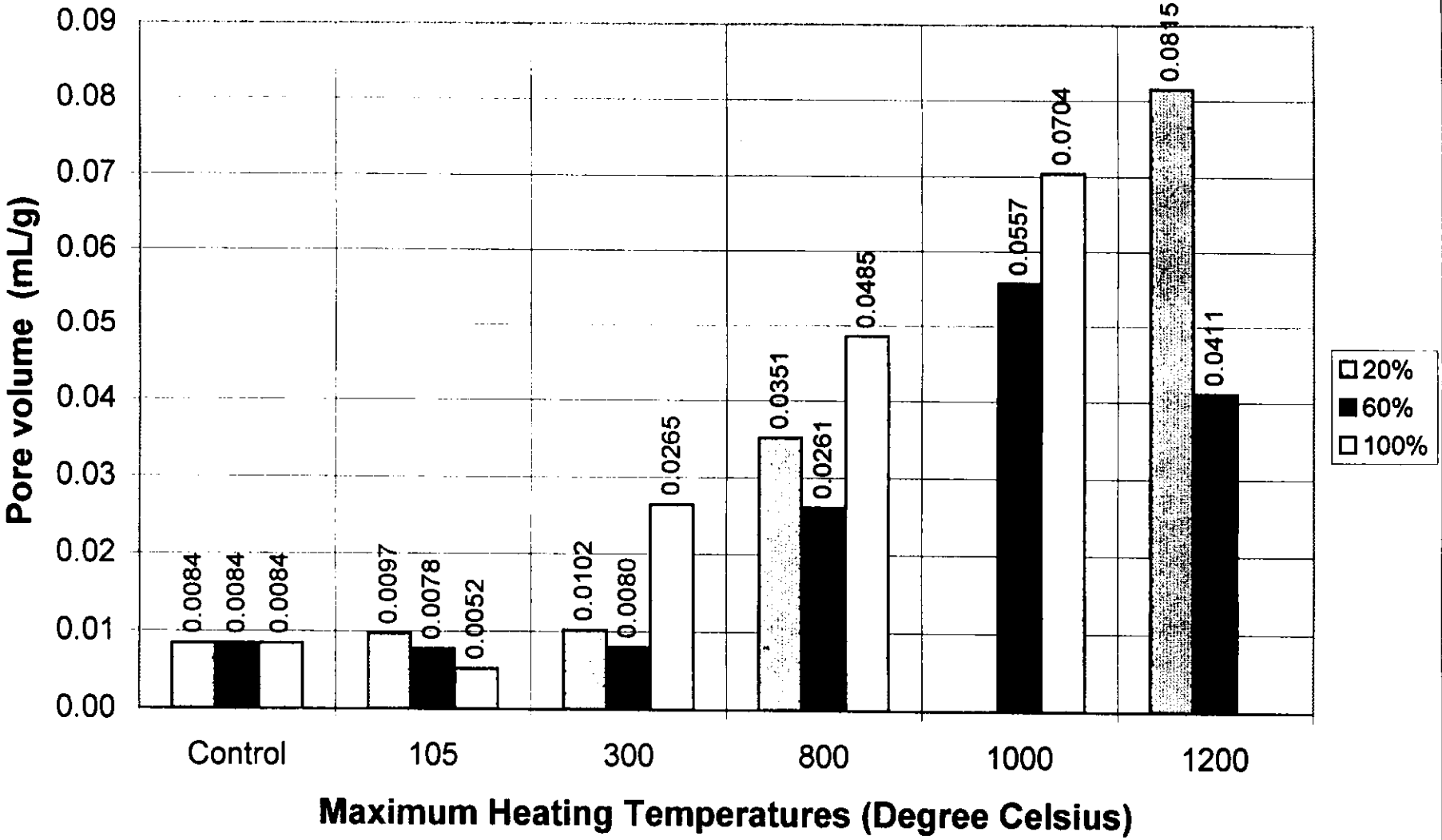

Fig. 4-53 Cumulative pore volume with diameter $\geq 0.1 \times 10^{-6}$m for concrete mix M-3F

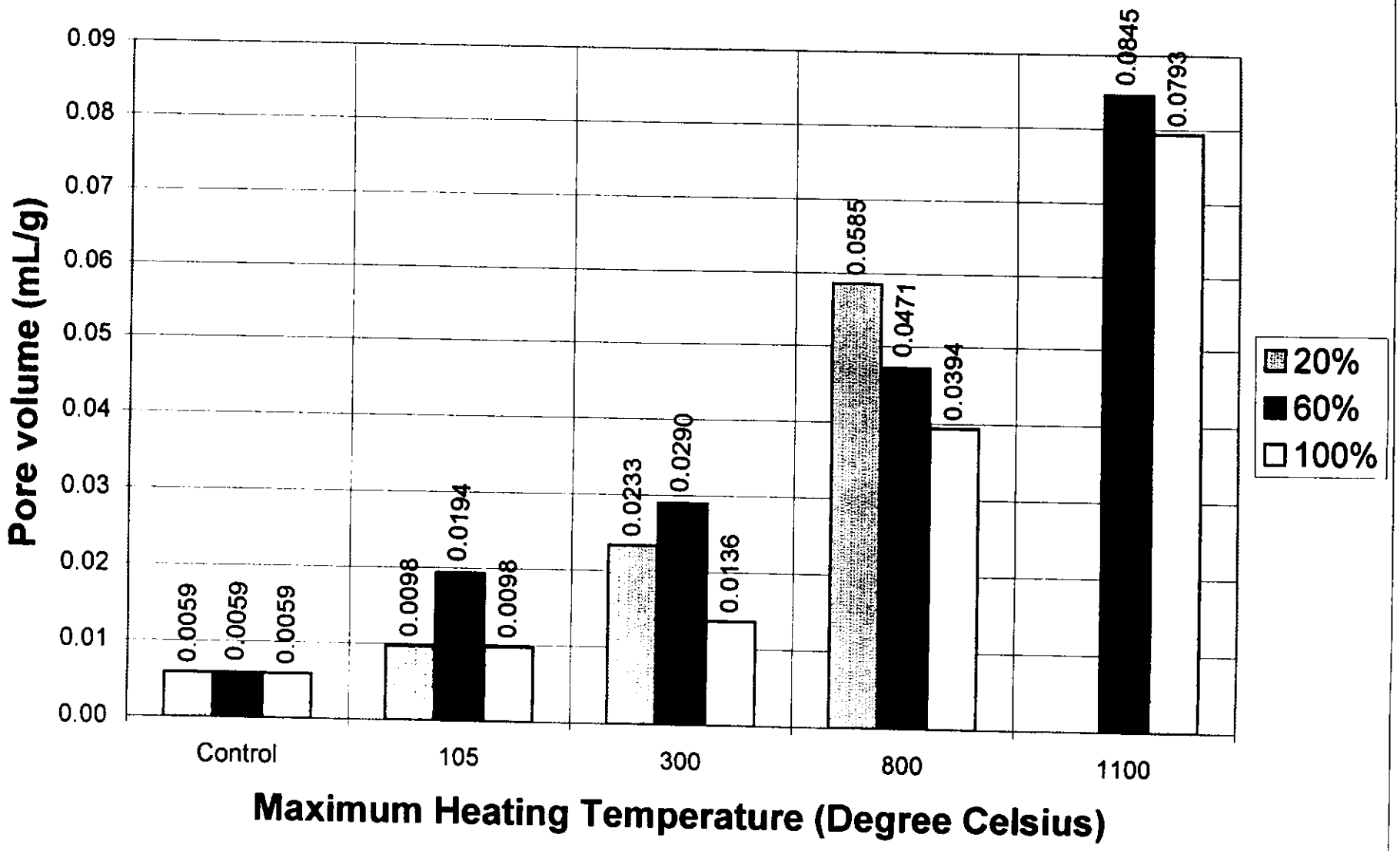

Fig. 4-54 Cumulative pore volume with diameter ≥ 1.3×10^{-6}m for concrete mix M-3F

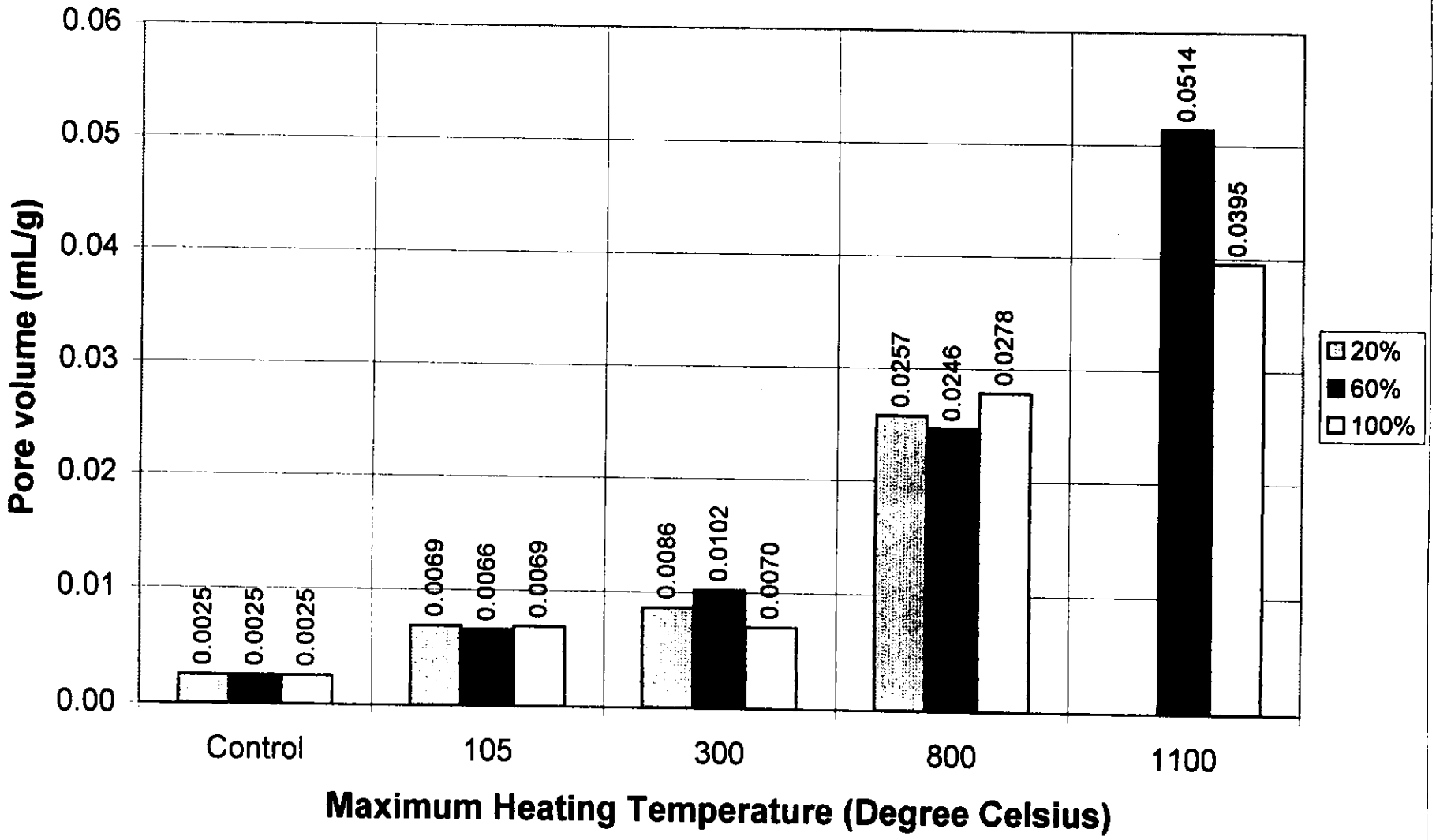

Fig. 4-55 Average Pore Diameter vs. Initial Moisture Content after Heating to Maximum Temperature of 105°C

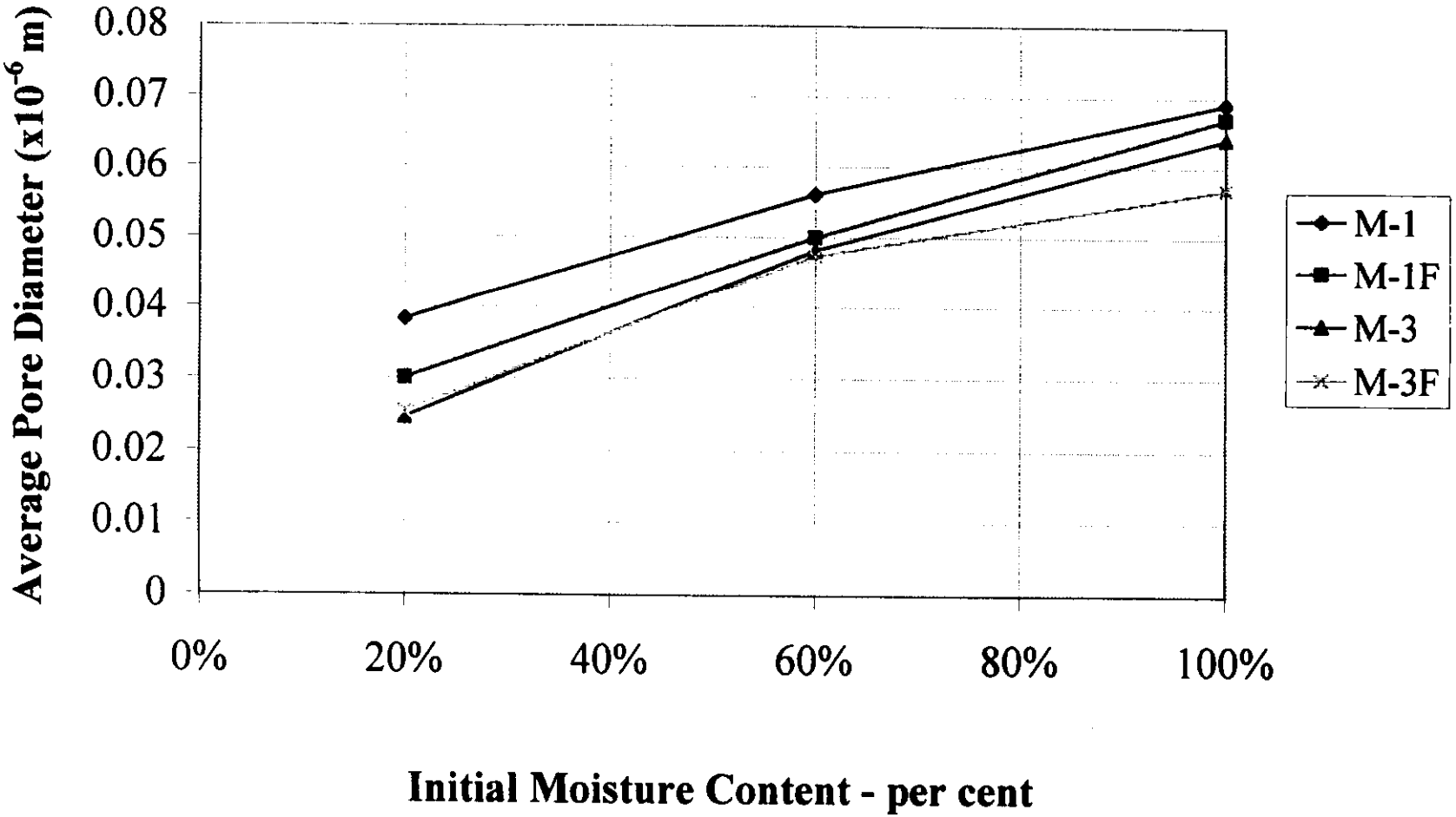

Fig. 4-56 Average Pore Diameter vs. Initial Moisture Content after Heating to Maximum Temperature of 300°C

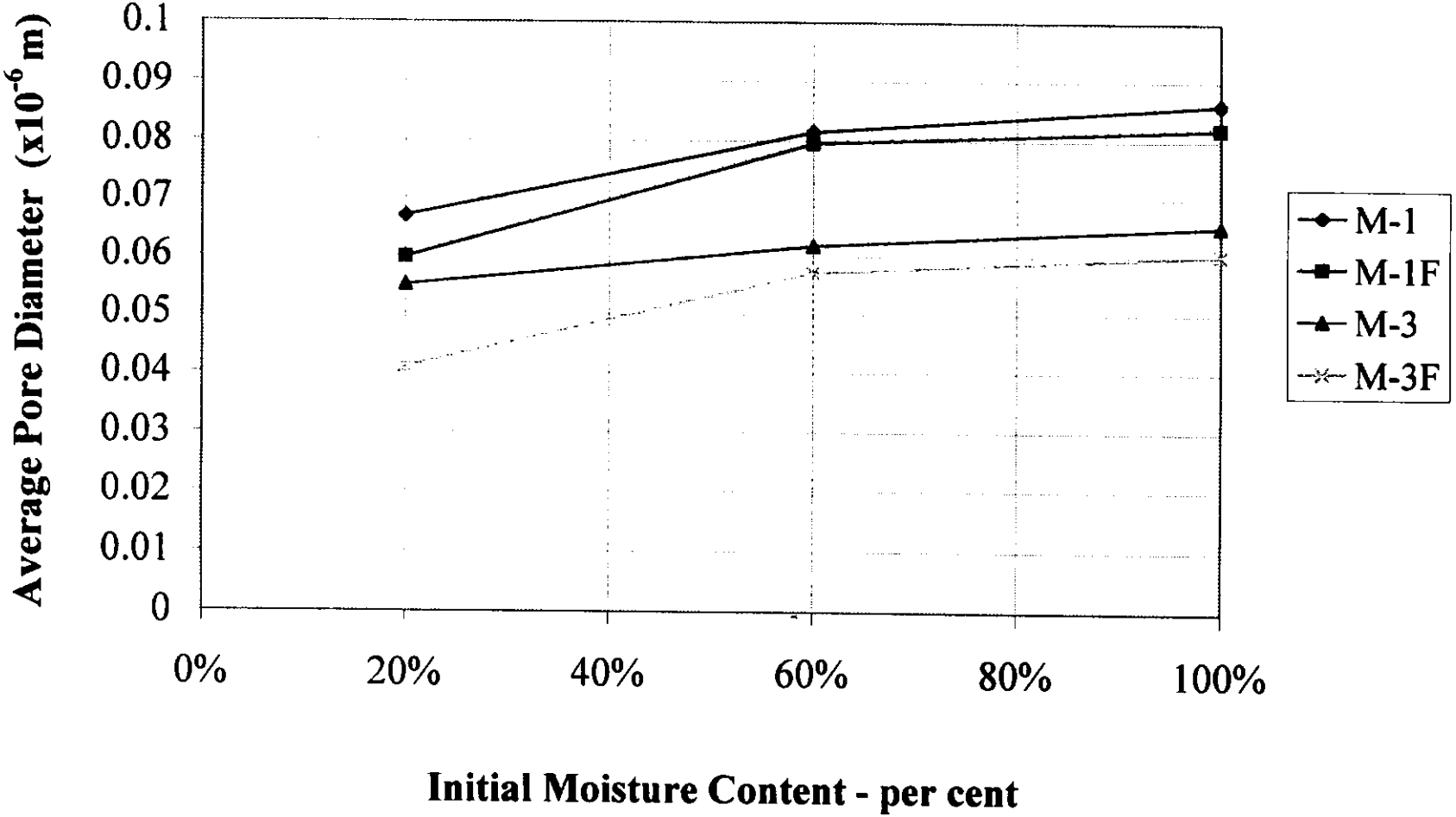

Fig. 4-57 Average Pore Diameter vs. Initial Moisture Content after Heating to Maximum Temperature of 800°C

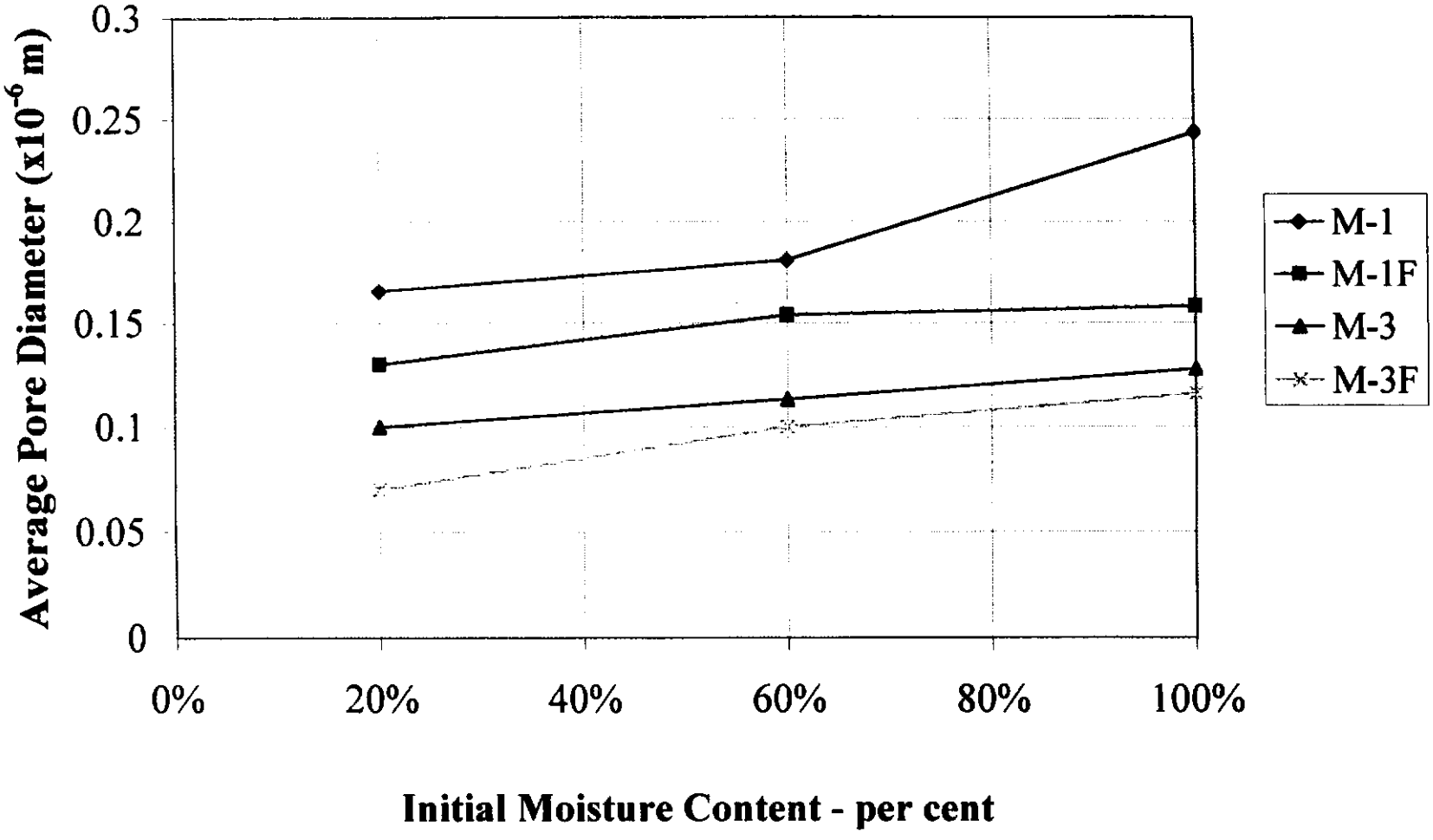

Fig. 4-58 Average Pore Diameter vs. Initial Moisture Content after Heating to Maximum Temperature of above 1000°C

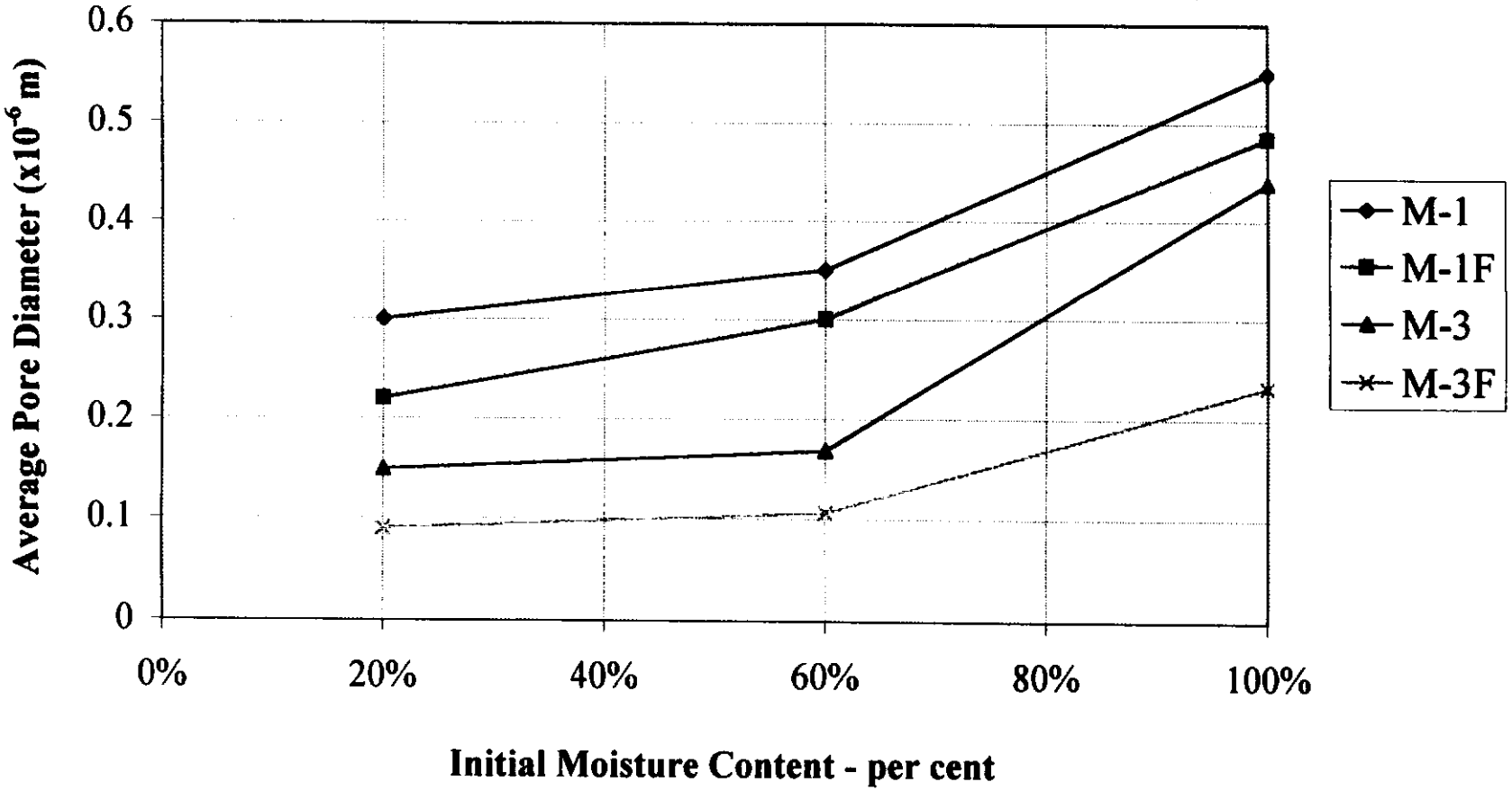

Fig. 4-59 Cumulative Intrusion Volume vs. Pore Diameter for Control Specimens that were not Heated

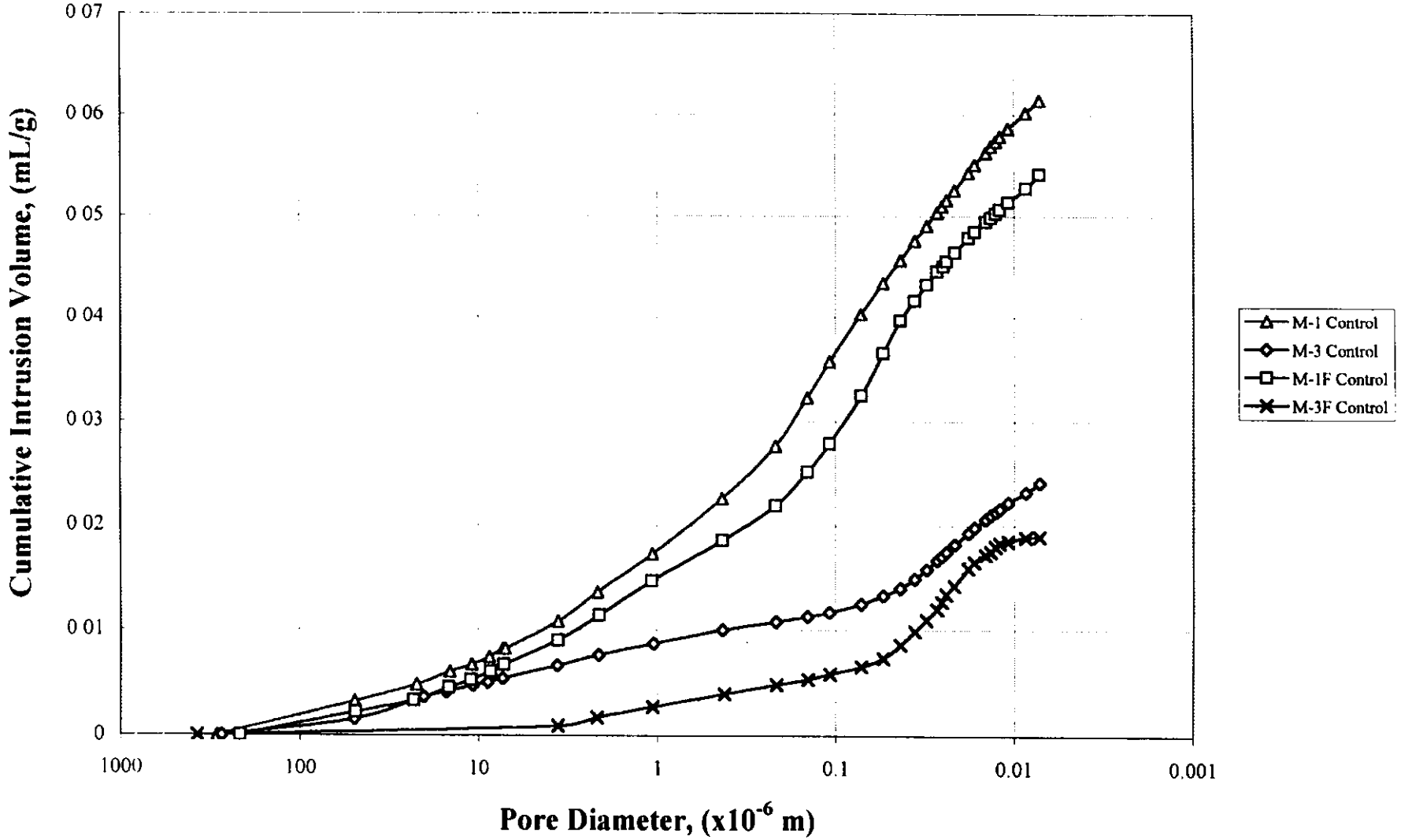

Fig. 4-60 Cumulative Intrusion Volume vs. Pore Diameter after Heating to a Maximum Temperature of 105 °C

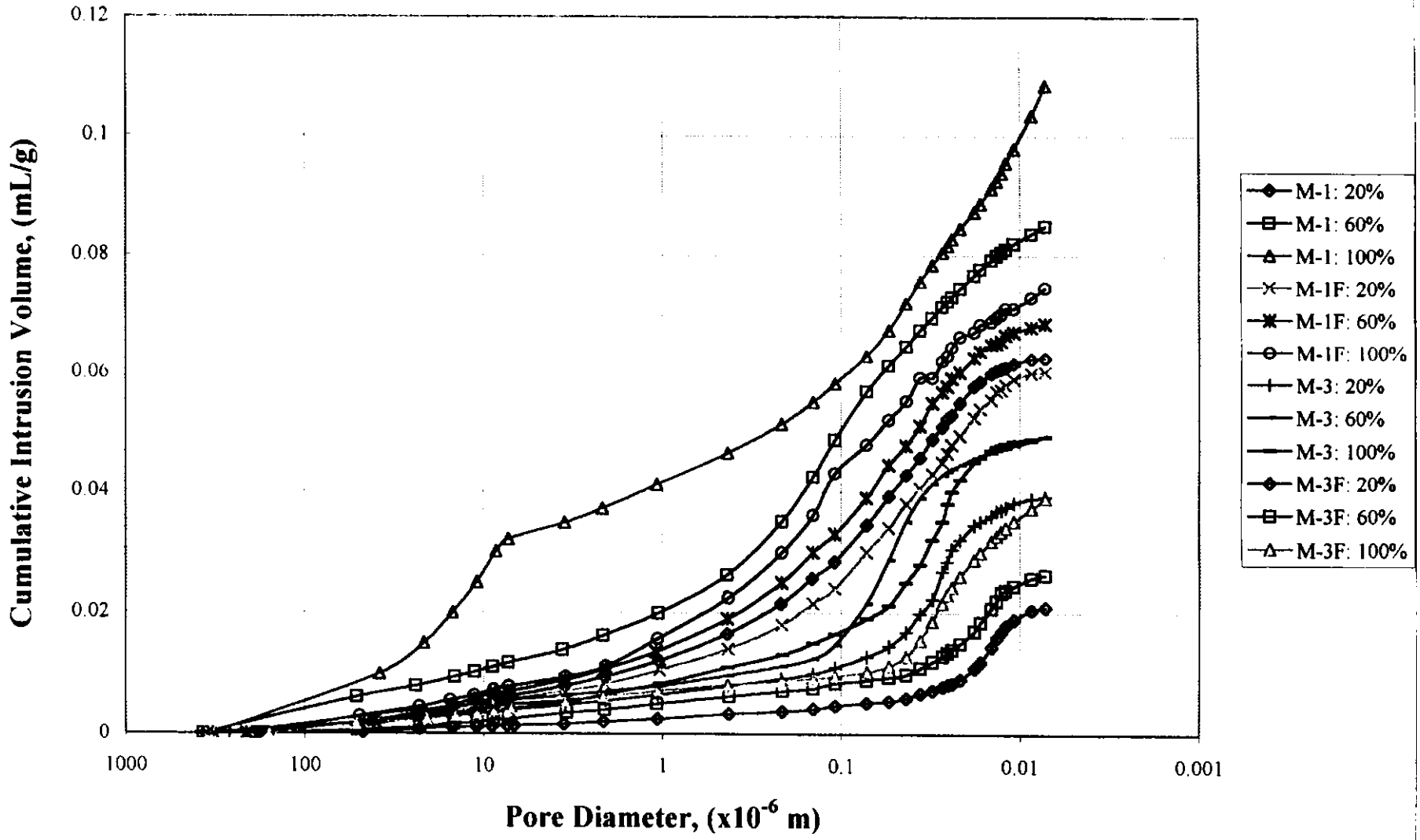

Fig. 4-61 Cumulative Intrusion Volume vs. Pore Diameter after Heating to a Maximum Temperature of 300 °C

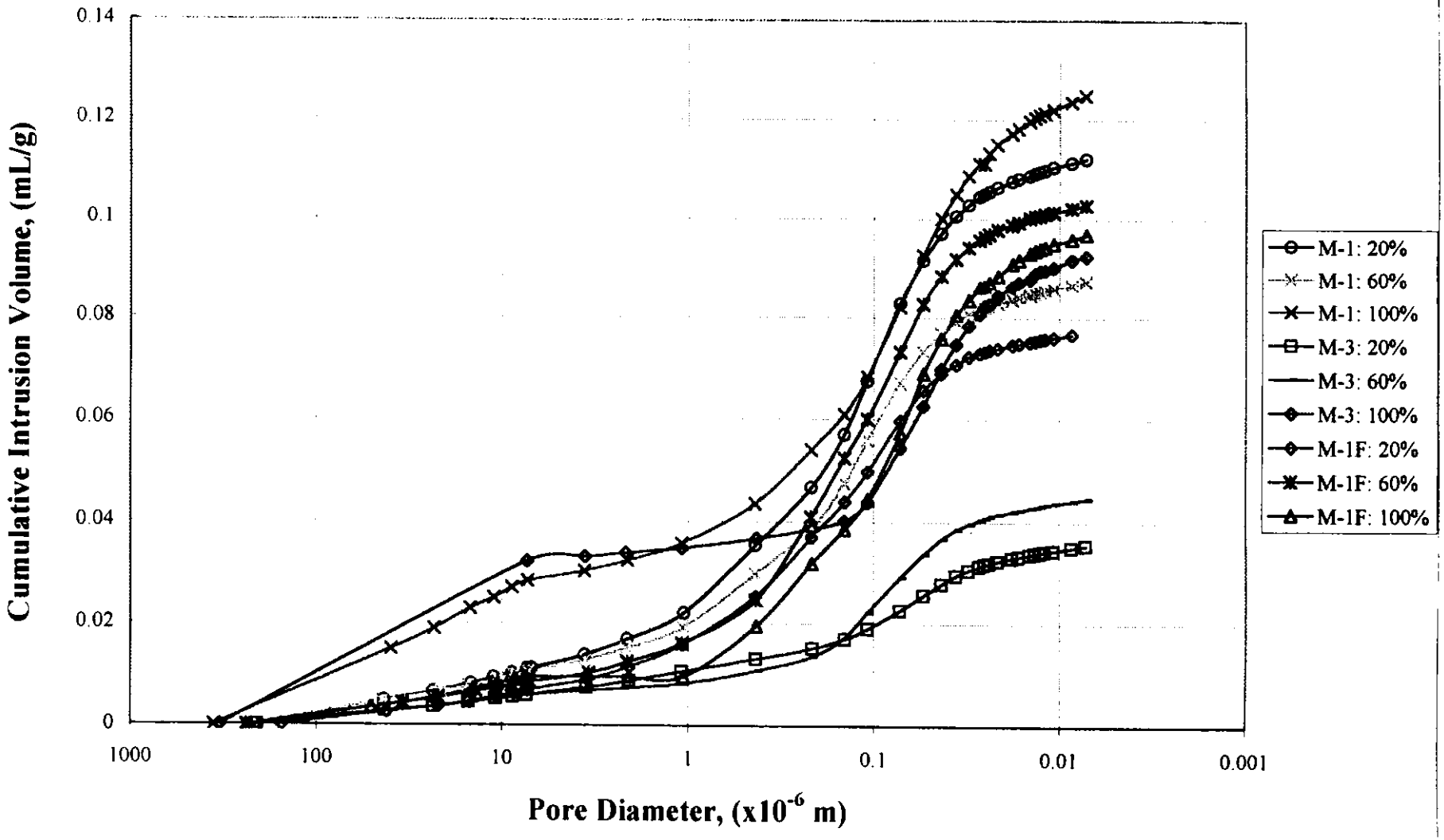

Fig. 4-62 Cumulative Intrusion Volume vs. Pore Diameter after Heating to a Maximum Temperature of 800 °C

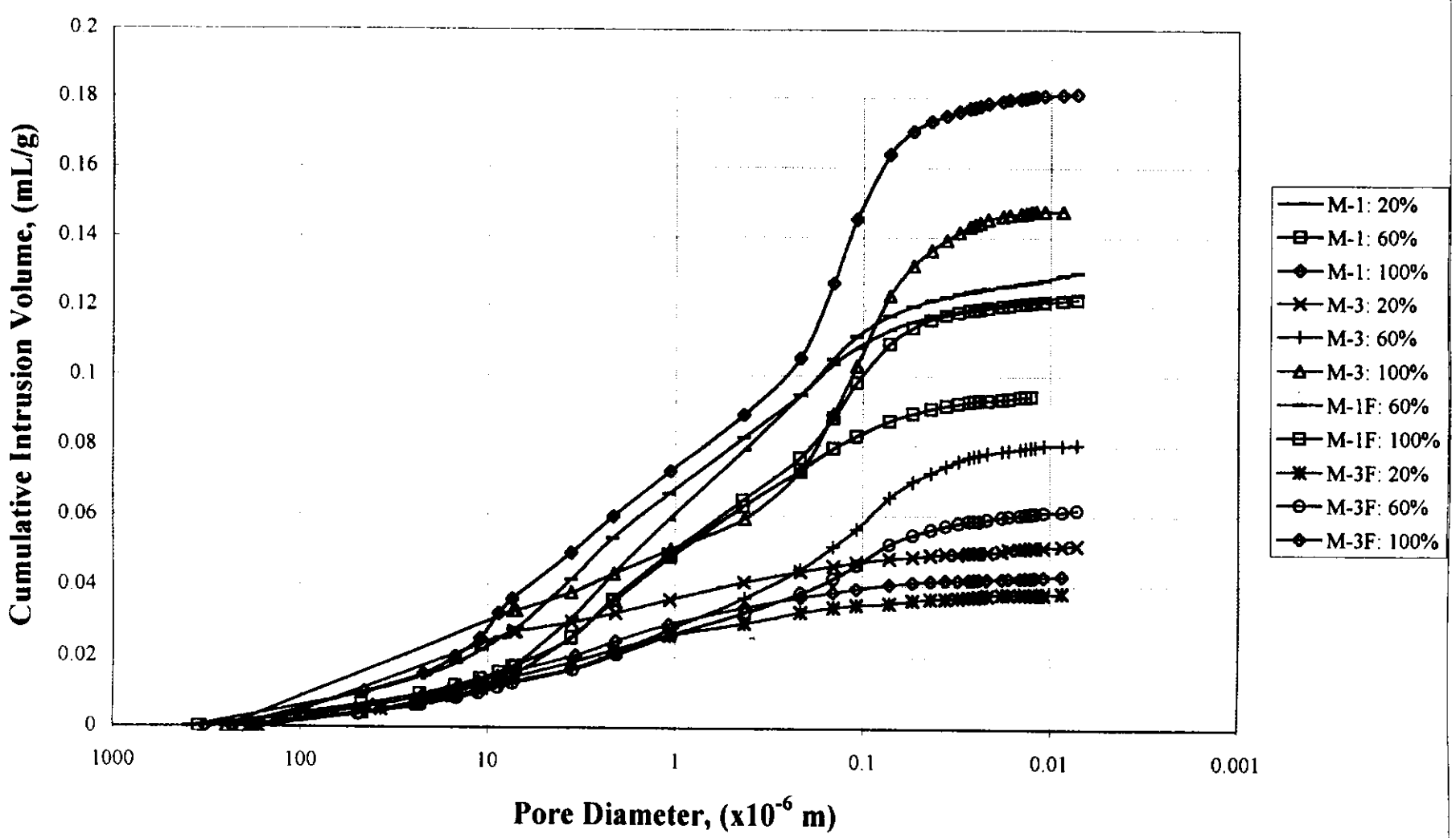

Fig. 4-63 Cumulative Intrusion Volume vs. Pore Diameter after Heating to a Maximum Temperature of 1100 °C

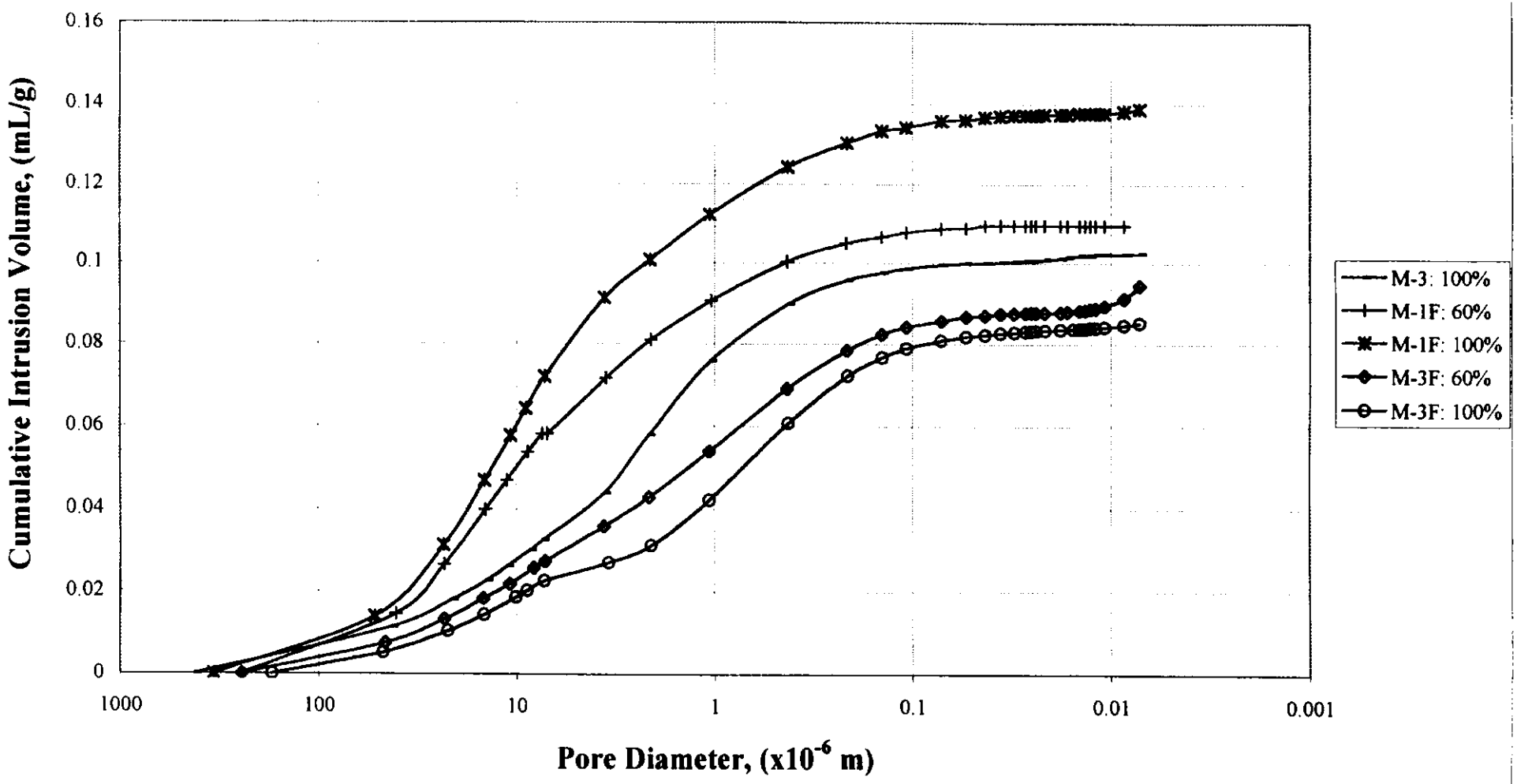

Fig. 4-64 Cumulative Intrusion Volume vs. Pore Diameter after Heating to a Maximum Temperature of 1200 °C